UNIVERSITY OF THE WITWATERSRAND

The Nonstandard Finite Difference Method Applied to Pharmacokinetic Models

Author:
Oluwaseun Francis Egbelowo

Supervisors:
Prof. Charis Harley
Dr. Byron A. Jacobs

A thesis submitted in fulfilment of the requirements for the degree of Doctor of Philosophy

in the

School of Computer Science and Applied Mathematics

WITS
UNIVERSITY

July 2018

Declaration of Authorship

I, Oluwaseun Francis Egbelowo, declare that this thesis titled, 'The Nonstandard Finite Difference Method Applied to Pharmacokinetic Models' and the work presented in it are my own. I confirm that:

- This work was done wholly or mainly while in candidature for a research degree at this University.
- Where any part of this thesis has previously been submitted for a degree or any other qualification at this University or any other institution, this has been clearly stated.
- Where I have consulted the published work of others, this is always clearly attributed.
- Where I have quoted from the work of others, the source is always given. With the exception of such quotations, this thesis is entirely my own work.
- I have acknowledged all main sources of help.
- Where the thesis is based on work done by myself jointly with others, I have made clear exactly what was done by others and what I have contributed myself.

Signed: 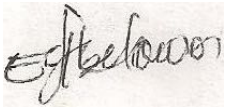

Date: 26/07/2018

"When you are about to lose courage, think beyond and trust in God's unlimited mercy and wisdom."

Oluwaseun Francis Egbelowo

UNIVERSITY OF THE WITWATERSRAND

Abstract

Faculty of Science
School of Computer Science and Applied Mathematics

Doctor of Philosophy

The Nonstandard Finite Difference Method Applied to Pharmacokinetic Models

by Oluwaseun Francis EGBELOWO

A good understanding of pharmacokinetic-pharmacodynamic can shed light on situations where one or the other needs to be optimized in drug discovery and development. As a result of this, pharmaceutical companies aim to develop new tools to support drug discovery and efficacious dose for clinical use. Drugs take a complicated journey through the body before they produce their desired therapeutic effects. Ultimately, these processes are usually best described by compartment pharmacokinetic-pharmacodynamics models. Pharmacokinetic (PK) models are commonly used to predict drug concentrations that drive controlled intravenous (I.V.) transfers (or infusion and oral transfers) while pharmacokinetic and pharmacodynamic (PD) interaction models are used to provide predictions of drug concentrations affecting the response of these clinical drugs. These PK/PD models leads to differential equations. Few of these differential equations can be solved exactly. Therefore, a lack of exact solutions to many of these differential equations leads to numerical approximation been used to determine the possible solution or behaviour of the differential equations. The aim of this thesis is to apply standard finite difference (SFD) and nonstandard finite difference (NSFD) methods to continuous-time pharmacokinetic- pharmacodynamic models. Another aim of this thesis is to provide a rigorous analysis of these models to gain insight into the dynamical features. This will allow us to also comment on the impact of certain key parameters. The NSFD method was shown to be dynamically consistent with the original continuous-time models. Also, the NSFD method is able to predict the concentration–time profile of a drug when there are alterations in the dosing regimen—this would not be possible were one to consider non-compartment analysis.

Furthermore, the NSFD method preserves significant properties of the analogous models and consequently gives reliable numerical results even when analytical solutions are not possible. The standard approaches to multi-compartment models assume linear dynamics over the duration of each time step, whereas the NSFD method assumes exponential dynamics. Thus, in the case of a linear model the NSFD method recovers the model dynamics exactly. This thesis illustrates the ability of the NSFD method to solve compartment PK models in a stable and robust fashion.

Acknowledgements

I am grateful to the Almighty God who has kept me in His arms throughout my study. Without Him, there is nothing I can do.

At this moment of accomplishment I am greatly indebted to my supervisors Prof. Charis Harley and Dr. Byron A. Jacobs for their tireless guidance, assistance, patience and unwavering faith in me. Without their supervision, this work would not have been possible. I also sincerely appreciate the useful discussion with Dr. M. Chapwanya and Prof. JM-S Lubuma.

To my lovely sweet heart, your love, tender care and support have kept me going through the years. Thanks to your commitment, trust, forgiveness and honesty. I give you full credit my darling wife for being a loving wife. Thanks so much for always encouraging me and pray for me. Temitope Egbelowo, I owe you a lot.

To my mother who taught me everything I know and stand for and raised me to be strong and independent man. Thank you mum. Thank you very much for your infallible love and support which has always been my strength. You have faithfully prayed for me my whole life and your prayers have always followed me. You are a personal friend of God and you planted the seed of Christ in me. I am grateful.

I am especially thankful to my son, Oluwaseun David Egbelowo, for sacrificing a lot of time and pleasure so that I could finish this degree. Your early mornings bye-bye and late nights hugs at the entrance was additional source of inspiration to me. Your Amen to every prayer brings me joys and hope. I consider myself the luckiest in the world to have such a lovely son. You are smarter than your age. You have made me stronger, better and more fulfilled than I could have ever imagined. My prayer for you is that you grow up believing in yourself as much I believe in you. I love you my adorable son.

I feel a deep sense of gratitude for my late father who formed part of my vision and taught me good things that really matter in life. Your plan was that immediately I finish my first degree I should enrolled for master programme but death knocked you down just a week for me to complete my National Youth Service Corps (NYSC). The good news is that your son has moved a step further. Be proud dad and rest on.

My sincere gratitude goes to my late brother, Abiodun Adewale Egbelowo who was until his death a pillar of support in all ramification.

I take this opportunity to express a deep sense of appreciation to Mr Sunday Babatunde for his support, advice and encouragement before and during my programme.

I would like to thank staff and postgraduate students of School of Computer Science and Applied Mathematics for their outstanding academic and social contribution which made the school an excellent place to do research. I express my sincere appreciation to Matthews Sejeso and Simphiwe Simelane for their co-operation, useful discussions and support.

To all my spiritual fathers, friends and well-wishers who have contributed to the successful completion of this thesis, I say a big THANK YOU.

Finally, I thank the Deutscher Akademischer Austauschdienst (DAAD), Council for Scientific and Industrial Research (CSIR), South Africa, African Institute for Mathematical Sciences (AIMS), and the University of the Witwatersrand, Johannesburg for the financial supports.

Contents

Declaration of Authorship i

Abstract iii

Acknowledgements v

Contents vii

List of Tables xiv

1 Introduction 1
- 1.1 Literature review . . . 2
- 1.2 Bioscience Models using NSFD Methods . . . 4
- 1.3 Pharmacokinetic modeling . . . 8
- 1.4 Thesis Motivation and Outline . . . 12

2 Methodologies 15
- 2.1 Introduction . . . 15
- 2.2 Finite Difference Method . . . 15
- 2.3 Runge-Kutta Method . . . 17
- 2.4 NSFD Modeling Fundamental Principles . . . 19
- 2.5 Stability, Consistency and Convergence . . . 23
- 2.6 Numerical Instabilities . . . 24
- 2.7 Elementary Stability . . . 25
- 2.8 Dynamical Consistency . . . 26

3 Linear and Nonlinear One Compartment Pharmacokinetic Model: Nonstandard Finite Difference Approach 29
- 3.1 One-compartmental Pharmacokinetic Models . . . 30
- 3.2 One-compartment Model: I.V. Bolus Injection . . . 32
  - 3.2.1 I.V. Bolus Injection: Linear Pharmacokinetic Model . . . 33
  - 3.2.2 I.V. Bolus Injection: Nonlinear Pharmacokinetic Model . . . 35

3.2.3 I.V. Bolus Injection: Linear and Nonlinear Pharmacokinetic Model . . . 40
3.3 One-compartment: I.V. Bolus Infusion . . . 42
3.3.1 I.V. bolus infusion: Linear pharmacokinetic model . . . 42
3.3.2 I.V. Bolus Infusion: Nonlinear Pharmacokinetic Model . . . 46
3.3.3 I.V. Bolus Infusion: Linear and Nonlinear Pharmacokinetic Model . . . 48
3.4 One-compartment: Extravascular Administration . . . 49
3.4.1 Extravascular Administration: Linear Pharmacokinetic Model 49
3.4.2 One-compartment: Extravascular Administration and I.V. Infusion . . . 54
3.4.3 Extravascular Administration: Linear and Nonlinear Pharmacokinetic Model . . . 55
3.5 Models Simulation . . . 56
3.5.1 I.V. Bolus Injection: Simulation . . . 57
3.5.1.1 I.V. Bolus Injection: Linear Pharmacokinetic Results 57
3.5.1.2 I.V. Bolus Injection: Nonlinear Pharmacokinetic Results . . . 59
3.5.1.3 I.V Bolus Injection: Linear and Nonlinear Pharmacokinetic Results . . . 60
3.5.2 I.V. Bolus Infusion: Simulation . . . 61
3.5.2.1 I.V. Bolus Infusion: Linear Pharmacokinetic Results 61
3.5.2.2 I.V. Bolus Infusion: Nonlinear Pharmacokinetic Results . . . 63
3.5.2.3 I.V. Bolus Infusion: Linear and Nonlinear Pharmacokinetic . . . 64
3.5.3 Extravascular Administration:Simulation . . . 65
3.5.3.1 Extravascular Administration: Linear Pharmacokinetic Results . . . 65
3.5.3.2 Extravascular Administration: Linear and Nonlinear Pharmacokinetic Results . . . 66
3.5.4 General Comparison . . . 67
3.6 Conclusion . . . 67

4 Nonstandard Finite Difference Method Applied to a Linear Pharmacokinetics Model 69
4.1 Introduction . . . 69
4.1.1 Nonstandard Finite Difference Method . . . 72
4.1.2 Phase Plane Analysis . . . 72
4.2 Results . . . 73
4.2.1 Compartmental Models for Pharmacokinetics . . . 73
4.2.2 Analytical Solution . . . 76
4.2.2.1 Case 1 . . . 76
4.2.2.2 Case 2 . . . 79
4.2.3 Remarks . . . 82

4.2.4 Nonstandard Finite Difference Scheme 85
4.2.4.1 Case 1 85
4.2.5 Case 2: 86
4.3 Discussion 87
4.3.1 Case 1: Simulation Results 88
4.3.2 Case 2: Simulation Results 89
4.4 Conclusions 92

5 Application of Nonstandard Finite Difference Method to 3-Compartment Pharmacokinietics Models 94
5.1 Introduction 94
5.2 Mathematical Model 97
5.3 Analytical Solution 99
5.3.1 Case 1: Analtytical solution 99
5.3.2 Case 2: Analtytical Solution 104
5.4 NSFD Scheme 108
5.4.1 Case 1: NSFD Scheme 108
5.4.2 Case 2: NSFD Scheme 112
5.5 Numerical Verifications and Comparison with other Schemes 116
5.6 Conclusion 120

6 Mathematical Analysis of Target-mediated Drug Disposition Models using Non-standard Finite Difference Methods 121
6.1 Introduction 121
6.2 One-compartment TMDD Model 122
6.2.1 Mathematical Analysis of One-compartment TMDD Model . 124
6.2.2 Construction and Analysis of the NSFD 126
6.3 Two-compartment TMDD Model 129
6.3.1 Mathematical Analysis of Two-compartment TMDD Model 130
6.3.2 Construction and Analysis of the NSFD 131
6.3.2.1 Analysis of the NSFD 132
6.4 Global Sensitivity Analysis 134
6.4.1 Background 134
6.4.2 Result 136
6.5 Concluding Remarks 138

7 Conclusion 139
7.1 Nonstandard Finite Difference Method 140
7.1.1 One-compartment Pharmacokinetic Models 140
7.1.2 Two-compartmnet Pharmacokinetic Models 141
7.1.3 Three-compartment Pharmacokinetic Models 141
7.1.4 Target-mediated Drug Disposition Models 142
7.2 Final note 142

Bibliography **144**

List of Figures

3.1 *Schematic representation of the one-compartment bolus I.V. bolus injection model.* . . . 33
3.2 *One-compartment IV bolus injection. Note how the concentrations of the drugs continuously decrease as the levels fall from C_0 to 0.* . . . 34
3.3 *Scheme of I.V. bolus injection with Michaelis-Menten elimination.* . . . 35
3.4 *Schematic representation of I.V. bolus infusion with both linear and Michealis-Menten elimination.* . . . 40
3.5 *Schematic representation of the one-compartment intravenous infusion.* 42
3.6 *Trajectory representation of the one-compartment i.v infusion. A drug is given at a more rapid infusion rate, a higher steady state drug concentration is obtained. But the time to reach steady state is the same.* . . . 43
3.7 *Schematic representation of IV infusion with Michaelis-Menten elimination.* . . . 46
3.8 *Scheme of IV infusion with both linear and Michealis-Menten elimination.* . . . 48
3.9 *One-compartment pharmacokinetic model for first-order drug absorption and first-order elimination.* . . . 50
3.10 *Scheme of both extravascular and I.V infusion administrations.* . . . 54
3.11 *Scheme of extravascular administration with both linear and Michealis-Menten elimination.* . . . 55
3.12 Plots showing the results obtained for time course of the plasma concentration of a drug after bolus injection from different algorithms for different steps size. We can see from all the plots that the 'exact' finite-difference scheme gives accurate result for all the step-sizes. . . . 58
3.13 *NSFD schemes (3.24), (3.26) and (3.34) respectively plotted against the exact scheme (3.35) and SFD scheme (3.17).* . . . 60
3.14 *Trajectory representation of the one-compartment i.v bolus injection model that follow both linear and nonlinear elimination.* . . . 61
3.15 Plots showing the results obtained from different algorithms for different steps size. We can see from all the plots that the 'exact' finite-difference scheme gives accurate result for all the step-sizes. . . . 62
3.16 *The concentration of the drug when (a) $h = 0.51613$ (b) $h = 6.4516$.* . . . 63
3.17 *The concentration of the drug where (a) $h = 0.75$ (b) $h = 3.3333$.* . . . 64
3.18 *Plasma concentration (C)-time curve for a drug given ins a single oral dose.* . . . 65

3.19 *3D plot of extravascular administration model (system of Equation 3.79-3.80). (a) The plot is obtained with the analytical method. (b) The plot is obtained with NSFD method. The solution obtained with NSFD method match the analytic solution very well.* 65
3.20 *Comparison of methods for one-compartment extravascular administration that follow both linear and nonlinear elimination.* 66
3.21 *In figure a-c we gives the comparison between the NSFD scheme for drug follow linear elimination and nonlinear eliminiation.* 67

4.1 Two-compartment model with intravenous (I.V.) infusion introduced into the plasma compartment. 75
4.2 Phase portrait representing $c(t)$ and $p(t)$. The arrows illustrates the trajectories of the system. 83
4.3 Phase portrait representing $c(t)$ and $p(t)$. The arrows illustrates the trajectories of the system. 83
4.4 Phase portrait (**a**) shows the steady state concentration is directly proportional to the infusion rate (I_0). Thus, a higher I_0 will result in a higher steady-state concentration, and (**b**) shows a higher elimination rate (k_{10}) will result in a lower steady-state concentration. 84
4.5 The concentration of the drug for Case 1 where $h = 0.53333$ in the (**a**) central compartment, and (**b**) peripheral compartment. 89
4.6 The concentration of the drug for Case 1 where $h = 5.3333$ in the (**a**) central compartment, and (**b**) peripheral compartment for a large time interval. 89
4.7 The concentration of the drug for Case 2 where $h = 10$ in the (**a**) central compartment, and (**b**) peripheral compartment. At the steady state, the rate of drug infusion (I_0) is equal to the elimination rate (k_{10}). 91
4.8 The concentration of the drug for Case 2 where $h = 26.667$ in the (**a**) central compartment, and (**b**) peripheral compartment. 91

5.1 A three-compartment pharmacokinetic model which assumes that all drug elimination occurs via the central compartment. 97
5.2 *The NSFD scheme (5.60) plotted against the exact scheme (5.30) - (5.32) and SFD scheme (5.62) showing concentration of the drug in each compartment for a small time interval ($h = 0.4000$).* 118
5.3 *The NSFD scheme (5.60) plotted against the exact scheme (5.30) - (5.32) and SFD scheme (5.62) showing concentration of the drug in each compartment for a large time interval ($h = 2.6667$).* 118
5.4 *The NSFD scheme (5.73) plotted against the exact scheme (5.45) and SFD scheme (5.77) showing concentration of the drug in each compartment for a small time interval ($h = 0.03$). We observe for this step size, all the methods considered mimic the dynamic properties of the differential equation.* 119

5.5 *The NSFD scheme (5.73) plotted against the exact scheme (5.45) and SFD scheme (5.77) showing concentration of the drug in each compartment for a large time interval ($h = 0.8299$). We observe for this step size, the SFD method could not mimic the dynamic properties of the differential equation as it introduce spurious solution.* 119

6.1 One-compartment TMDD reaction model [1]. 123
6.2 The NSFD scheme (6.11) showing the concentration-time profile for $0 \leq t \leq 1$ of (a) the free ligand L, and (b) the free receptor R (blue) and the ligand-receptor complex P (red). 128
6.3 The NSFD scheme (6.11) showing the concentration-time profile for $0 \leq t \leq 20$ of (a) the free ligand L, and (b) the free receptor R (blue) and the ligand-receptor complex P (red). 129
6.4 Two-compartment TMDD reaction model. 130
6.5 The NSFD scheme (6.23) showing the concentration-time profile for $0 \leq t \leq 1$ of (a) tissue M, (b) the free ligand L, and (c) the free receptor R (blue) and the ligand-receptor complex P (red). 134
6.6 The NSFD scheme (6.23) showing the concentration-time profile for $0 \leq t \leq 20$ of (a) tissue M, (b) the free ligand L, and (c) the free receptor R (blue) and the ligand-receptor complex P (red). 134
6.7 First order effects $S_1(blue)$ and total effects S_{Tot} (red) of the six parameters using Sobol's method of Sensitivity Analysis for one-compartment TMDD model. 137
6.8 First order effects $S_1(blue)$ and total effects S_{Tot} (red) of thesix parameters using Sobol's method of Sensitivity Analysis for two-compartment TMDD model. 138

List of Tables

3.1 The variables of importance and their meaning 32
3.2 The numerical results for IV bolus model (3.1). 59
3.3 The numerical results for the I.V. bolus infusion model (3.45). . . . 63
3.4 The absolute error results of Equations (3.67) for C with parameters values $R = 0.5$, $K_m = 4$, and $V_{max} = 2$. 64
3.5 The numerical results for the extravascular administration model. . 66

4.1 Values for sisomicin kinetic parameters derived from two-compartment open model analysis of serum data after intravenous (I.V.) administration. These values are visualized in Figure 4.1 and are obtained from the work by Péchère et al. [2]. 74
4.2 The absolute error results for the system of equations given by (4.3) for $c(t)$ with parameter values $k_{10} = 0.0094$, $k_{12} = 0.0405$, and $k_{21} = 0.0291$. 90
4.3 The absolute error results for the system of equations given by (4.3) for p with parameter values $k_{10} = 0.0094$, $k_{12} = 0.0405$, and $k_{21} = 0.0291$. 90
4.4 The absolute error results for the system of equations given by (4.4) for $c(t)$ with parameter values $k_{10} = 0.0094$, $k_{12} = 0.0405$, $k_{21} = 0.0291$ and $I_0 = 1$. 92
4.5 The absolute error results for the system of equations given by (4.4) for $p(t)$ with parameter values $k_{10} = 0.0094$, $k_{12} = 0.0405$, $k_{21} = 0.0291$ and $I_0 = 1$. 92

5.1 Pharmacokinetics of Remifentani parameters derived from three-compartment open model analysis after intravenous (I.V.) administration. These values are visualized in Figure 5.2 and are obtained from the work by Cascone et al. [3]. 96
5.2 The absolute error results for the system of equations given in Equation (5.2) for C_1 with parameter values in Table 5.1. 117
5.3 The absolute error results for the system of equations given in Equation (5.2) for C_2 with parameter values in Table 5.1. 117
5.4 The absolute error results for the system of equations given in Equation (5.2) for C_3 with parameter values in Table 5.1. 118

6.1 Values and ranges for parameters for the one and two-compartment TMDD models, (6.1) and (6.17). 123

6.2 First order indices and the total indices for one-compartment TMDD model. 137

This thesis is dedicated to the Lord Jesus Christ the giver of knowledge, wisdom, inspiration, mercy and grace.

Chapter 1

Introduction

"So many fail because they don't get started - they don't go. They don't overcome inertia. They don't begin."

W. Clement Stone

Many real life problems are usually best described by differential equations. Few of these differential equations can be solved exactly and it's not always easy (or possible) to find exact solutions to many of these. Several researchers have tried to develop accurate and fast methods capable of producing approximations to problems whose exact solutions are difficult to find, due to their complexity, by adopting various standard finite difference methods (e.g Finite Difference Method, Finite Volume Method, Boundary Element Method, Spectral Method, Runge-Kutta etc.). These methods are often the only practical and viable way to solve these differential equations. We employed the standard finite difference (SFD) scheme as a basis for our computational work. In the case where the equation involves nonlinear terms, the nonlinear terms are often not properly approximated. When the nonlinear terms are essential to the description of the problem employing linearized equations cannot capture the impact of the nonlinear terms. This leads to numerical instabilities which arise from the incorrect modelling of derivatives and nonlinear terms in these equations [4]. Numerical instabilities in a discrete

model of a differential equation are said to occur if there exist solutions to the SFD equations that do not correspond to any solution of the differential equation [5].

In recent years, advances in research have allowed researchers to cater for the numerical instabilities that occur when using SFD methods. Researchers believe that numerical methods that approximate differential equations are expected to exhibit similar behaviour with the continuous models. A numerical method is deemed consistent if the truncation error vanishes as the relevant step size approaches zero. The nonstandard finite difference (NSFD) schemes developed by Mickens et al. [6–10] were proposed to compensate for the weaknesses of methods such as the SFD methods; numerical instabilities being a prime example. As commented on by Liao and Ding [11], with regard to the positivity, boundedness, and monotonicity of solutions, NSFD schemes have performed better than SFD schemes. Because it is more flexible in its construction, an NSFD scheme can more easily preserve certain properties and structures obeyed by the original equations and can have better dynamical consistency for dynamical problems [11]. The advantages of NSFD methods have been observed when being employed for many numerical applications. González-Parra et al. [12, 13] developed some NSFD methods to preserve the positivity condition and population conservation law of biological models. Heat transfer problems have also been considered via this method in Jordan [14] and Malek [15]. As such we will employ this method in our work as an extension of the comparison work done via the SFD method.

1.1 Literature review

NSFD approach is still in the early stages of its development. After the pioneering work of Mickens [4], Mickens et al. [16] have shown the advantage of using complicated denominator functions in constructing FD models of ordinary differential equations (ODEs). They discuss the influence on the solutions of FD schemes of using a variety of denominator functions in the discrete modelling of the derivative for any ODE. Mickens et al. [17] extended the work of Mickens et al. [16]. They

show how to construct a class of FD schemes for two coupled first-order ODE's that do not have numerical instabilities. They considered differential equations that are assumed to have only a single (real) fixed point. Illustrations of such schemes are given for the Duffing and Van der Pol equations.

Mickens [18] presented novel FD schemes used to numerically integrate the time-dependent Shrödinger equation. The schemes are explicit and use Euler-type expressions for the discrete time derivative. Also in [19] Mickens constructs a new class of NSFD schemes for the Fisher partial differential equation. These schemes have the property that, in the appropriate limits, the discrete models obtained are either exact or the "best" FD schemes for the corresponding differential equation.

Anguelov and Lubuma [20] formalized the transfer of essential properties of the solution of a differential equation to the solution of a discrete scheme as qualitative stability with respect to the properties. This helped to motivate some rules used in the design of nonstandard finite difference schemes. They considered extensions of some models, and numerical examples confirming the efficiency of the nonstandard approach are provided.

Lubuma and Patidar [21] considered singular perturbation problems defined by first-order (systems of) ordinary differential equations, second-order ordinary differential equations, advection-reaction equations and reaction-diffusion equations. They provide some complements to the theory of non-standard finite difference method. They use this theory to design non-standard schemes which replicate the physical properties of the exact solution. They provide several numerical simulations that support the theory.

Cole [22] introduced the NSTD method to construct a high accuracy finite-difference time-domain (FDTD) algorithm to solve Maxwell's equations. This method is 10,000 times more accurate than the standard Yee algorithm. He also introduced nonstandard second-order FD methods into the Yee algorithm. Using μ/h (grid spaces per wavelength = 8), he achieved the same accuracy as the standard Yee algorithm does at $\mu/h = 1140$. Similarly, Momoniat [23] studied the regularized

long wave equation (RLW). He used a modified form of the RLW equation as a criterion for selecting the "best" NSFD scheme for solving the RLW equation. He showed that the modified equation performed well by preserving the three conserved quantities and capturing the single solitary wave solution accurately.

Chen et al. [24] investigated the appearance of spurious solutions when first order ODEs are discretized using Runge-Kutta schemes. They concluded that the reliability of the numerical solutions to a particular ODE could be verified only by constructing several discrete models and comparing their numerical results with the known properties of the exact solutions. However, Mickens [25] demonstrated that by constructing NSFD schemes all difficulties found by Chen et al. [24] can be eliminated, and that qualitatively correct numerical solutions are obtained for all values of the step size. Similarly, Markus et al. [26], constructed a simple nonstandard forward Euler scheme to solve a system of three ordinary nonlinear differential equations that models photoconductivity in semiconductors which successfully eliminates numerical instabilities. The models, when integrated with a conventional fourth-order Runge-Kutta algorithm produces numerically- induced chaos. In order to help determine the best FD scheme, it was found useful to test the local stability of the scheme by direct inspection of the eigenvalues dependent on the step size. The proper choice of the scheme and the nonlocal substitutions proved to be critical for the performance of the scheme.

1.2 Bioscience Models using NSFD Methods

NSFD methods have recorded remarkable successes when applied to bioscience models. We present such a biosciences model and will employ SFD schemes as well as NSFD methods.

Anguelov et al. [27] produced an article on the numerical computation and analysis of a problem related to the research of Kamgang et al. [28] where threshold conditions for epidemiological models and the global stability of the disease-free

equilibrium (DFE) are studied. Anguelov et al. [27] established a discrete counterpart of the main continuous result that guarantees the global asymptotic stability (GAS) of the DFE for general epidemiological models. They then designed NSFD schemes in which the Metzler matrix structure of the continuous model is carefully incorporated and both Mickens' rules [29] on the denominator of the discrete derivative and the nonlocal approximation of nonlinear terms are used in an innovative way. As a result of these strategies, their NSFD schemes are proved to be dynamically consistent with the continuous model, i.e, they replicate their basic features, including the GAS of the DFE, the linear stability of the endemic equilibrium (EE), the positivity of the solutions, the dissipativity of the system, and its inherent conservation law. The general analysis is done in detail for the MSEIR model for which the NSFD theta method is implemented, with emphasis on the computational aspects such at its convergence, or local truncation error. Numerical simulations that illustrate the theoretical results are provided.

Anguelov et al. [30] designed, analyzed and implemented nonstandard finite difference (NSFD) schemes for some differential models in biosciences. The NSFD schemes are reliable in three directions. They are topologically dynamically consistent for one dimensional models. They can replicate the global asymptotic stability of the disease-free equilibrium of the MSEIR model in epidemiology whenever the basic reproduction number is less than 1. They preserved the positivity and boundedness property of solutions of advection-reaction and reaction-diffusion equations.

Elsheikh et al. [31] designed and analysed a NSFD numerical scheme for the numerical solution of the HIV-malaria co-infection model with a distributed delay representing the incubation period of the malaria parasite in the mosquitoes. They studied a number of qualitative properties of sub-models to come up with efficient numerical methods for the full co-infection model. They observed that one of the salient features of these methods was that they preserve positivity of the solution which is essential while studying epidemiological models. They presented numerical

simulations which confirmed the theoretical findings.

In the work of Ding et al. [32] though they employed the NSFD method to derive a set of difference equations for the epidemic model with vaccination, they violated the NSFD rules. They show that when $h < h_o$ (h is the step size and $h_o = \frac{1}{d+\alpha+\gamma}$), the discretized model preserves positivity and global dynamics of the continuous model. This is a contradiction to the NSFD rules that put no restriction on the step size. Obaid et al. [33] formulated and analysed an unconditionally stable NSFD method for a mathematical model of HIV transmission dynamics. They studied the dynamics of this model using the qualitative theory of dynamical systems. They show that the qualitative features of the continuous model are preserved by the numerical method proposed. This method also preserves the positivity solution, which is an essential requirement when modelling epidemic diseases. Comparisons are also made with other conventional approaches that are routinely used for such problems.

Lubuma et al. [34] considered the SIS-model extended to a Volterra equation which exhibits complex behaviour such as the backward bifurcation phenomenon. They designed a NSFD scheme which is reliable in replicating there complex dynamics. They show that the NSFD scheme has no spurious fixed points.

Anguelov et al. [35] constructed a family of NSFD schemes that are dynamically consistent with the MSEIR model in the sense that they replicate the global asymptotic stability of the disease-free equilibrium, the local asymptotic stability of the endemic equilibrium, as well as the positivity of exact solutions and the conservation of the population of the continuous model. In [36] Anguelov et al. built upon their previous article, Anguelov et al. [35], by presenting some NSFD methods for the MSEIR model and compared their results with the standard methods usually implemented in scientific software. They show that NSFD schemes are superior to the standard ones with respect to their qualitative properties and the CPU running time. Furthermore, it is shown that non-local approximations of

non-linear terms in the equations can be of utmost importance when capturing the dynamics of the system.

Chapwanya et al. [37] considered the basic SIR epidemiological model with the Michealis-Menten formulation of the contact rate. From a study of the Michealis-Menten basic enzymatic reaction, they designed two types of NSFD schemes for the SIR model: exact-related schemes based on the Lambert W function and schemes obtained by using Mickens's rules of more complex denominator functions for discrete derivatives and non-local approximations of non-linear terms. They compared and investigated the performance of the two types of schemes by showing that they are dynamically consistent with the continuous model. Numerical simulations that supported the theory and demonstrate the computational the power of NSFD schemes were presented.

Garba et al. [38] considered a deterministic continuous-time model for the transmission dynamics of two strains of an arbitrary disease in the presence of an imperfect vaccine. The model is rigorously analysed, to gain insights into its dynamical features. The analysis reveals that it undergoes a vaccine-induced backward bifurcation when the associated reproduction threshold is less that unity. They presented two FD methods for numerically solving the model. The central objective is to determine which of the two methods gives solutions that are dynamically consistent with those of the continuous-time model. The first method is an implicit method, being a Gauss-Siedel-like algorithm. However, this was shown to suffer numerous scheme-dependent problems when trying to preserve many of the main essential dynamical features of the model, particularly when relatively large step-sizes are used in the simulations. On the other hand, the second numerical method, constructed based on Mickens' NSFD discretization framework, was shown to be free of any numerical instabilities and contrived behaviour regardless of the size of the step-size used in the numerical simulations.

Lubuma et al. [39] designed and investigated the reliability of various NSFD

schemes for SIS-type epidemiological models. For a classical SIS-ODE model, they constructed a non-standard Runge-Kutta method, which is shown to be of order four-this is a first in the field. They also considered two NSFD schemes which faithfully replicate the property of the continuous model requiring the value $R_o = 1$ (where R_o is the basic reproduction parameter as a forward bifurcation): the disease-free equilibrium is globally asymptotically stable when $R_o < 1$; it is unstable when $R_o > 1$, however there appears a unique locally asymptotically stable endemic equilibrium in this case. The latter schemes are further used to derive NSFD schemes that are dynamically consistent with the positivity and boundedness properties of the SIS-diffusion model for the spatial spread of disease. Numerical simulations that support the theory are provided.

Extensive literature of the NSFD can be found in Patidar [40] and [41].

1.3 Pharmacokinetic modeling

The first attempt into what led to pharmacokinetics was described by Andrew Buchanan in his work *Physiological effects of the inhalation of ether* [42] in which he pointed out that for short ether inhalations, the speed of recovery of the ether was related to redistribution of ether in the body. Pharmacokinetics is the science of the kinetics of drug absorption, distribution, and elimination (more precisely relating to excretion and the metabolism). The mathematical representation of this work started with Michaelis and Menten [43] who first developed the now well-known Michaelis–Menten equation to describe enzyme kinetics; later this equation was also used to describe the elimination kinetics of drugs. Widmark and Tandberg [44] in 1924 published equations now known as (a) the one-compartment open model with bolus intravenous injection and multiple doses administered at uniform intervals and (b) the one-compartment open model with constant rate intravenous infusion [44]. Though the full concept of pharmacokinetic was introduced by Teorell [45], Holford and Sheiner [46] defined pharmacokinetic as a branch of pharmacology that employs mathematical models to better understand how drugs are absorbed,

distributed, metabolized and excreted by the body. It has been well reported recently that the Food and Drug Administration (FDA) and other drug regulatory agencies have been using modeling and simulation to assist in making informed decisions. Furthermore, pharmaceutical companies are expected to justify their dose, their choice of patient population, and their dosing regimen, not just through clinical trials, but also through modeling and simulation [47, 48].

After a drug is released from its dosage form, the drug is absorbed into the surrounding tissue, the body, or both. As commented on by Shargel et al. [49], the distribution through and elimination of the drug in the body varies for each patient but can be characterized using mathematical models and statistics. Being able to characterize drug distribution and elimination is an important prerequisite to be able to determine or modify the dosing regimens of individuals and groups of patients. From among the three main types of pharmacokinetic (PK) models—compartment, physiologic and statistical moment approach models—compartmentally-based models are known to be a very simple and useful tool in pharmacokinetic [49]. In essence, a compartment model provides a simple way of grouping all the tissues into one or more compartments where drugs move to and from the central or plasma compartment. Assuming a drug is given by intravenous (I.V.) injection and that the drug dissolves (distributes) rapidly in the body fluids, one may employ a one-compartment PK model that can describe the situation as a tank containing a volume of fluid that is rapidly equilibrated with the drug [49]. The concentration of the drug in the tank after a given dose is governed by two parameters, namely the fluid volume of the tank that will dilute the drug, and the elimination rate of the drug per unit of time—these are both assumed constant for a given drug [49]. Simplistic as this model may be with regards to drug distribution and elimination in the human body, a drug's PK properties can frequently be described via such a one-compartment open model. Assuming such a model, the drug is both added to and eliminated from a central compartment which represents plasma and highly-perfused tissues that rapidly equilibrate with the drug. When an I.V. dose of drug is given, the drug enters directly into the central compartment while elimination of

the drug occurs from the central compartment given that the organs involved in drug elimination, primarily the kidney and liver, are well-perfused tissues.

In a two-compartment model, the drug can move between the central or plasma compartment to and from the peripheral or tissue compartment [49]. Although the peripheral compartment does not represent a specific tissue, the mass balance accounts for the drug present in all the tissues. Knowing the parameters of either the one- or two-compartment model, one can estimate the amount of drug left in the body and the amount of drug eliminated from the body at any time. A drug that follows the pharmacokinetic of a two-compartment model does not equilibrate rapidly throughout the body, as is assumed for a one-compartment model [50]. In the former, the drug distributes into two compartments, the central compartment and the peripheral compartment. The central compartment represents the blood, extracellular fluid, and highly-perfused tissues. The drug distributes rapidly and uniformly in the central compartment. The peripheral compartment contains tissues in which the drug equilibrates more slowly. Drug transfer between the two compartments is assumed to take place by first-order processes. We will be considering all these models in this thesis.

The simplicity and flexibility of the compartment model is the principal reason for its wide application. A major advantage of such models is that the time course of the drug in the body may be monitored quantitatively with a limited amount of data [51]. Furthermore, these models account accurately for the mass balance of the drug in the body and the amount of drug eliminated [1]. Compartment models have successfully been applied for the prediction of the pharmacokinetic of the drug and the development of dosage regimens. Moreover, compartment models are very useful in relating plasma drug levels to pharmacodynamic (PD) and toxic effects in the body [51]. Underlying physiologic mechanisms can also be obtained via such a model through model testing of the data. Thus, compartment analysis may lead to a more accurate description of the underlying physiologic processes and the kinetics involved. In clinical PK literature, drug data comparisons are

[1] Mass balance includes the drug in the plasma, the drug in the tissue pool, and the amount of drug eliminated after dosage administration.

based on compartment models and the easy tabulation of important parameters accomplished [51].

In practice, PK models seldom consider all the rate processes ongoing in the body [50]. Due to the complexity models which incorporate such information pose, simplifying assumptions are often made so that solutions may be obtained. Traditional PK models, being simplified mathematical expressions, are based on the assumption of a linear relationship between the dose of a drug and its concentration [52]. In a linear model, these rate coefficients, called k, are assumed to be constant. However, such assumptions regarding the linearity of the model do not necessarily describe the actual physical processes as accurately as a non-linear relationship may. In fact, the non-linearities seen in such models are related to drug absorption, distribution, metabolism and excretion, and the pharmacokinetic of drug action. Another example where simplifying assumptions are made pertains to the number of tissue compartments in a perfusion model. Multi-compartment models were developed to explain the observation that, after a rapid I.V. injection, the plasma level–time curve does not decline linearly as a single, first-order rate process [50]. The plasma level–time curve reflects first-order elimination of the drug from the body only after distribution equilibrium, or plasma drug equilibrium with peripheral tissues occurs. Therefore, while the number of tissue compartments in a perfusion model does vary with the drug, the tissues or organs that have no drug penetration are invariably excluded from consideration. Organs such as the brain, the bones, and other parts of the central nervous system are often excluded, as most drugs have little penetration into these organs [49]. To describe each organ separately with a differential equation would make the model very complex and mathematically difficult to solve. Under such circumstances more sophisticated methods of solution need to be employed. The focus of this thesis are on well-known compartment models [1, 3, 53–59], particularly since our focus is to provide justification for the use of the NSFD method.

1.4 Thesis Motivation and Outline

Mathematical analysis of pharmacological models is becoming increasingly important for drug development. While this is important, most pharmacological systems are complex or non-linear systems and require numerical techniques to obtain the solution. In recent years, the food and drug administration (FDA) uses modeling and simulation extensively in their review of new drug applications (NDAs) to making informed decisions [48]. Also the pharmaceutical companies are required to provide modeling and simulations results when filing for NDA. In the light of aforementioned facts the development and optimization of PK/PD modeling methods could bring tremendous benefit to the drug research and development. Hence, new numerical approaches could be of help.

This thesis contributes to the area of pharmacokinetic analysis. Specifically, it introduces new techniques for solving pharmacokinetic models. These techniques provide an improved numerical solution to continuous–time pharmacokinetic models by constructing discrete models when compared with standard finite difference methods. Also, it provide a framework for the study of the dynamic flow of drugs in the body. The primary objective of this thesis is to apply SFD and NSFD methods to continuous-time pharmacokinetic models and prove that NSFD methods is dynamically consistent with the original continuous-time models. Also, to provide a rigorous analysis of these models to gain insight into the dynamical features. This will allow us to comment on the impact of certain key parameters. For each of the model considered in this thesis, the itemize below was consider:

1. Design SFD schemes for pharmacokinetic models as a means of:
    a. Comparing with the NSFD schemes;
    b. Considering the impact of parameter choices.
2. Design NSFD schemes for pharmacokinetic models that will be:
    a. Free of numerical instabilities;

   b. Dynamically consistent.

3. Investigate the impact of parameter choices when using NSFD methods. This will act as another means of comparison with SFD schemes.

The contributions of this thesis can be summarized as follows:

- ✓ Introduction of new techniques for solving pharmacokinetic models. This we believe lays a new foundation for solving pharmacokinetic models.
- ✓ A description and investigation into dynamics of pharmacokinetic models are provided.
- ✓ 'Exact' finite difference scheme are provided for all the linear pharmacokinetic models studied in this thesis. It is shown that the approach produce solutions of better quality than the standard finite difference schemes.
- ✓ NSFD schemes that are dynamical consistency with the continuous analogue differential are provided for the nonlinear pharmacokinetic models.
- ✓ A qualitative understanding of the behaviour of the solutions and local stability of the numerical solution near steady states was determined.
- ✓ The most contributing parameters were determined with the use of global sensitivity analysis.

The contributions are detailed as outline:

- In Chapter 1, a brief overview is given and relevant literature is reviewed.
- Chapter 2 presents the methods and concepts that are put to extensive use throughout this thesis.
- In Chapter 3, one compartment pharmacokinetic models was described. The one compartment model was consider for three different dose regimens. These models leads to linear and nonlinear ordinary differential equations (ODE). The ODEs was solved using the SFD and NSFD methods.

- In Chapter 4, the concept of two compartment pharmacokinetic models was described. NSFD scheme was structured for relevant system of equations which models this pharamcokinetic process. The results obtained was compared with standard methods.

- In Chapter 5, three compartment pharmacokinetic models is described. NSFD scheme is derived for three-compartment pharmacokinetic models. For the case when the system is homogeneous (models arising from IV bolus injection mode of administration), 'exact' finite difference scheme is given while in the case of non-homogeneous (models arising from IV infusion route of administration), scheme that has the same qualitative behaviour as the analytical solution for all step-sizes is provided.

- In Chapter 6, mathematical analysis of system of nonlinear ordinary differential equations (ODE) arising from target mediated drug disposition (TMDD) models was carried out. NSFD schemes are structured for the models. The global sensitivity analysis (GSA) of TMDD parameters was studied in one and two-compartment models.

- The summary of the work done in this thesis are presented in Chapter 7.

Chapter 2

Methodologies

"Everything must be taken into account. If the fact will not fit the theory—let the theory go."

Agatha Christie

2.1 Introduction

This Chapter review the methodologies used throughout this thesis and explain the important concepts a scheme must possess.

2.2 Finite Difference Method

While the implementation of the NSFD method is the focus of this research, we employ the finite difference method as means of comparison. We define finite difference methods as numerical methods used for the solution of differential equations by approximating them with difference equations, in which finite differences approximate the derivatives.

We introduce the concept of the finite difference method from Taylor's theorem, where h is termed the step size between the values of the independent variable x. Where we have to increase x by h, then according to Taylor's theorem, we could create a Taylor series expansion.

$$f(x+h) = f(x) + hf'(x) + \frac{h^2}{2!}f''(x) + \cdots \tag{2.1}$$

such that

$$f'(x) = \frac{f(x+h) - f(x)}{h} + \mathcal{O}(h). \tag{2.2}$$

Assuming that $h \to 0$ then,

$$f'(x) \approx \frac{f(x+h) - f(x)}{h} \quad \text{or} \quad f'(x_n) \approx \frac{f(x_n+h) - f(x_n)}{h} = \frac{f_{n+1} - f_n}{h}. \tag{2.3}$$

Similarly, if we expand $f(x)$ at $f(x-h)$ then,

$$f(x-h) = f(x) - hf'(x) + \frac{h^2}{2!}f''(x)\cdots \tag{2.4}$$

such that,

$$f'(x) = \frac{f(x) - f(x-h)}{h} + \mathcal{O}(h), \tag{2.5}$$

which, if $h \to 0$, gives,

$$f'(x) \approx \frac{f(x) - f(x-h)}{h} \quad \text{or} \quad f'(x_n) \approx \frac{f(x_n) - f(x_n-h)}{h} = \frac{f_n - f_{n-1}}{h}. \tag{2.6}$$

Subtracting the Taylor series expansion of $f(x-h)$ from that of $f(x+h)$ provides us with

$$f(x+h) - f(x-h) = 2hf'(x) + \frac{2h^3}{3!}f'''(x) + \cdots \tag{2.7}$$

such that,

$$f'(x) = \frac{f(x+h) - f(x-h)}{2h} + \mathcal{O}(h^2) \tag{2.8}$$

which, under the assumption that $h \to 0$, provides us with a third approximation for the derivative

$$f'(x) \approx \frac{f(x+h) - f(x-h)}{2h} \quad \text{or} \quad f'(x_n) \approx \frac{f(x_n+h) - f(x_n-h)}{2h} = \frac{f_{n+1} - f_{n-1}}{2h}. \tag{2.9}$$

Equations (2.3), (2.6) and (2.9) are known as forward difference, backward difference and central difference approximations to the first order derivative, respectively. The approximation given by Equation (2.9) has an error of $\mathcal{O}(h^2)$, and is deemed the most accurate of the three approximations provided.

2.3 Runge-Kutta Method

In a similar fashion with the finite difference scheme, we introduce the concept of the Runge-Kutta method from Taylor's theorem, where h is the step size between the values of the independent variable x [60]. Consider

$$x' = f(t, x). \tag{2.10}$$

Let's denote the time at the nth time step by t_n and the computed solution at the nth time-step by x_n. The step size h is then given by $h = t_n - t_{n-1}$. Then, the Taylor's series expansion of Equation (2.10) is given by

$$x(t_{n+1}) = x(t_n) + hx'(t_n) + \frac{h^2}{2!}x''(t_n) + \mathcal{O}(h^3). \tag{2.11}$$

Differentiating Equation (2.10), we have

$$x''(t_n) = f_t(t_n, x_n) + f_x(t_n, x_n)x'(t_n). \tag{2.12}$$

$x'(t)$ is given in Equation (2.10), therefore Equation (2.12) becomes

$$x''(t_n) = f_t(t_n, x_n) + f_x(t_n, x_n)f(t_n, x_n). \tag{2.13}$$

Substituting Equations (2.10) and (2.13) into Equation (2.11), we have

$$x_{n+1} = x_n + hf(t_n, x_n) + \frac{h^2}{2}\left(f_t(t_n, x_n) + f_x(t_n, x_n)f(t_n, x_n)\right) + \mathcal{O}(h^3). \tag{2.14}$$

With some manipulations, we have

$$x_{n+1} = x_n + \frac{h}{2}f(t_n, x_n) + \frac{h}{2}f(t_n, x_n) + \frac{h^2}{2}\left(f_t(t_n, x_n) + f_x(t_n, x_n)f(t_n, x_n)\right) + \mathcal{O}(h^3). \tag{2.15}$$

$$x_{n+1} = x_n + \frac{h}{2}f(t_n, x_n) + \frac{h}{2}\left[f(t_n, x_n) + h\left(f_t(t_n, x_n) + f_x(t_n, x_n)f(t_n, x_n)\right)\right] + \mathcal{O}(h^3). \tag{2.16}$$

Using Multi variable Taylor series, we know that

$$f(t + h, x + hf(t, x)) = f(t, x) + h\left(f_t(t, x) + f_x(t, x)f(t, x)\right) + \mathcal{O}(h^2). \tag{2.17}$$

Therefore, using Equation (2.17), Equation (2.16) becomes

$$x_{n+1} = x_n + \frac{h}{2}f(t_n, x_n) + \frac{h}{2}f(t_n + h, x_n + hf(t_n, x_n)) + \mathcal{O}(h^3). \tag{2.18}$$

From Equation (2.18) if

$$k_1 = f(t_n, x_n), \tag{2.19}$$

$$k_2 = f(t_n + h, x_n + hk_1), \tag{2.20}$$

then classical second order Runge-Kutta method is given as

$$x_{n+1} = x_n + h(\frac{1}{2}k_1 + \frac{1}{2}k_2). \tag{2.21}$$

The approximation given by Equation (2.21) has a local truncated error $\mathcal{O}(h^3)$. This second order Runge-Kutta method is also known as Heun's method.

The most widely used method is the fourth-order Runge-Kutta method which can be developed in the similar fashion to the second order Runge-Kutta. The local truncation error of the fourth-order Runge-Kutta method is $\mathcal{O}(h^5)$. Equation (2.10)

can be solved using the classical fourth-order Runge-Kutta as follows:

$$x_{n+1} = x_n + \frac{1}{6}(k_1 + 2k_2 + 2k_3 + k_4), \tag{2.22}$$

where

$$k_1 = hf(t_n, x_n), \tag{2.23}$$

$$k_2 = hf(t_n + \frac{h}{2}, x_n + \frac{k_1}{2}), \tag{2.24}$$

$$k_3 = hf(t_n + \frac{h}{2}, x_n + \frac{k_2}{2}), \tag{2.25}$$

$$k_4 = hf(t_n + \frac{h}{2}, x_n + k_3). \tag{2.26}$$

The approximation given by Equation (2.22) subjected to k_i, $i = 1, 2, 3, 4$ has an error of $\mathcal{O}(h^5)$ and thus is deemed the most accurate of all the approximations provided.

2.4 NSFD Modeling Fundamental Principles

NSFD methods provide numerical solutions to differential equations by constructing discrete models. They preserve the significant properties of their continuous analogues and consequently give reliable numerical results. The following rules were given by Mickens in [29] for constructing an NSFD scheme:

Rule 1. The orders of the discrete representation of the derivative must be equal to the orders of the corresponding derivatives appearing in the differential equations.

Remark 2.1. If the order of the discrete representations for derivatives are larger than those occurring in the differential equations, then numerical instabilities will occur.

Rule 2. Denominator functions for the discrete representations for derivatives must, in general, be expressed in terms of more complicated functions of the step-sizes than those conventionally used.

Remark 2.2. Consider a first-order differential equation of the form:

$$\frac{du}{dt} = f(t, u). \tag{2.27}$$

The conventional denominator h of the system in (2.27) is:

$$\frac{du}{dt} \to \frac{u_{k+1} - u_k}{h}, \tag{2.28}$$

which is replaced by a nonnegative function $\phi(h)$ where,

$$\phi(h) = h + \mathcal{O}(h^2). \tag{2.29}$$

In the above, we have:

$$h = \Delta t, \quad t \to t_k = hk, \quad u(t) \to u_k, \tag{2.30}$$

where k is an integer. The exact discrete representations of Equation (2.27) are given as:

$$\frac{du}{dt} \to \frac{u_{k+1} - \varphi(h)u_k}{\phi(h)}, \tag{2.31}$$

where,

$$\varphi(h) = 1 + \mathcal{O}(h). \tag{2.32}$$

Rule 3. Nonlinear terms must, in general, be modeled by nonlocal discrete representations on the computational grid. When using the SFD method, the derivative is always spread over two or more grids points. However, nonlinear terms

are always modeled locally. This leads to one of the problems we encountered when using SFD method.

Remark 2.3. The nonlinear terms that occur in $f(t,u)$ are approximated in a nonlocal way by a suitable function of several points on the mesh. For example, Mickens' approximation of nonlinear terms [7, 61, 62] is given as:

$$u^2 \approx u_k u_{k+1} \quad \text{and} \quad u^3 \approx \frac{2u_{k+1}^2 u_k^2}{u_{k+1}+u_k}, \tag{2.33}$$

Erdogan and Ozis' approximation of the nonlinear term, which was clearly stated in [62], is given as:

$$u^2 \approx u_k u_{k+1} \quad \text{and} \quad u^3 \approx \frac{1}{2}u_k^2(3u_{k+1}-u_k). \tag{2.34}$$

Rule 4. All the special conditions that correspond to either the differential equation and/or its solutions should also correspond to the difference equation and/or its solutions.

Remark 2.4. For example, the system described in Equation (2.27) is called time-invariant if the behavior of the system does not explicitly depend on the absolute time. In other words, if $f(t_1,u) = f(t_2,u)$ for any two times t_1 and t_2, then the system is time-invariant. If the discrete representation of the same model does not also have this property, numerical instabilities may occur.

Rule 5. The discrete scheme should not introduce extraneous or spurious solutions.

Remark 2.5. The discrete representation of the derivative must, in general, converge to the same fixed-point solutions as the corresponding derivative. If it does otherwise, numerical instabilities may occur.

These set rules for the construction of the discrete models that have the capability to replicate the properties of the exact solution culminated to the formal definition of NSFD schemes by Anguelov and Lubuma [20]. They considered a dynamical system on an interval $D \subset \mathbb{R}$ defined by equation (2.27), as well as numerical

scheme of the form [30]:

$$u^{k+1} = G(h; u^k), \tag{2.35}$$

which is a discrete dynamical system on D. The function $G = G(h) = G(h; u)$ must satisfy the usual consistency conditions for the argument u:

$$G(0, u) = u \qquad \text{and} \qquad \frac{dG(0)}{dh} = f(u). \tag{2.36}$$

Definition 2.6 (Anguelov and Lubuma [20])**.** A finite difference equation (2.35) that determines approximate solutions u^k to the solution $u(t)$ of a differential equation (2.27) is called a nonstandard finite difference (NSFD) scheme if at least one of the following two conditions is met:

a. The classical denominator h of the discrete derivative is replaced by a non-negative function $\phi(h)$ such that

$$\phi(h) = h + \mathcal{O}(h^2) \quad \text{as} \quad h \to 0; \tag{2.37}$$

b. Nonlinear terms that occur on the right-hand side of equation (2.27) are approximated in a nonlocal way, i.e., by a suitable function of several points of the mesh.

Definition 2.7 (Anguelov and Lubuma [20])**.** Assume that the solution of problem (2.27) satisfies some property P. The difference equation (2.35) is called (qualitatively) stable with respect to property P (or P-stable) if, for every $h > 0$, the set of discrete solutions satisfies property P.

Equations (2.27) and (2.35) are said to have the same general solution if and only if,

$$u_k = u(t_k). \tag{2.38}$$

for arbitrary values of h.

Definition 2.8. The method (2.35) is called exact difference scheme of (2.27), if the relation (2.38) between the discrete solution u_k and the exact solution $u(t_k)$ holds.

2.5 Stability, Consistency and Convergence

In pharmacokinetic modeling, the long time behaviour of the models converge to the steady state. Therefore, any method to be used to solve the models arising from pharmacokinetic must follow this phenomenon. The classical method, most used for pharmacokinetic models has inherent with them a number of potential problems (1) the modeling is not unique, (2) the step size is a constant h and numerical methods are investigated for "small" h by letting h tend to 0; and (3) the inappropriate modeling of a differential equation by a difference equation can lead to numerical instabilities. All of these problems are related to the issues of stability, consistency and convergence which arise in the use of finite-difference schemes [63]. Hence, having best numerical method means that the question relating to stability, consistency and convergence do not arise [4].

Stability: In numerical analysis, stability is a desirable property of numerical method. Therefore, a numerical method is said to be stable if the errors at any stage of the computation does not grow in the course of the computational processes [64]. Stability of a discretization refers to a quantitative measure of the well-posedness of the discrete problem. For example, a SFD method is stable if the errors (truncation, round-off errors) decay as the computation proceeds from one marching step to the next i.e as the grid spacing tends to zero the SFD method become stable.

Consistency: A numerical scheme is consistent if the method approximating differential equation become exact as the time step size tend to zero. For a method to be consistent, the truncation error should vanish as the step size approaches zero.

Convergence: A numerical method is said to be convergence if the solution of the numerical method approaches exact solution of the original differential equation in the course of the computation progresses. A stable and consistent process of discretization leads to convergence of the solution.

To illustrate the concepts above, we considered a linear difference equation with constant coefficients of the form [65]

$$x_n = Ax_{n-1} + v_n \tag{2.39}$$

Definition 2.9. The difference equation (2.39) is stable if for any choice of x_0, $\|\mathbf{x}_n\|$ is bounded as $n \to \infty$.

Definition 2.10. The difference equation (2.39) is convergent if for any choice of x_0, $\|\mathbf{x}_n\| \to 0$ as $n \to \infty$.

2.6 Numerical Instabilities

An opposite of numerical stability is numerical instability. A numerical method is said to be numerically unstable if the growth of errors is unbounded as the computation progresses. Also, we say that a computation is numerically unstable if the uncertainty of the input values is grossly magnified by the numerical method. In the case the numerical algorithm tends to the exact solution in some limit, it may not converge to the correct solution because of truncation errors that can magnified causing deviation from the exact solution to grow [66].

Some of the well know standard numerical method (Euler, R-K method) are associated with some degree of stability and their stability depend on the time step size. They are only conditionally stable. In these methods, numerical instabilities can occur if one or more of the following occur [5]:

- The step-size h becomes equal to or larger than a threshold value h_0 i.e $h \geq h_0$;

- The order of the discrete SFD model is larger than the order of the corresponding differential equation;
- The number of fixed points of the SFD scheme is larger than the number of fixed points of the corresponding differential equation.

The concept of elementary stability explained by Anguelov and Lubuma [20, 61] is abundantly used in the literature to overcome the numerical instabilities.

2.7 Elementary Stability

The concept of elementary stability pertains to a number of fixed points and their relationship to the behaviour of the other solutions around them. Generally, fixed points which attract the solutions in some neighborhood, when the argument increases to infinity, are called stable; those that repulse the solutions are called unstable [61]. For hyperbolic fixed points $\bar{u}$,

$$J \equiv f'(\bar{u}) \neq 0, \tag{2.40}$$

the asymptotic behaviour of solutions of (2.27) with initial condition near $\bar{u}$ may be reduced to the behaviour of solutions of the linear equation

$$\frac{d\epsilon}{dt} = J\epsilon. \tag{2.41}$$

Definition 2.11 (Anguelov and Lubuma [20])**.** A hyperbolic fixed point $\bar{u}$ is called linearly stable provided that the solution ϵ of the equation (2.41) corresponding to any small enough initial condition $\epsilon(0) = \epsilon_0$, $|\epsilon| \ll 1$ say, satisfies $\lim_{t\to\infty} \epsilon(t) = 0$. This is equivalent to saying that $J < 0$ in equation (2.40). Otherwise, the fixed point is called linearly unstable.

The discrete analogue of the continuous case (2.41) is given as

$$\epsilon_{k+1} = J_h\epsilon_k \quad \text{with} \quad J_h = \frac{\partial G}{\partial u}. \tag{2.42}$$

Definition 2.12 (Anguelov and Lubuma [20]). Assume that a hyperbolic fixed point $\bar{u}$ of the differential equation in (2.27) is a solution of the discrete method (2.35). We say that the constant solution (or fixed point) $\bar{u}$ is linearly stable provided that the solution (ϵ_k) of the equation (2.42) corresponding to any small enough initial condition $\epsilon(0) = \epsilon_0$, $|\epsilon| \ll 1$ say, satisfies $\lim_{t\to\infty} \epsilon_k = 0$. This is equivalent to saying that $|J_k| < 0$ in equation (2.42). Otherwise, the fixed point is called linearly unstable.

Definition 2.13 (Anguelov and Lubuma [20]). The finite difference method (2.35) is called elementary stable if for any value of the step size h, its only fixed points $\bar{u}$ are those of the differential equation (2.27), the linear stability properties of each $\bar{u}$ being the same for both the differential equation and the discrete method.

The substitute for elementary stability is a concept introduced in [67], where it is referred to as topological dynamic consistency. They proved that if the condition (2.43) holds for a discrete model of the form (2.35) then

$$\frac{dG(h;u)}{du} > 0, \tag{2.43}$$

then condition (2.43) is necessary and sufficient for the scheme (2.35) to be qualitatively stable with respect to monotone dependence on the initial value.

2.8 Dynamical Consistency

In this section we review simple differential models for which NSFD methods are qualitatively consistent with the original continuous time models they approximated. Consider the combustion model [68]:

$$\frac{du}{dt} = u^2(1-u) \quad u(0) = u_0 > 0. \tag{2.44}$$

There are three fixed points in equation (2.44)

$$\bar{u}^{(1)} = \bar{u}^{(2)} = 0, \quad \bar{u}^{(3)} = 1. \tag{2.45}$$

For this equation the non-standard scheme is taken to be

$$\frac{u_{k+1}-u_k}{\phi(h)} = 2(u_k)^2 - u_{k+1}u_k - u_{k+1}(u_k)^2, \tag{2.46}$$

where u^2 and u^3 have been approximated as

$$u^2 \to 2(u_k)^2 - u_{k+1}u_k, \quad u^3 \to u_{k+1}(u_k)^2. \tag{2.47}$$

$\phi(h)$ is determined via a consideration of equation (2.44) which allows us to let

$$f(u) = u^2(1-u), \quad f(\bar{u}) = 0. \tag{2.48}$$

Equation (2.48) has three real solutions which we denote by $\{\bar{u}^i, i = 1, 2, 3\}$. Now define R_i as

$$R_i = \frac{df}{du}\Big|_{u=\bar{u}^{(i)}} \tag{2.49}$$

and take R^* to be

$$R^* = max\{|R_i|; \quad i = 1, 2, 3\}. \tag{2.50}$$

Note that $\phi(h, R^*)$ has to satisfy

$$\phi = h + \mathcal{O}(R^*h^2), \quad 0 < \phi < \frac{1}{R^*}. \tag{2.51}$$

Using equation (2.50) and our fixed points (2.45) we see that $R^* = 1$ since for $\bar{u}^{(1)} = \bar{u}^{(2)} = 0$. Given ϕ as

$$\phi(h, R^*) = \frac{1 - e^{-R^*h}}{R^*}, \tag{2.52}$$

the denominator function $\phi(h)$ for (2.44) is

$$\phi(h) = 1 - e^{-h}. \tag{2.53}$$

Thus the NSFD scheme of (2.44) is

$$u_{k+1} = \frac{(1 + 2(1 - e^{-h})u_k)u_k}{1 + (1 - e^{-h})[u_k + (u_k)^2]}. \tag{2.54}$$

Equation (2.44) has the property that all solutions, for $u_o > 0$ move monotonically towards the fixed point $\bar{u}^3 = 1$. This is because $\bar{u}^3$ is the only stable fixed point while $\bar{u}^1$ and $\bar{u}^2$ are unstable fixed points. Using the fact that $\phi(h)$, given by equation (2.53), has the property

$$0 < \phi(h) < 1, \quad h > 0. \tag{2.55}$$

It is clear that Equation (2.44) has exactly the same properties as the solutions obtained for (2.54):

1. Equation (2.54) has three fixed points located at $\bar{u}^1 = \bar{u}^2 = 0$ and $\bar{u}^3 = 1$.
2. Fixed points $\bar{u}^1 = \bar{u}^2 = 0$ are unstable while $\bar{u}^3 = 1$ is stable.
3. For $u_o > 0$, the u_k monotonically approach $\bar{u}^3 = 1$.

Scheme (2.54) preserves the positivity and the boundedness of the solutions as well as the asymptotic stability of the fixed point $y = 1$.

Chapter 3

Linear and Nonlinear One Compartment Pharmacokinetic Model: Nonstandard Finite Difference Approach

"There is no one giant step that does it. It's a lot of little steps."

Peter A. Cohen

Some of the work in this Chapter appear in:

Oluwaseun Egbelowo. Nonlinear Elimination of Drugs in One-Compartment Pharmacokinetic Models: Nonstandard Finite Difference Approach for Various Routes of Administration. Math. Comput. Appl. 2018, 23, 27.

3.1 One-compartmental Pharmacokinetic Models

In a one-compartment model the body is assumed to be a single compartment and the drug absorbed achieves instantaneous distribution throughout the body, metabolizing between tissues. The drug output is characterized by an elimination rate. In this study, three dose regimen models are considered:

- One-compartment model - I.V. bolus injection,
- One-compartment model - I.V. bolus infusion,
- One-compartment model - Extravascular administration.

Compartment models play a significant role in understanding the dynamics of concentration of the drug in the body. In most cases, these compartment models are described by autonomous linear or nonlinear ordinary differential equations. At the therapeutic doses, the change in the amount of drug in the body due to absorption, distribution, metabolism or excretion, is proportional to its dose. In such situation the rate processes are said to follow a linear kinetics. The term linear simply means that if the dose is increased, the plasma concentration will be increased proportionally. However, nonlinearity in pharmacokinetics arises when therapeutic drug concentrations are high enough to saturate an enzyme. In the case when the nonlinearity in the system is complex or when the number of compartments in the model becomes large or when the kinetics becomes complex, such as in the work of Michaelis-Menten, exact solutions are not obtainable and hence the need for numerical methods arises [69]. Some of the well known standard numerical schemes produce unnecessary oscillations, introduce extraneous or spurious solutions, and converge to fixed-point solutions different from the corresponding derivative. Hence one observes the occurrence of numerical instabilities. The NSFD scheme was developed by Mickens as an alternative method providing an approximate solution to a wide range of differential equations and catering for the numerical instabilities

that occur when using standard methods. NSFD method have been well reported in recent years mainly because they are efficient and and preserve qualitative properties, see for example [4, 7, 70–79] which give the relevant background materials on this topic.

A standard finite difference (SFD) scheme is said to be 'exact' for a particular differential equation if its local truncated error is exactly zero for its general solution [80, 81]. In other words, when the analytical solution of a differential equation can be matched exactly with its corresponding SFD equation then the 'exact' finite difference solution exists[1] [79]. The idea of 'exact' finite difference was first conceived by Mickens [81, 82] who has shown that an exact explicit scheme is easily obtained from the knowledge of its analytical solution. Therefore, 'exact' finite difference schemes are designed in such a fashion that the difference equation has the same general solution as the corresponding differential equation. In this situation where exact solutions exist, the solution can be re-structured in such a way to obtain the 'exact' finite difference scheme. But in the case where exact solutions are not possible, the rules proposed by Mickens [81] will be deployed. In such a situation the method is called a NSFD method [61]. The consequence of these rules is that while the scheme may not be 'exact', qualitative properties of the corresponding differential equations for all step-sizes are preserved and thus elementary numerical instabilities that can arise are eliminated. The remainder of this chapter is organized as follows. A one-compartment pharmacokinetic model with drugs administered by I.V. bolus injection is presented in Section 2 and I.V. bolus infusion model is solved in Section 3. Section 4 provides solutions to one compartment pharmacokinetic models when the drug is administered by extravascular administration. Numerical simulations are provided for the models in the Section 5. Conclusions are provided in the Section 6.

[1] If exact general solutions of a differential equation are explicitly known, then an 'exact' finite difference scheme exists.

Variable	Meaning
C	Concentration of drug in central compartment.
V_{max}	The maximum rate of change of concentration.
K_m	The Michaelis-Menten constant.
k_a	The absorption rate constant for oral administration.
k_{el}	Elimination rate of drug leaving central compartment.
V_1	The apparent volume of distribution.

TABLE 3.1: The variables of importance and their meaning

3.2 One-compartment Model: I.V. Bolus Injection

When drugs are administered by I.V. bolus injection, the entire dose administered enters the bloodstream directly and is able to produce pharmacological effects. This is followed by the immediate onset of action by distribution of the drug through the circulatory system to all the tissues in the body. Hence, it is possible to assume that a drug given by IV bolus injection is rapidly mixed. We understand that if you inject directly into the bloodstream it is immediately in the bloodstream and does not have to be absorbed. The concentration at time 0, corresponds to the dose given therefore, it is described as an I.V. bolus injection route of administration. We considered this mode of administration in three different elimination processes: 1) drugs given via an I.V. bolus injection, distributed as a one-compartment model, eliminated only by linear pharmacokinetic, 2) drugs given via an I.V. bolus injection, distributed as a one-compartment model, eliminated only by nonlinear pharmacokinetic, and 3) drugs given via an I.V. bolus injection, distributed as a one-compartment model, and eliminated by both linear and nonlinear processes. We solved the differential equation arising from these elimination processes with the concept of NSFD as a means of comparison with the SFD.

3.2.1 I.V. Bolus Injection: Linear Pharmacokinetic Model

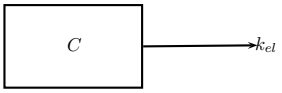

FIGURE 3.1: *Schematic representation of the one-compartment bolus I.V. bolus injection model.*

The process by which a drug administered by IV bolus injection, distributed as a one-compartment and eliminated by linear pharmacokinetic is depicted diagrammatically as shown in Figure 3.1. The differential equation for the compartment as represented in Figure 3.1 is given as

$$\frac{dC}{dt} = -k_{el}C, \tag{3.1}$$

with initial condition

$$C(0) = C_0, \qquad k_{el} > 0.$$

It is one of the most appropriate for drugs which rapidly distribute between plasma and other tissues. Here $C = C(t)$ is the concentration of the drug in the body as a function of real time. k_{el} is the elimination rate of the drug, V_1 is the apparent volume of distribution while D is the initial dose. The analytical solution of this is obtained and given as

$$C(t) = C_0 e^{-k_{el}t}. \tag{3.2}$$

It is very easy to see from the exact solution of the model that the solution monotonically approaches 0 as $t \to \infty$. This can be seen in the Figure 3.2.

We are now able to provide the 'exact' finite-difference scheme for Equation (3.1). Since the model is linear, the only fixed point is given as

$$\bar{C} = 0.$$

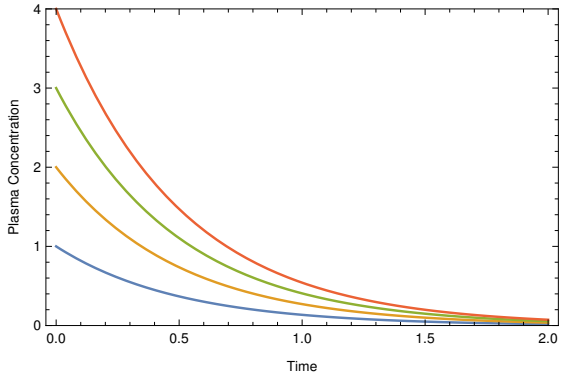

FIGURE 3.2: *One-compartment IV bolus injection. Note how the concentrations of the drugs continuously decrease as the levels fall from C_0 to 0.*

For this equation the 'exact' finite difference scheme is taken to be

$$\frac{C_{k+1} - C_k}{\phi(h, k_{el})} = -k_{el} C_k \tag{3.3}$$

Equation (3.1) is a decay equation, and its exact scheme is known and is given by Equations (3.4) - (3.5) by Mickens [81].

$$\phi(h, k_{el}) = \frac{1 - e^{-k_{el} h}}{k_{el}}. \tag{3.4}$$

Therefore, the NSFD scheme of equation (3.1) is given by the scheme [68, 81]

$$\frac{C_{k+1} - C_k}{\frac{1 - e^{-k_{el} h}}{k_{el}}} = -k_{el} C_k \tag{3.5}$$

This result is to be contrasted with the standard forward-Euler scheme. Now consider the SFD method for Equation (3.1)

$$\frac{C_{k+1} - C_k}{h} = -k_{el} C_k, \tag{3.6}$$

where h is the step-size. Its corresponding difference equation will be

$$C_{k+1} = C_k (1 - h k_{el}) \tag{3.7}$$

with the solution

$$C_k = C_0 (1 - h k_{el})^k. \tag{3.8}$$

Equation (3.8) gives the following results:

(i) if $0 < hk_{el} < 1$, C_k monotonically tends to 0.

(ii) if $hk_{el} = 1$, $C_k = 0$ for $k \geq 1$.

(iii) if $1 < hk_{el} < 2$, C_k tends to 0 with an oscillating amplitude via an alternating sign at each step.

(iv) if $hk_{el} = 2$, C_k oscillates with a constant amplitude C_0.

(v) if $hk_{el} > 2$, C_k oscillates with an increasing amplitude.

As a result, the SFD scheme in Equation (3.6) has the same qualitative behaviour as the analytical solution of the pharmacokinetic model if [81]

$$0 < hk_{el} \ll 1. \tag{3.9}$$

In turn, the NSFD scheme (3.5) gave accurate results without the requirement (3.9) as needed by the SFD scheme.

3.2.2 I.V. Bolus Injection: Nonlinear Pharmacokinetic Model

The equation that describes the elimination of a drug that is distributed in the body as a one-compartment and is eliminated by nonlinear (Michaelis-Menten) pharmacokinetic after an I.V. bolus injection is given as [55]

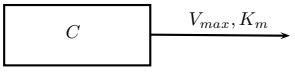

FIGURE 3.3: *Scheme of I.V. bolus injection with Michaelis-Menten elimination.*

$$\frac{dC}{dt} = -\frac{V_{max}C}{K_m + C} \qquad V_{max} > 0, \quad K_m > 0, \tag{3.10}$$

with initial condition

$$C(0) = C_0. \tag{3.11}$$

V_{max} is the maximal velocity of the metabolism and K_m is Michaelis constant. Michaelis-Menten kinetics is also called capacity-limited metabolism, saturable metabolism, or mixed-order kinetics [56].

The function $C(t)$, that is the solution to the differential equation (3.10), has no closed form expression. The explicit closed-form solution of the one-compartment IV bolus injection model that follow Michaelis-Menten kinetics given in equation (3.10) is expressible in terms of the Lambert W-function as

$$C(t) = K_m W\left(\frac{C_0 e^{\frac{C_0}{K_m} - \frac{V_{\max} t}{K_m}}}{K_m}\right). \tag{3.12}$$

Definition 3.1. The Lambert W function is defined to be a multivalued (single valued in the case of PK applications) inverse of the function $x \mapsto xe^x$ satisfying [83]

$$y = W(x) \tag{3.13}$$

such that

$$x = ye^y, \tag{3.14}$$

which can be writing as

$$x = W(x)e^{W(x)}. \tag{3.15}$$

Where W is Lambert's function. Equation (3.12) satisfies the transcendental Equation (3.15).

The exact finite difference scheme of (3.12) is given as [84]

$$C_{k+1} = K_m W\left(\frac{C_k e^{\frac{C_k}{K_m} - \frac{V_{\max} h}{K_m}}}{K_m}\right). \tag{3.16}$$

A SFD scheme for the Michaelis-Menten equation (3.10) might take a form such as

$$\frac{C_{k+1} - C_k}{h} = -\frac{V_{max} C_k}{K_m + C_k}. \tag{3.17}$$

We will provide NSFD schemes for Equation (3.10) for the case when (3.10) is discretize using the concept of: semi-implicit forward-Euler, implicit forward-Euler and explicit forward-Euler [37, 84, 85]. A systematic approach is used to determine the denominator functions which has enabled us to rediscover the NSFD schemes (3.24), (3.26) and (3.34). The processes are shown under each cases below.

Case 1: Semi-implicit forward-Euler

The NSFD here is obtained from semi-implicit forward-Euler discretization as

$$\frac{C_{k+1} - C_k}{h} = -\frac{V_{max} C_{k+1}}{K_m + C_k}. \tag{3.18}$$

Equation (3.18) can be rewritten in the form

$$C_{k+1} = \frac{K_m C_k + C_k^2}{(K_m + hV_{max}) + C_k}. \tag{3.19}$$

Then we can use the fact that

$$1 + \frac{hV_{max}}{K_m} = e^{\frac{hV_{max}}{K_m}} + O(V_{max}^2 h^2 / K_m^2), \tag{3.20}$$

we can make the replacements

$$1 + \frac{hV_{max}}{K_m} = e^{\frac{hV_{max}}{K_m}}, \tag{3.21}$$

which implies

$$h \to \frac{K_m(e^{\frac{hV_{max}}{K_m}} - 1)}{V_{max}}. \tag{3.22}$$

Therefore, the denominator function for the semi-implicit forward-Euler is given as

$$\phi_1(h, V_{max}, K_m) = \frac{K_m(e^{\frac{hV_{max}}{K_m}} - 1)}{V_{max}}. \tag{3.23}$$

The NSFD semi-implicit discretization of Equation (3.10) is

$$\frac{C_{k+1}-C_k}{\phi_1(h)} = -\frac{V_{max}C_{k+1}}{K_m+C_k}. \tag{3.24}$$

Case 2: Implicit forward-Euler

We also note that when Equation (3.10) is discretize using implicit discretization as

$$\frac{C_{k+1}-C_k}{h} = -\frac{V_{max}C_{k+1}}{K_m+C_{k+1}}, \tag{3.25}$$

and following the same process from Equation (3.18) to (3.22), we obtain the same denominator function given in Equation (3.23). Therefore the NSFD for the Equation (3.10) when it is discretize using implicit forward-Euler is

$$\frac{C_{k+1}-C_k}{\phi_1(h)} = -\frac{V_{max}C_{k+1}}{K_m+C_{k+1}}. \tag{3.26}$$

From computational point of view, equation (3.26) is equivalent to [37]

$$C_{k+1} = \frac{1}{2}\left(C_k - K_m - hV_{\max} + \sqrt{(hV_{\max}+K_m-C_k)^{\,2}+4C_kK_m}\right) \tag{3.27}$$

which has a unique non-negative root.

Case 3: Explicit forward-Euler

NSFD scheme in this case is obtained from explicit forward-Euler as

$$\frac{C_{k+1}-C_k}{h} = -\frac{V_{max}C_k}{K_m+C_k}, \tag{3.28}$$

Equation (3.28) can be rewritten in the form

$$C_{k+1} = \frac{C_k(K_m-hV_{max})+C_k^2}{K_m+C_k}. \tag{3.29}$$

Then we can use the fact that

$$1 - \frac{hV_{max}}{K_m} = e^{\frac{-hV_{max}}{K_m}} + O(V_{max}^2 h^2 / K_m^2), \tag{3.30}$$

we can make the replacements

$$1 - \frac{hV_{max}}{K_m} = e^{\frac{-hV_{max}}{K_m}}, \tag{3.31}$$

which implies

$$h \to \frac{K_m(1 - e^{\frac{-hV_{max}}{K_m}})}{V_{max}}. \tag{3.32}$$

Therefore, the denominator function for the explicit forward-Euler is given as

$$\phi_2(h) = \frac{K_m(1 - e^{\frac{-hV_{max}}{K_m}})}{V_{max}}. \tag{3.33}$$

Similarly NSFD discretization of Equation (3.10) is

$$\frac{C_{k+1} - C_k}{\phi_2(h)} = -\frac{V_{max} C_k}{K_m + C_k}. \tag{3.34}$$

From the three cases we have seen that the denominator function obtained depends on the discretization method.

The result of Equation (3.10) obtained in term of the Lambert function as in Equation (3.16) can be rewritten in the form

$$\frac{C_{k+1} - C_k}{\phi_2(h)} = \frac{K_m W\left(\frac{C_k e^{\frac{C_k}{K_m} - \frac{V_{\max} h}{K_m}}}{K_m}\right) - C_k}{\phi_2(h)}. \tag{3.35}$$

which serves as a means of comparison with the results obtained from the three cases above. Equation (3.35) serves as the true solution.

3.2.3 I.V. Bolus Injection: Linear and Nonlinear Pharmacokinetic Model

The other possible route of drugs elimination is mixed drug elimination. In this elimination process, drug may be eliminated by both linear (first-order) and nonlinear (Michaelis-Menten) processes. Therefore, the equation that describes a

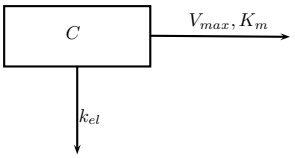

FIGURE 3.4: *Schematic representation of I.V. bolus infusion with both linear and Michealis-Menten elimination.*

drug that is eliminated by both first-order and Michaelis-Menten kinetics after IV bolus injection is given by

$$\frac{dC}{dt} = -k_{el}C - \frac{V_{max}C}{K_m + C}, \tag{3.36}$$

where k_{el} is the first-order rate constant representing the sum of all first-order elimination processes, while second term of Equation (3.36) representing the saturable process.

There are two fixed points in Equation (3.36)

$$\bar{C}^{(1)} = 0, \quad \bar{C}^{(2)} = \frac{-k_{el}K_m - V_{\max}}{k_{el}}. \tag{3.37}$$

The SFD scheme of (3.36) is given as

$$\frac{C_{k+1} - C_k}{h} = -k_{el}C_{k+1} - \frac{V_{max}C_{k+1}}{K_m + C_k}. \tag{3.38}$$

This can be rewritten in the form

$$C_{k+1} = \frac{K_m C_k + C_k^2}{(K_m + hk_{el}K_m + hV_{max}) + C_k + hk_{el}C_k}. \tag{3.39}$$

Then we can use the fact that

$$1+\frac{h(k_{el}K_m+V_{max})}{K_m}=e^{\frac{h(k_{el}K_m+V_{max})}{K_m}}+O((hk_{el}K_m+hV_{max})^2/K_m^2), \tag{3.40}$$

we can make the replacements

$$1+\frac{h(k_{el}K_m+V_{max})}{K_m}=e^{\frac{h(k_{el}K_m+V_{max})}{K_m}}, \tag{3.41}$$

which implies

$$h\rightarrow\frac{K_m e^{\frac{h(k_{el}K_m+V_{max})}{K_m}}-K_m}{k_{el}K_m+V_{max}}. \tag{3.42}$$

Therefore, the denominator function for equation (3.38) is

$$\phi_3(h,k_{el},V_{max},K_m)=\frac{K_m e^{\frac{h(k_{el}K_m+V_{max})}{K_m}}-K_m}{k_{el}K_m+V_{max}}, \tag{3.43}$$

then, the NSFD scheme for the Equation (3.36) is structured as

$$\frac{C_{k+1}-C_k}{\phi_3(h)}=-k_{el}C_{k+1}-\frac{V_{max}C_{k+1}}{K_m+C_k}. \tag{3.44}$$

It is clear that (3.36) has exactly the same properties as the solutions obtained for (3.44):

1. Equation (3.44) has two fixed points located at $\bar{C}^{(1)}=0, \quad \bar{C}^{(2)}=\frac{-k_{el}K_m-V_{\max}}{k_{el}}$.
2. Fixed points $\bar{C}^{(1)}$ is biologically possible while $\bar{C}^{(2)}$ is biologically impossible.
3. Fixed point $\bar{C}^{(1)}$ is locally asymptotically.
4. Applying condition (2.43) on equation (3.44) we realize that fixed point $\bar{C}^{(1)}$ is globally asymptotically stable.

Scheme (3.44) preserves the positivity, the asymptotic stability of the fixed point $\bar{C}^{(1)}=0$ and globally asymptotically stable properties. Therefore, for all h we have the replication of all topological dynamical properties, a concept introduced in [67].

3.3 One-compartment: I.V. Bolus Infusion

The I.V. bolus infusion process is the process of infusing a drug at a constant rate. The drug input is constant and equal to the rate of infusion of the drug. On starting the infusion there is no drug in the body and therefore no elimination. The concentration of the drug in the body then rises, but as the drug concentration increases, so does the rate of elimination. Thus, the rate of elimination will keep rising until it matches the rate of infusion. The concentration of the drug in the body is then constant and is said to have reached a steady state. A similar approach is used for the I.V bolus injection process. This section describe I.V. bolus infusion route of administration. We considered this mode of administration in three different elimination processes: 1) drugs given by I.V. bolus infusion, distributed as a one-compartment model, eliminated only by linear pharmacokinetic, 2) drugs given by I.V. bolus infusion, distributed as a one-compartment model, eliminated only by nonlinear pharmacokinetic, and 3) drugs given by I.V. bolus infusion, distributed as a one-compartment model, and eliminated by both linear (first-order) and nonlinear (Michaelis-Menten) processes.

3.3.1 I.V. bolus infusion: Linear pharmacokinetic model

In this case when drug is given by infusion and the drug is excreted in a linear way, the equation used to described this process is given in Equation (3.45). The schematic representation of this situation is given below. This process is described

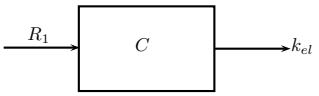

FIGURE 3.5: *Schematic representation of the one-compartment intravenous infusion.*

with the expression:

$$\frac{dC}{dt} = R - k_{el}C \quad C(0) = 0, \tag{3.45}$$

where $R = \frac{R_1}{V_1}$ is the flow rate of the drug, R_1 is the infusion rate per unit time, C is the concentration of the drug present at time t, V_1 is the apparent volume of distribution and $k_{el}C$ is the rate of the drug coming out (this is a first order process). To find $C(t)$, we need to integrate this from time 0 to time t, knowing that $C(0) = 0$ (i.e., we are starting with zero drug in the body). If we integrate, the C is described by the equation:

$$C(t) = \frac{R}{k_{el}}\left(1 - e^{-k_{el}t}\right) \tag{3.46}$$

for which steady state concentration is reached after infinite infusion time. That is as

$$t \to \infty, \qquad e^{-k_{el}t} \to 0. \tag{3.47}$$

Equation (3.46) reduce to steady-state concentration $C(\infty)$ as follows

$$C(\infty) = \frac{R}{k_{el}}. \tag{3.48}$$

We obtained the 'exact' finite difference scheme of Equation (3.45) with initial

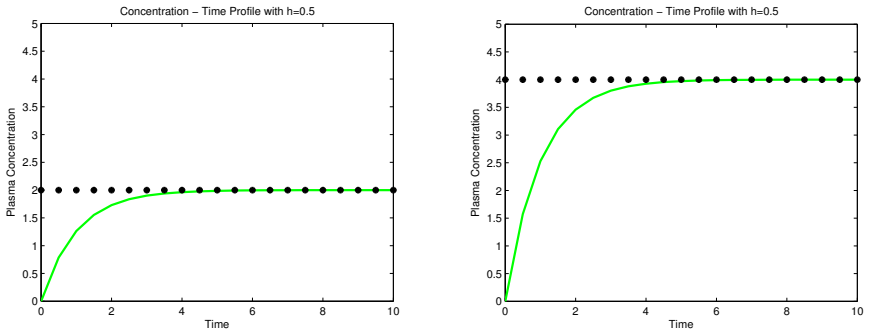

(a) (b)

FIGURE 3.6: *Trajectory representation of the one-compartment i.v infusion. A drug is given at a more rapid infusion rate, a higher steady state drug concentration is obtained. But the time to reach steady state is the same.*

condition $C(t_0) = C_0$ as follow

$$C(t) = \frac{R}{k_{el}} + C_0 e^{-k_{el}(t-t_0)} - \frac{R}{k_{el}} e^{-k_{el}(t-t_0)}. \tag{3.49}$$

Making the substitutions

$$\begin{cases} t_0 \to t_k = hk, \\ t \to t_{k+1} = h(k+1), \\ C_0 \to C_k, \\ C(t) \to C_{k+1}, \end{cases} \tag{3.50}$$

and with little algebraic manipulation, we have the 'exact' finite difference scheme

$$C_{k+1} - C_k = (\frac{R}{k_{el}} - C_k)(1 - e^{-k_{el}h}). \tag{3.51}$$

Equation (3.51) can be written in the form

$$\frac{C_{k+1} - C_k}{\frac{1-e^{-k_{el}h}}{k_{el}}} = R - k_{el}C_k. \tag{3.52}$$

Equation (3.52) is the 'exact' finite difference scheme of Equation (3.45) which is obtained in Mickens [86].

We proceed by constructing a SFD scheme for Equation (3.45) as a comparison with the 'exact' finite difference scheme given in Equation (3.52) as follows

$$\frac{C_{k+1} - C_k}{h} = R - k_{el}C_k, \tag{3.53}$$

where h is the step-size. Its corresponding difference equation will be

$$C_{k+1} = hR + C_k(1 - hk_{el}), \tag{3.54}$$

where Equation (3.54) is a first order nonhomogeneous difference equation. We can transform it into a first order homogeneous difference equation. To do this, we take

note of the steady state from Equation (3.54) and create a sequence Q_n. Firstly,

$$C = C(1 - hk_{el}) + hR, \tag{3.55}$$

$$C^* = \frac{R}{k_{el}}, \tag{3.56}$$

since $k_{el} > 0$. We create a new sequence, Q_n, so that:

$$Q_n = C_n - C^* \tag{3.57}$$

The difference equation that corresponds to Q_n will have a steady state at $Q^* = 0$ as required. Therefore,

$$Q_{n+1} = C_{n+1} - C^* = C_n(1 - hk_{el}) + hR - C^* \tag{3.58}$$

$$= (1 - hk_{el})(Q_n + C^*) + hR - C^* \tag{3.59}$$

$$= Q_n - Q_n hk_{el} - \frac{R}{k_{el}} hk_{el} + hR \tag{3.60}$$

$$= Q_n(1 - hk_{el}). \tag{3.61}$$

The closed form solution is:

$$Q_n = (1 - hk_{el})^n Q_0 \tag{3.62}$$

or

$$C_n - C^* = (1 - hk_{el})^n (C_0 - C_*) \tag{3.63}$$

$$C_n = (1 - hk_{el})^n (C_0 - C_*) + C^* \tag{3.64}$$

$$= (1 - hk_{el})^n (C_0 - \frac{R}{k_{el}}) + \frac{R}{k_{el}} \tag{3.65}$$

$$C_n = C_0(1 - hk_{el})^n + R\frac{1 - (1 - hk_{el})^n}{k_{el}}. \tag{3.66}$$

The solution, given by equation (3.66), gives the following results:

(i) if $0 < hk_{el} < 1$, C_k monotonically tends to $\frac{R}{k_{el}}$.

(ii) if $hk_{el} = 1$, $C_k = \frac{R}{k_{el}}$ for $k \geq 1$.

(iii) if $1 < hk_{el} < 2$, C_k tends to $\frac{R}{k_{el}}$ with an oscillating amplitude via an alternating sign at each step.

(iv) if $hk_{el} = 2$, C_k oscillates with a constant amplitude $\frac{2R}{k_{el}}$.

(v) if $hk_{el} > 2$, C_k oscillates with an increasing amplitude.

From these results, we conclude that this model will have numerical instabilities for all cases except for cases (i) and (ii). Cases (i) and (ii) have the same qualitative behaviour as the original differential equation. The NSFD scheme from Equation (3.52) in turn, gave accurate results for all the cases given above.

3.3.2 I.V. Bolus Infusion: Nonlinear Pharmacokinetic Model

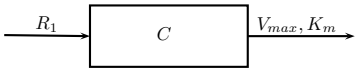

FIGURE 3.7: *Schematic representation of IV infusion with Michaelis-Menten elimination.*

If the drug is administered by constant infusion and is eliminated only by nonlinear pharmacokinetic, then the equation that describes the rate of change of the plasma concentration is given by

$$\frac{dC}{dt} = R - \frac{V_{max}C}{K_m + C} \qquad V_{max} > 0, \quad K_m > 0, \tag{3.67}$$

with initial condition

$$C(0) = 0.$$

All the parameters are identical to models (3.10) and (3.45). Solving Equation (3.67) using the concept of the Lambert function with the aid of Mathematica, we obtain

$$C(t) = \frac{-K_m V_{\max} W\left(-\frac{\exp(L(t)+M(t))}{K_m V_{\max}}\right) - RK_m}{R - V_{\max}}, \tag{3.68}$$

where

$$\begin{cases} L(t) = -\frac{R^2 t}{K_m V_{\max}} - \frac{R^2 Q}{K_m V_{\max}(R-V_{\max})^2} + \frac{2RQ}{K_m (R-V_{\max})^2}, \\ M(t) = -\frac{V_{\max} Q}{K_m (R-V_{\max})^2} - \frac{t V_{\max}}{K_m} + \frac{2Rt}{K_m} - \frac{R^2}{V_{\max}(R-V_{\max})} + \frac{R}{R-V_{\max}}. \\ Q = -K_m V_{\max} \log\left(RK_m e^{-\frac{R}{V_{\max}}}\right) - RK_m, \end{cases} \tag{3.69}$$

Equation (3.68) can be written in the form

$$\frac{C_{k+1} - C_k}{\phi_1(h)} = \frac{\frac{-K_m V_{\max} W\left(-\frac{\exp(L_1+M_1)}{K_m V_{\max}}\right) - RK_m}{R-V_{\max}} - C_k}{\phi_1(h)}. \tag{3.70}$$

where $L_1 = L(h)$ and $M_1 = M(h)$. The steady-state concentration of Equation (3.67) can be determined by the following equation:

$$C_{ss1} = \frac{K_m R}{V_{max} - R}. \tag{3.71}$$

The NSFD scheme for Equation (3.67) is structured as

$$\frac{C_{k+1} - C_k}{\phi_1(h)} = R - \frac{V_{max} C_{k+1}}{K_m + C_k}, \tag{3.72}$$

where $\phi_1(h)$ is obtained as before and defined as Equation (3.23). Compared Equation (3.72) with the SFD scheme, such as

$$\frac{C_{k+1} - C_k}{h} = R - \frac{V_{max} C_k}{K_m + C_k}, \tag{3.73}$$

clearly shows that the NSFD scheme is dynamically consistent with the original differential equation for any step size. Figure 3.17 presents numerical solutions of equation (3.73). We observed for all the steps-sizes, the numerical functions have similar qualitative behaviour as the corresponding solution of the differential equation (3.67). A geometrical analysis of equation (3.72) shows that C_k converges to the fixed point C_{ss1}.

3.3.3 I.V. Bolus Infusion: Linear and Nonlinear Pharmacokinetic Model

If the drug is eliminated by parallel pathways consisting of both linear and nonlinear pharmacokinetic Equation (3.67) may be extended to Equation (3.74)

$$\frac{dC}{dt} = R - k_{el}C - \frac{V_{max}C}{K_m + C} \quad C(t=0) = 0, \tag{3.74}$$

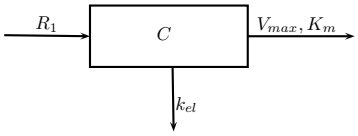

FIGURE 3.8: *Scheme of IV infusion with both linear and Michealis-Menten elimination.*

All the parameters are identical to models in Equation (3.10) and (3.45). The biologicsl relevant steady-state concentration of Equation (3.74) can be determined by the following equation:

$$C_{ss2} = \frac{(R - k_{el}K_m - V_{max}) + \sqrt{(R - k_{el}K_m - V_{max})^2 + 4Rk_{el}K_m}}{2k_{el}}. \tag{3.75}$$

The NSFD scheme of (3.74) is given as

$$\frac{C_{k+1} - C_k}{\phi_3(h)} = R - k_{el}C_{k+1} - \frac{V_{max}C_{k+1}}{K_m + C_k}, \tag{3.76}$$

re-arranging equation (3.76), we have

$$C_{k+1} = \frac{K_mC_k + C_k^2 + \phi_3(h)RK_m + \phi_3(h)RC_k}{K_m + C_k + \phi_3(h)K_mk_{el} + \phi_3(h)k_{el}C_k + \phi_3(h)V_{max}} \tag{3.77}$$

where $\phi_3(h)$ is given in Equation (3.43). The SFD scheme of equation is given as

$$\frac{C_{k+1} - C_k}{h} = R - k_{el}C_k - \frac{V_{max}C_k}{K_m + C_k}. \tag{3.78}$$

Therefore, scheme (3.77) preserved two main properties:

1. The positivity condition.

2. The existence of the equilibrium state given by equation (3.75).

3.4 One-compartment: Extravascular Administration

A drug given via the extravascular route of administration undergoes the process of absorption before it gets to the systemic circulation. This type of drug delivery is complicated by the variable at the site of absorption. The absorption of a drug from the gastrointestinal tract (GIT) depends on the following: anatomy and physiology of the absorption site, physiochemical properties of the drug, and physiochemical properties of the dosage form. Initially, the entire drug is in the site of absorption and none has yet reached the systemic circulation. Most drugs administered extravascularly act systemically. In such cases, systemic absorption is a prerequisite for efficacy. This section describes the extravascular route of administration. We consider this mode of administration via two different elimination processes: 1) drugs given by extravascular administration, distributed as a one-compartment model, eliminated only by linear pharmacokinetic, 2) drugs given by extravascular administration, distributed as a one-compartment model, eliminated by both linear and nonlinear processes.

3.4.1 Extravascular Administration: Linear Pharmacokinetic Model

When a drug is administered through extravascular administration and eliminated by a linear process the situation is describe by Equations (3.79) and (3.80). Equation (3.79) describes the drug at the site of absorption before it reaches the systemic

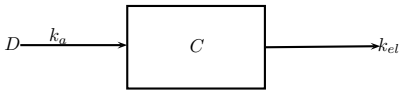

FIGURE 3.9: *One-compartment pharmacokinetic model for first-order drug absorption and first-order elimination.*

circulation while Equation (3.80) describes the concentration of the drug at the systemic circulation. D is the amount of drug in the GIT at any time t, k_a is the first-order absorption rate constant, C is the plasma concentration of the drug in the body, V_1 is the apparent volume of distribution and k_{el} is the elimination rate. Therefore, the disappearance rate of the drug from the GIT is given by (equation for drug in GIT),

$$\frac{dD}{dt} = -k_a D, \qquad D(0) = D_0. \tag{3.79}$$

Rate of change of the concentration of the drug is given as

$$\frac{dC}{dt} = k_a D/V_1 - k_{el}C, \qquad C(0) = 0, \tag{3.80}$$

where C is the concentration of the drug available at the absorption site. The equation below describes the time course of the plasma concentration of the drug that follows the oral route of administration.

$$C(t) = \frac{k_a D_0}{V_1(k_a - k_{el})}\left(e^{-k_{el}t} - e^{-k_a t}\right), \qquad k_a \neq k_{el}, \tag{3.81}$$

where D_0 is the dose of the administered drug, k_a is the constant of the absorption, and k_{el} is the rate of elimination. At $t = \infty$ (at later time intervals) the above equation reduces to (i.e when $e^{-k_a t} \approx 0$)

$$C(t) = \frac{k_a D_0}{V_1(k_a - k_{el})}e^{-k_{el}t}. \tag{3.82}$$

The 'exact' finite-difference scheme of the model is derived from the analytical solution. Since Equations (3.79) and (3.80) can be solved simultaneously we proceed

as follows [87]:

$$\begin{cases} \frac{dD}{dt} = -k_a D \\ \\ \frac{dC}{dt} = k_a D - k_{el} C, \end{cases} \tag{3.83}$$

with initial conditions

$$D_0 = D(t_0), \qquad C_0 = C(t_0). \tag{3.84}$$

The particular solution of Equation (3.83) is

$$D = 0, \qquad C = 0. \tag{3.85}$$

Considering the system of equation in (3.83), we have the corresponding matrix

$$M = \begin{pmatrix} -k_a & 0 \\ k_a & -k_{el} \end{pmatrix}.$$

The matrix has eigenvalues λ that are the solution of $det(M - \lambda I) = 0$ or $\lambda^2 - tra(M)\lambda + det(M) = 0$. Therefore we have the eigenvalue equation to be

$$\lambda^2 + (k_a + k_{el})\lambda + k_a k_{el} = 0, \tag{3.86}$$

which provide the eigenvalues

$$\lambda_1 = -k_a, \qquad \lambda_2 = -k_{el}. \tag{3.87}$$

Suppose $v = \begin{pmatrix} v_1 \\ v_2 \end{pmatrix}$ is the eigenvector corresponding to a generic eigenvalue λ, then $(M - \lambda I)v = 0$. Hence we have that

$$\begin{pmatrix} -k_a - \lambda_{1,2} & 0 \\ k_a & -k_{el} - \lambda_{1,2} \end{pmatrix} \begin{pmatrix} v_1 \\ v_2 \end{pmatrix} = \begin{pmatrix} 0 \\ 0 \end{pmatrix},$$

which gives

$$\begin{cases} (-k_a - \lambda_{1,2})v_1 = 0 \\ \\ k_a v_1 + (-k_{el} - \lambda_{1,2})v_2 = 0. \end{cases} \tag{3.88}$$

Thus,

$$v = \begin{pmatrix} v_1 \\ v_2 \end{pmatrix} = \begin{pmatrix} \frac{k_{el}+\lambda_{1,2}}{k_a} \\ 1 \end{pmatrix},$$

giving the general solution of the system as

$$D(t) = A\left(\frac{k_{el}+\lambda_1}{k_a}\right)e^{\lambda_1 t} + B\left(\frac{k_{el}+\lambda_2}{k_a}\right)e^{\lambda_2 t} \tag{3.89}$$

$$C(t) = Ae^{\lambda_1 t} + Be^{\lambda_2 t}. \tag{3.90}$$

To calculate A and B, we use the initial values given in Equation (3.84) and Equation (3.90) becomes

$$C(t_0) = Ae^{\lambda_1 t_0} + Be^{\lambda_2 t_0} = C_0, \tag{3.91}$$

$$A = C_0 e^{-\lambda_1 t_0} - Be^{t_0(\lambda_2 - \lambda_1)}. \tag{3.92}$$

From Equation (3.89) we have that

$$D(t_0) = A\left(\frac{k_{el}+\lambda_1}{k_a}\right)e^{\lambda_1 t_0} + B\left(\frac{k_{el}+\lambda_2}{k_a}\right)e^{\lambda_2 t_0} = D_0. \tag{3.93}$$

Substituting Equation (3.92) into Equation (3.93) and with little algebraic manipulation we have

$$B = \left(\frac{k_a}{\lambda_2 - \lambda_1}\right)D_0 e^{-\lambda_2 t_0} - \left(\frac{k_{el}+\lambda_1}{\lambda_2 - \lambda_1}\right)C_0 e^{-\lambda_2 t_0}. \tag{3.94}$$

Substituting Equation (3.94) into (3.92) we have

$$A = C_0 e^{-\lambda_1 t_0} - \left(\frac{k_a}{\lambda_2 - \lambda_1}\right)D_0 e^{-\lambda_1 t_0} + \left(\frac{k_{el}+\lambda_1}{\lambda_2 - \lambda_1}\right)C_0 e^{-\lambda_1 t_0}. \tag{3.95}$$

Substituting Equations (3.94) and (3.95) into Equation (3.90) with some manipulation we have

$$C(t) = -\left(\frac{k_a}{\lambda_2 - \lambda_1}\right)\left[\left(D_0 - \frac{k_{el} + \lambda_2}{k_a}C_0\right)e^{\lambda_1(t-t_0)}\right] + \left(\frac{k_a}{\lambda_2 - \lambda_1}\right)\left[\left(D_0 - \frac{\lambda_1 + k_{el}}{k_a}C_0\right)e^{\lambda_2(t-t_0)}\right]. \tag{3.96}$$

The 'exact' finite-difference scheme of Equation (3.83) is obtained by making the following transformation in Equation (3.96)

$$\begin{cases} t_0 \to t_k = hk, \\ t \to t_{k+1} = h(k+1), \\ D_0 \to D_k, \\ D(t) \to D_{k+1}, \\ C_0 \to C_k, \\ C(t) \to C_{k+1}, \end{cases} \tag{3.97}$$

$$C_{k+1} = -\left(\frac{k_a}{\lambda_2 - \lambda_1}\right)\left[\left(D_k - \frac{\lambda_2 + k_{el}}{k_a}C_k\right)e^{\lambda_1 h}\right] + \left(\frac{k_a}{\lambda_2 - \lambda_1}\right)\left[\left(D_k - \frac{\lambda_1 + k_{el}}{k_a}C_k\right)e^{\lambda_2 h}\right], \tag{3.98}$$

from there, we have

$$C_{k+1} - C_k\left(\frac{\lambda_2 e^{\lambda_1 h} - \lambda_1 e^{\lambda_2 h}}{\lambda_2 - \lambda_1}\right) = (k_a D_k - k_{el}C_k)\left(\frac{e^{\lambda_2 h} - e^{\lambda_1 h}}{\lambda_2 - \lambda_1}\right), \tag{3.99}$$

giving the 'exact' finite-difference scheme as

$$\begin{cases} \dfrac{D_{k+1} - \varphi D_k}{\phi} = -k_a D_k \\ \dfrac{C_{k+1} - \varphi C_k}{\phi} = k_a D_k - k_{el}C_k, \end{cases} \tag{3.100}$$

where

$$\varphi = \frac{k_a e^{-k_{el}h} - k_{el} e^{-k_a h}}{k_a - k_{el}}, \qquad \phi = \frac{e^{-k_{el}h} - e^{-k_a h}}{k_a - k_{el}}. \tag{3.101}$$

The 'exact' finite difference result obtained in (3.100) will be compared with the SFD scheme

$$\begin{cases} \dfrac{D_{k+1} - D_k}{h} = -k_a D_k \\ \dfrac{C_{k+1} - C_k}{h} = k_a D_k - k_{el} C_k. \end{cases} \tag{3.102}$$

3.4.2 One-compartment: Extravascular Administration and I.V. Infusion

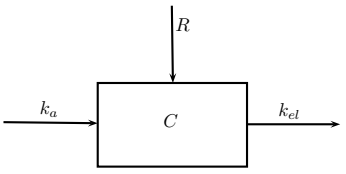

FIGURE 3.10: *Scheme of both extravascular and I.V infusion administrations.*

Suppose that, as the drug is been administered by extravascular mode of administration the drug is also administered by I.V. infusion at a rate R. Then the concentration of drug in the body is given as

$$\begin{cases} \dfrac{dD}{dt} = -k_a D \\ \dfrac{dC}{dt} = k_a D - k_{el} C + R. \end{cases} \tag{3.103}$$

The 'exact' finite-difference scheme of (3.103) can be obtained from the analytical solution of (3.103). Using the same concept we used from Equation (3.84) - (3.88) except that the particular solution for Equation (3.103) is given as

$$D = 0, \qquad C = \frac{R}{k_{el}}, \tag{3.104}$$

and the general solution becomes

$$D(t) = A\left(\frac{k_{el}+\lambda_1}{k_a}\right)e^{\lambda_1 t} + B\left(\frac{k_{el}+\lambda_2}{k_a}\right)e^{\lambda_2 t} \tag{3.105}$$

$$C(t) = \frac{R}{k_{el}} + Ae^{\lambda_1 t} + Be^{\lambda_2 t}. \tag{3.106}$$

Applying similar step we follow from (3.91) - (3.99) to Equations (3.105) and (3.106) we get 'exact' finite difference scheme (3.103) to be

$$\begin{cases} \dfrac{D_{k+1}-\varphi D_k}{\phi} = -k_a D_k \\ \dfrac{C_{k+1}-\varphi C_k}{\phi} = k_a D_k - k_{el}C_k + \frac{\theta}{\phi}R, \end{cases} \tag{3.107}$$

where,

$$\frac{\theta}{\phi}(h) = 1 + \mathcal{O}(h). \tag{3.108}$$

φ and ϕ are given as (3.101) and θ is given below

$$\theta = \frac{(\lambda_2-\lambda_1) - (\lambda_2+k_{el})e^{\lambda_1 h} + (\lambda_1+k_{el})e^{\lambda_2 h}}{k_{el}(\lambda_2-\lambda_1)^2}. \tag{3.109}$$

The NSFD scheme of equation (3.107) is dynamically consistent with equation (3.103). Also, the scheme is exact finite difference representation of equation (3.103).

3.4.3 Extravascular Administration: Linear and Nonlinear Pharmacokinetic Model

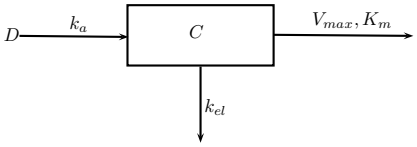

FIGURE 3.11: *Scheme of extravascular administration with both linear and Michealis-Menten elimination.*

In a situation when the drug is administered by the extravascular mode of administration and the drug is eliminated by parallel pathways consisting of both linear and nonlinear pharmacokinetic, Equation (3.110) is employed. Consider:

$$\begin{cases} \dfrac{dD}{dt} = -k_a D \\ \dfrac{dC}{dt} = k_a D - k_{el} C - \frac{V_{max} C}{K_m + C}, \end{cases} \tag{3.110}$$

with initial conditions $D_0 = D(t_0)$ and $C_0 = C(t_0)$. The NSFD scheme of Equation (3.110) is given as

$$\begin{cases} \dfrac{D_{k+1} - \varphi D_k}{\phi} = -k_a D_k \\ \dfrac{C_{k+1} - \varphi C_k}{\phi} = k_a D_k - k_{el} C_k - \frac{V_{max} C_k}{K_m + C_k}, \end{cases} \tag{3.111}$$

and it compare with SFD of the form

$$\begin{cases} \dfrac{D_{k+1} - D_k}{h} = -k_a D_k \\ \dfrac{C_{k+1} - C_k}{h} = k_a D_k - k_{el} C_k - \frac{V_{max} C_k}{K_m + C_k}. \end{cases} \tag{3.112}$$

Note that apart from equation (3.111), there are many possible NSFD schemes for extravascular administration: linear and nonlinear pharmacokinetic model (3.110).

3.5 Models Simulation

In this study one-compartment models (I.V. bolus injection, I.V. bolus infusion and extravascular) are considered for simulations. The methods compared are the SFD methods, and the in-built function `ODE45` in MATLAB, with the focus of the study being the NSFD method. In order to perform a useful comparison, these methods were tested under similar conditions corresponding to the intended practical application. The purpose of the tests will be to compare accuracy and stability. All the simulations were performed by using MATLAB and Mathematica. The numerical results are presented. Using the above, we proceed with the

examination of accuracy. For varying step-sizes employing the methods described, we examine the figures and the numerical results. We carry out the numerical calculations in MATHEMATICA, and the results are then processed in MATLAB to generate visual representations.

3.5.1 I.V. Bolus Injection: Simulation

3.5.1.1 I.V. Bolus Injection: Linear Pharmacokinetic Results

The plots in Figure 3.12 describe scheme (3.5) in comparison with Equation (3.6) by drawing them on the phase line. The phase plots were provided for each solution yielded by Equation (3.8). It is clearly seen from the figures that the 'exact' finite-difference scheme behaves exactly like the analytical solution while the solutions obtained using explicit Euler method is only consistent for $hk_{el} < 1$. Furthermore, ODE45 and exact finite difference scheme coincide in the nodes of the exact finite difference grid, but ODE45 solution requires possibly a larger amount of time steps. 'Exact' finite-difference scheme produced the same results as the one obtained with the analytical solution.

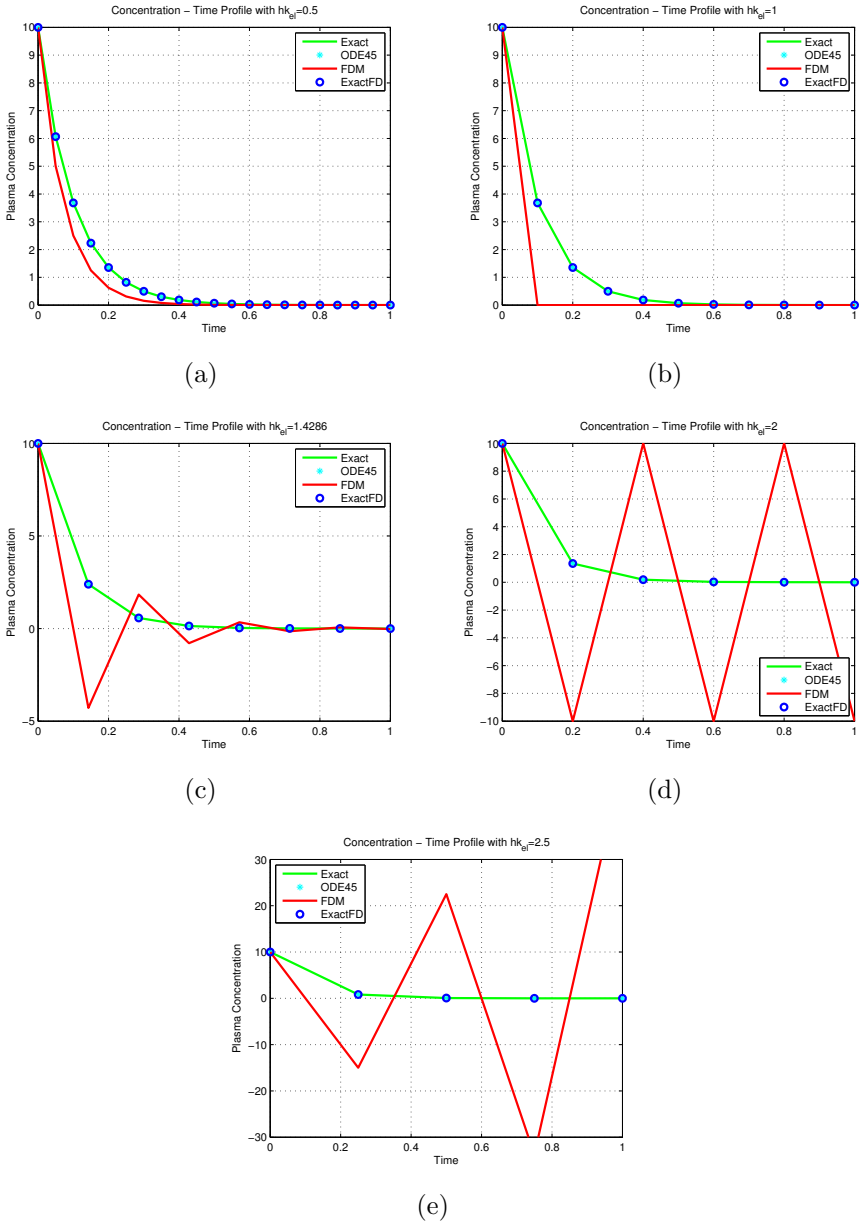

FIGURE 3.12: Plots showing the results obtained for time course of the plasma concentration of a drug after bolus injection from different algorithms for different steps size. We can see from all the plots that the 'exact' finite-difference scheme gives accurate result for all the step-sizes.

In Table 3.2, we present the results obtained after solving the I.V. bolus injection linear pharmacokinetic model with integration time step $h = 0.1$. We compare results of different methods with the analytical solution over a long period of time. We note that the 'exact' finite difference scheme obtained gives the same results as the analytical solution.

TABLE 3.2: The numerical results for IV bolus model (3.1).

Numerical Results					
t	**Euler**	**Heun**	**Runge-Kutta**	**NSFD**	**Exact**
0.0	2.00000	2.00000	2.00000	2.00000	2.00000
0.1	1.63746	1.64000	1.63747	1.63746	1.63746
0.2	1.28000	1.34480	1.34065	1.34064	1.34064
0.3	1.02400	1.10274	1.09763	1.09762	1.09762
0.4	0.83838	0.90424	0.89867	0.89866	0.89866
0.5	0.68641	0.74148	0.73577	0.73576	0.73576
0.6	0.52429	0.60801	0.60240	0.60239	0.60239
0.7	0.41943	0.49857	0.49320	0.49319	0.49319
0.8	0.33554	0.40883	0.40380	0.40379	0.40379
0.9	0.26844	0.33524	0.33061	0.33060	0.33060
1.0	0.21475	0.27490	0.27068	0.27067	0.27067

3.5.1.2 I.V. Bolus Injection: Nonlinear Pharmacokinetic Results

We present the results of the case when the drug is administered by I.V. bolus injection and eliminated by Michaelis-Menten elimination. NSFD schemes in Equations (3.24), (3.26), (3.34) and SFD scheme in Equation (3.17) are compared with exact scheme in Equation (3.35) obtained through the use of Lambert function as shown in Figure 3.13. For all these schemes, SFD schemes can produce negative solutions when the step size is increase above some threshold. This is not possible with NSFD schemes for any value of the step size.

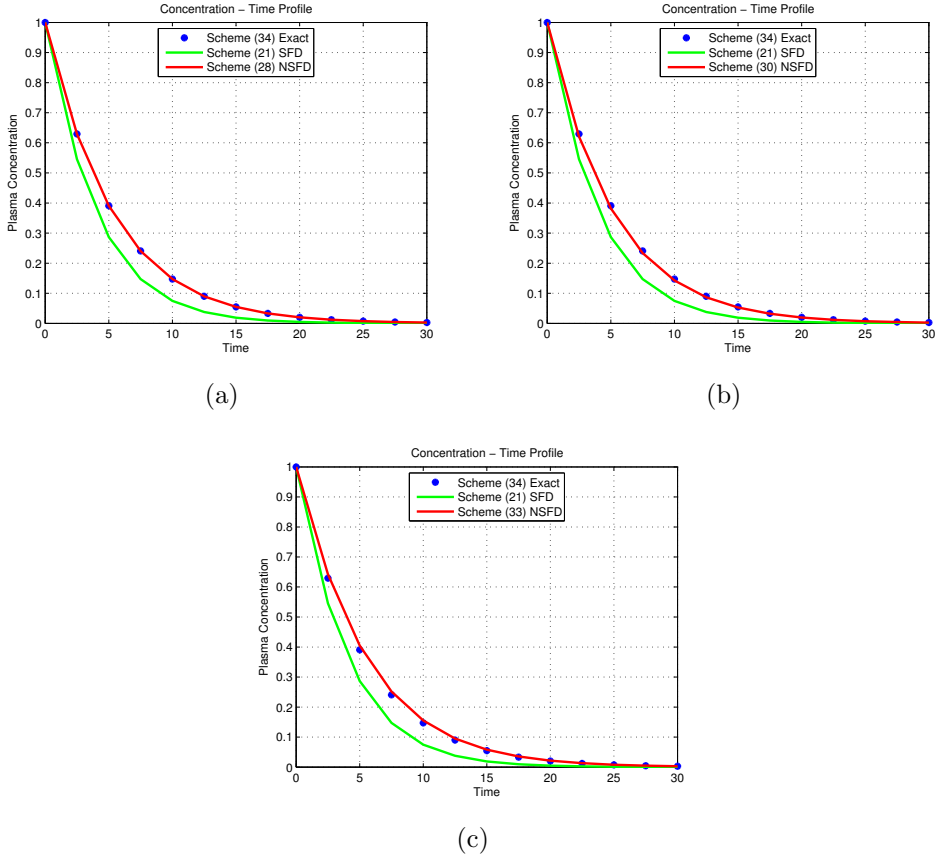

FIGURE 3.13: *NSFD schemes (3.24), (3.26) and (3.34) respectively plotted against the exact scheme (3.35) and SFD scheme (3.17).*

3.5.1.3 I.V Bolus Injection: Linear and Nonlinear Pharmacokinetic Results

Simulations of the equation that describe a drug that is eliminated by both first order and Michaelis - Menten kinetics after I.V. bolus injection are provided. Figure 3.14 shows the comparison of SFD scheme in Equation (3.38) and NSFD scheme in Equation (3.44) with MATLAB built-in function ODE45. For any step size, NSFD method performed better than the SFD method.

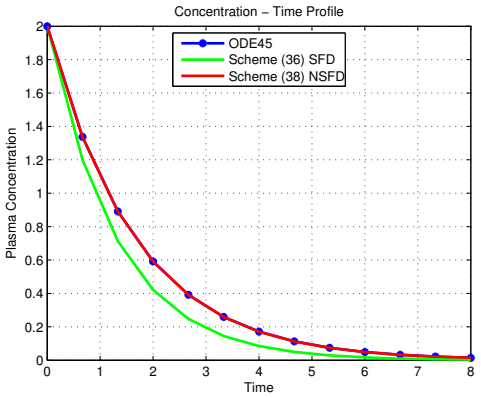

FIGURE 3.14: *Trajectory representation of the one-compartment i.v bolus injection model that follow both linear and nonlinear elimination.*

3.5.2 I.V. Bolus Infusion: Simulation

3.5.2.1 I.V. Bolus Infusion: Linear Pharmacokinetic Results

Similarly with the I.V. bolus infusion model, we present the 'exact' finite difference scheme, Equation (3.52), in comparison with SFD scheme, Equation (3.53). The figures represents the plasma concentration-time profile for a drug that follow IV infusion. At time zero ($t = 0$), no drug was present in the body. Then, the drug level gradually increases until the steady state is reached. Once the drug has reached the steady-state, the elimination rate of the drug equals the infusion rate. We expect any algorithm used for this model to capture this phenomenon. Thus it is observed from the figures that regardless of the step-size the 'exact' finite-difference scheme is consistent and accurate but numerical instabilities occurs for $hk_{el} \geq 1$ in the case of SFD scheme. Though the MATLAB built in function ODE45 gives results that are consistent and accurate, the 'exact' finite difference scheme returns a more accurate result (see Table 3.3). Also, ODE45 performs adaptive time-step algorithm and is likely to be computationally more expensive than the NSFD algorithm.

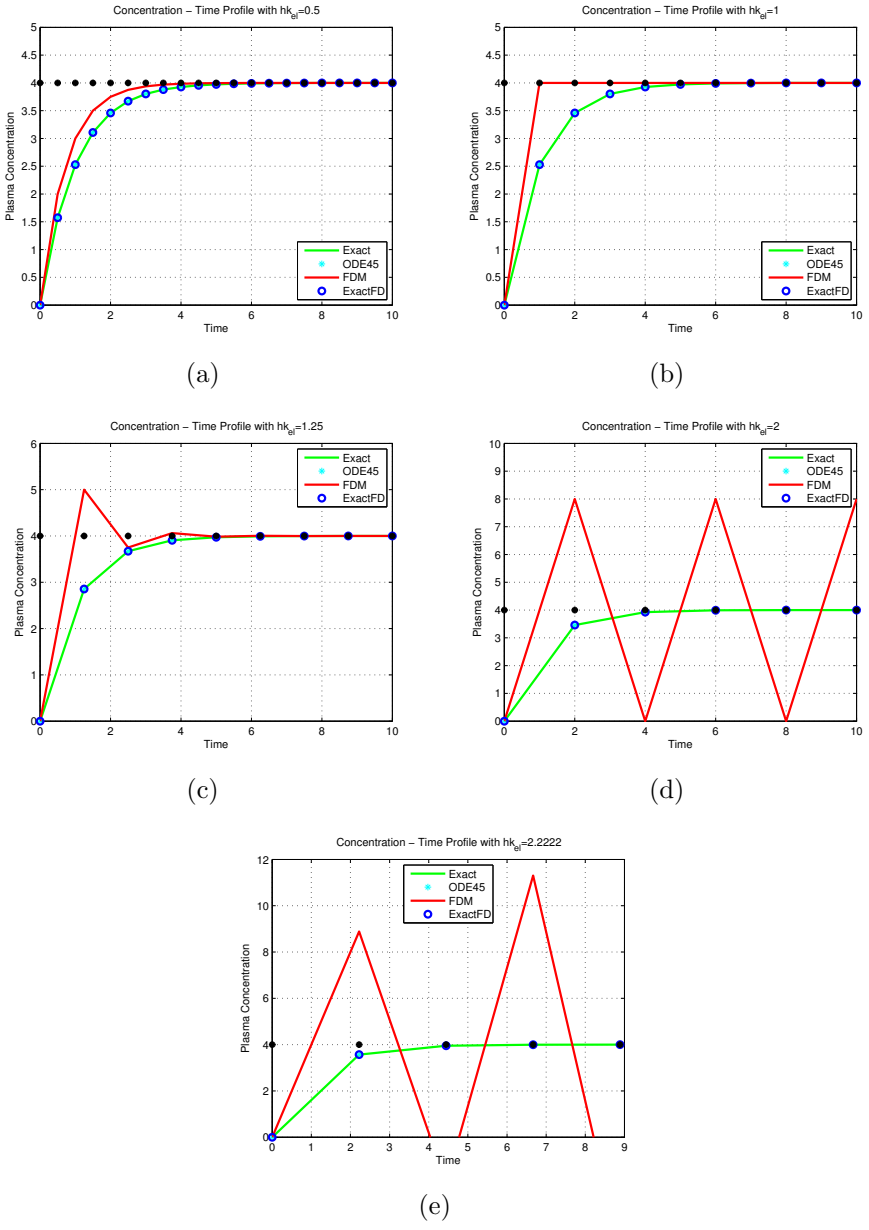

FIGURE 3.15: Plots showing the results obtained from different algorithms for different steps size. We can see from all the plots that the 'exact' finite-difference scheme gives accurate result for all the step-sizes.

Table 3.3 shows the results obtained with different numerical methods when we considered I.V bolus infusion linear pharmacokinetic model.

TABLE 3.3: The numerical results for the I.V. bolus infusion model (3.45).

Numerical Results					
t	**Euler**	**Heun**	**Runge-Kutta**	**Exact FD**	**Exact**
0.0	0.00000	0.00000	0.00000	0.00000	0.00000
0.1	0.18127	0.18000	0.18127	0.18127	0.18127
0.2	0.36000	0.32760	0.32968	0.32968	0.32968
0.3	0.48800	0.44863	0.45118	0.45119	0.45119
0.4	0.58081	0.54788	0.55067	0.55067	0.55067
0.5	0.65680	0.62926	0.63211	0.63212	0.63212
0.6	0.73786	0.69599	0.69880	0.69881	0.69881
0.7	0.79028	0.75071	0.75340	0.75340	0.75340
0.8	0.83223	0.79559	0.79810	0.79810	0.79810
0.9	0.86578	0.83238	0.83470	0.83470	0.83470
1.0	0.89263	0.86255	0.86466	0.86466	0.86466

3.5.2.2 I.V. Bolus Infusion: Nonlinear Pharmacokinetic Results

The results of the case when the drug is administered by I.V, bolus infusion and eliminated by Michaelis-Menten elimination is presented. NSFD scheme (3.72) and SFD scheme (3.73) are compared with ODE45. From Figure 3.16 we could see that regardless of what the step-size is, the NSFD scheme (3.72) converges to the steady state.

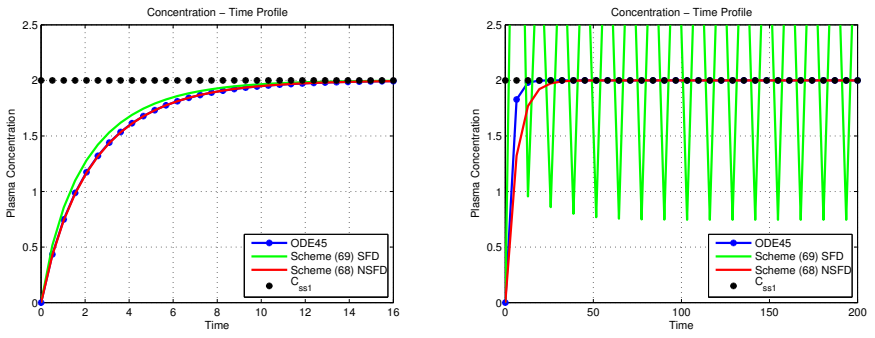

(a) (b)

FIGURE 3.16: *The concentration of the drug when (a)* $h = 0.51613$ *(b)* $h = 6.4516$.

Table 3.4 gives the simulation of the I.V. bolus infusion that follow nonlinear pharmacokinetic.

TABLE 3.4: The absolute error results of Equations (3.67) for C with parameters values $R = 0.5$, $K_m = 4$, and $V_{max} = 2$.

Absolute Error for $C(t)$			
N	**h**	**Error in Scheme 3.73 (SFD)**	**Error in Scheme 3.72 (NSFD)**
2	4.000	1.027	0.108
4	2.000	0.338	0.030
8	1.000	0.115	0.007
16	0.500	0.051	0.002
32	0.250	0.024	0.000
64	0.125	0.012	0.000
128	0.062	0.006	0.000
256	0.031	0.003	0.000
512	0.016	0.001	0.000
1024	0.008	0.001	0.000

3.5.2.3 I.V. Bolus Infusion: Linear and Nonlinear Pharmacokinetic

Figure 3.17 shows the simulation results of the NSFD scheme (3.76) and SFD scheme (3.78) in comparison with ODE45 in Matlab.

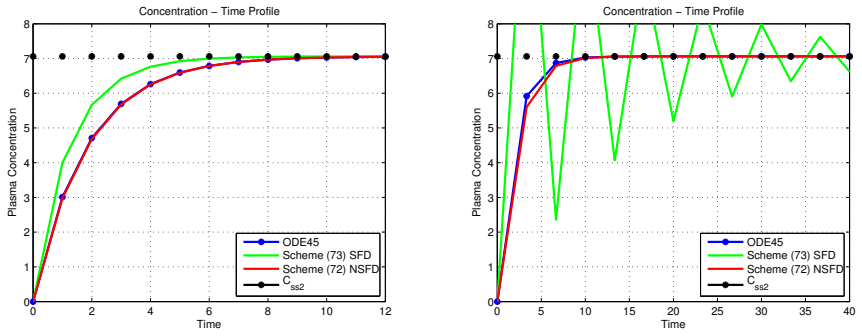

(a) (b)

FIGURE 3.17: *The concentration of the drug where (a)* $h = 0.75$ *(b)* $h = 3.3333$.

3.5.3 Extravascular Administration:Simulation

3.5.3.1 Extravascular Administration: Linear Pharmacokinetic Results

Results of the one compartment pharmacokinetic model administered by an extravascular mode of administration and following linear elimination. The C in NSFD scheme (3.100), SFD scheme (3.102), ODE45 and are compared with exact solution (3.81) as shown in Figure 3.18. The schemes obtained from the model using different methods are tested under similar conditions. Simulations are provided for $h = 0.5$ and $h = 1$. The NSFD scheme (3.100) produce the same result as exact solution (3.81). Also, Figure 3.19 shows that NSFD scheme of equations (3.79-3.80) correctly mimic the analytical solution of the system even when plotted in 3D.

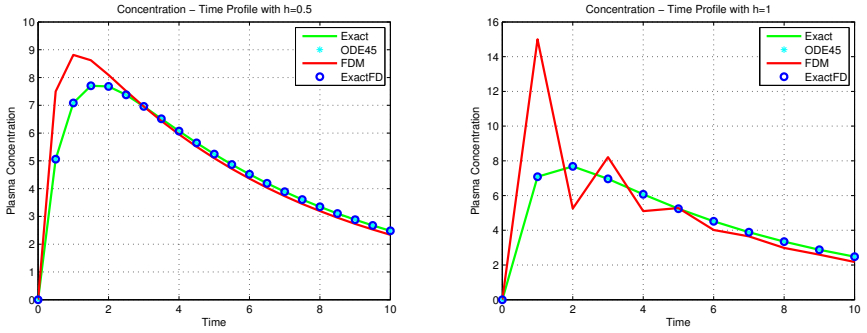

(a) (b)

FIGURE 3.18: *Plasma concentration (C)-time curve for a drug given ins a single oral dose.*

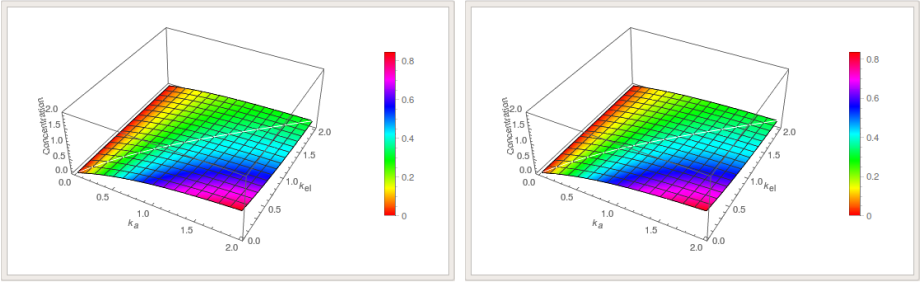

(a) (b)

FIGURE 3.19: *3D plot of extravascular administration model (system of Equation 3.79-3.80). (a) The plot is obtained with the analytical method. (b) The plot is obtained with NSFD method. The solution obtained with NSFD method match the analytic solution very well.*

Table 3.5 shows numerical results for the 'exact finite-difference scheme for extravascular administration model in comparison with standard methods (Euler, Heun and Runge-Kutta) and the analytical solution for plasma concentration C. It easy to see that the numerical results for the 'exact' finite difference scheme is the same for any value of t as the analytical solution.

TABLE 3.5: The numerical results for the extravascular administration model.

Numerical Results					
t	**Euler**	**Heun**	**Runge-Kutta**	**Exact FD**	**Exact**
0.0	0.00000	0.00000	0.00000	0.00000	0.00000
0.1	0.15000	0.13763	0.13823	0.13823	0.13823
0.2	0.27525	0.25411	0.25514	0.25514	0.25514
0.3	0.37950	0.35241	0.35374	0.35374	0.35374
0.4	0.46592	0.43508	0.43661	0.43661	0.43661
0.5	0.53723	0.50432	0.50597	0.50597	0.50597
0.6	0.59573	0.56203	0.56373	0.56374	0.56374
0.7	0.64337	0.60983	0.61154	0.61154	0.61154
0.8	0.68180	0.64912	0.65080	0.65081	0.65081
0.9	0.71245	0.68112	0.68275	0.68275	0.68275
1.0	0.73651	0.70686	0.70842	0.70842	0.70842

3.5.3.2 Extravascular Administration: Linear and Nonlinear Pharmacokinetic Results

Figure 3.20 shows the simulated plasma concentration C for extravascular administration that follows linear and nonlinear pharmacokinetic processes.

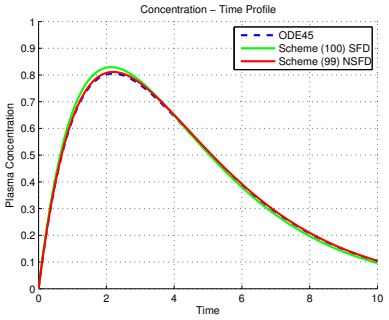

FIGURE 3.20: *Comparison of methods for one-compartment extravascular administration that follow both linear and nonlinear elimination.*

3.5.4 General Comparison

Figure 3.21 is the comparison of the models with linear elimination, and linear and nonlinear elimination for different routes of administration. As we observe from the Figure 3.21a -3.21c the models that comprise both linear and nonlinear elimination excreted drug faster that the model with only linear elimination in all the mode of drug administration (I.V. injection, I.V. infusion and extravascular administration) considered in this thesis. In reality, this phenomenon is expected. Administration of different doses of drugs with nonlinear pharmacokinetic may not result in parallel plasma concentration versus time profiles expected for drugs with linear pharmacokinetic.

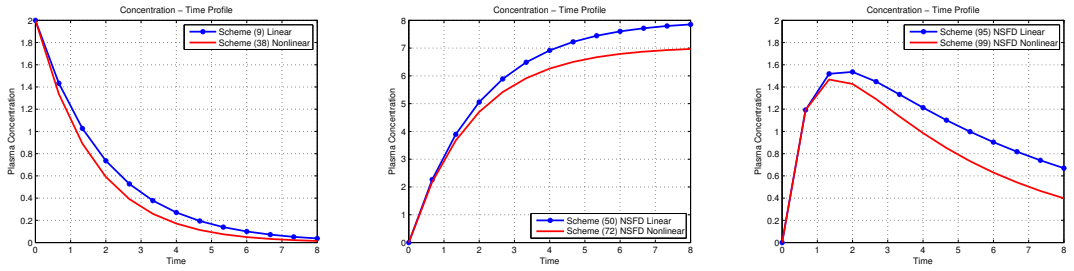

(a) I.V. injection (b) I.V. infusion (c) Extravascular administration

FIGURE 3.21: *In figure a-c we gives the comparison between the NSFD scheme for drug follow linear elimination and nonlinear eliminiation.*

3.6 Conclusion

In this chapter, we have presented a one compartment pharmacokinetic models with different routes of administration. In each of the models, we presented the efficiency of the NSFD method in comparison to standard methods. From the results obtained we observe that the stability of the NSFD scheme is independent of the chosen step-sizes and the step-sizes can be chosen as one wishes. This is not the case with standard methods such as Euler and Heun methods. Under such circumstances step-sizes must be chosen in a reasonable domain otherwise numerical instabilities will occur. The numerical simulations verify that NSFD schemes are

efficient and accurate. The major payoff is that we are able to generate numerical schemes that are dynamically consistent with respect to positivity, fixed-points and their stability properties. Furthermore, monotonicity properties of some of the schemes were preserved.

Chapter 4

Nonstandard Finite Difference Method Applied to a Linear Pharmacokinetics Model

"The enchanting charms of this sublime science reveal only to those who have the courage to go deeply into it."

Carl Friedrich Gauss

The work in this chapter appeared in:

Oluwaseun Egbelowo, Charis Harley and Byron Jacobs. Nonstandard Finite Difference Method Applied to a Linear Pharmacokinetics Model. Bioengineering. 2017; 4(2):40.

4.1 Introduction

The main purpose of this chapter is the application of NSFD method to two-pharmacokinetic models. Pharmacokinetic modeling is the mathematical representation of the behaviour of a drug in the body or an area of the body created to

describe the pharmacologic or physiologic kinetics characteristics[1]. These models can assist in simulating the biological processes involved in the kinetic behaviour of a drug after it has been introduced into the body, leading to a better understanding of its dynamic effects. Mathematical modeling is currently a common tool in the study of physiological and biochemical systems. It can be developed from non-compartmental representations to large scale multi- compartment models. In the case of compartment models, mass-balance equations are used to represent each compartment. A compartment is defined as a group of tissues with similar blood flow and drug affinity. This is used to model the transport processes between interconnected volumes, such as the movement of drugs and hormones in the human body. Compartment models assume that there is rapid and perfect mixing so that the drug concentration remain the same in each compartment. The complex transport processes are approximated by assuming that the flow rates between the compartments are proportional to the concentration difference in the compartments.

One of the early uses of compartment models was reported by Widmark [88]. He used a compartment model to develop a mathematical model that describes the propagation of alcohol in the body. Compartment models have proved to be a great advantage when screening drugs used by humans at any instant in time. The number of compartments in the model depends on the rate of drug distribution to different parts of the body. Studies most frequently use one- or two-compartment models. When the drug is eliminated, the drug concentration in the systemic circulation and in all tissues decline at the same rate because of the rapid distribution equilibrium. Drugs that follow this behavior follow the one-compartment pharmacokinetic model, while in two-compartment models the movement of the administered drug is distributed instantaneously to some tissues and slowly to other tissues. In this case a two-compartment pharmacokinetic model can be used to describe the pharmacokinetic behaviour of the drug. However, if the distribution of the drug happened at three different rates a three-compartment model would be applicable.

[1]Pharmacokinetics is the study of the basic processes that determine the duration and intensity of a drug effect within an organism.

This chapter is aimed at the well-known two-compartment model. We have chosen to consider the two-compartment model in this study, given that the one-compartment model assumes immediate distribution of the drug and attainment of equilibrium throughout the body. Realistically however, very few drugs display these characteristics, and hence we turn to a two-compartment model for consideration. While still a simplification of the actual physics of the problem, it is a well-justified model as commented on above. This model is capable of providing data on rates in and out of specific organs, which is of interest. The work conducted here is done with the aim of introducing a numerical method which may be employed in future research for the solution of models which are non-linear and describe multiple compartments. As such, we propose and illustrate the use of a numerical method of solution, namely the nonstandard finite difference method (NSFD), capable of efficiently obtaining solutions which are not only accurate but maintain the underlying dynamics of the system of equations. This choice of method impacts on whether we are able to consider non-compartment models; the NSFD is not amenable to the simulation of non-compartment models as it provides a meta-analysis of the inter-compartment dynamics, whereas non-compartment models are unable to describe these meta-dynamics and instead conduct parameter estimation of the entire system as a whole through the use of experimental data. The advantage of the NSFD method is the ability to predict the concentration–time profile of a drug when there are alterations in the dosing regimen—this would not be possible were one to consider non-compartment analysis. Another advantage of the NSFD method is that it preserves significant properties of the analogous models and consequently gives reliable numerical results even when analytical solutions are not possible. The standard approaches to multi-compartment models assume linear dynamics over the duration of each time step, whereas the NSFD method assumes exponential dynamics. Thus, in the case of a linear model the NSFD method recovers the model dynamics exactly. This chapter illustrates the ability of the NSFD method to solve a two-compartment PK model in a stable and robust fashion, with the ability of being extended to non-linear and/or multi-compartment models.

4.1.1 Nonstandard Finite Difference Method

The initial foundation of NSFD schemes came from exact finite difference schemes [89]. It is thought that numerical methods that approximate differential systems are expected to be consistent with the original differential systems. Mickens [63] provides a theorem which states that each ordinary differential equation corresponds to an "exact" finite difference scheme. He also introduces the NSFD method for designing schemes that are dynamically consistent with the original differential systems, preserve physical properties, obtain reliable results and require less effort to implement than those obtained via standard methods [4]. In this study, we employ the NSFD method to obtain solutions for the two-compartment I.V. bolus injection and the two-compartment I.V. infusion models. We furthermore, conduct a comparative analysis by also considering an analytical solution, the SFD method and ODE45 in MATLAB (MathWorks, Natick, Massachusetts, U.S.A). The purpose of this paper is to obtain an "exact" finite difference scheme for a linear PK model using the procedure of Mickens [7]. In this fashion we hope to prove the degree to which this method may provide meaningful solutions to equations within this context.

4.1.2 Phase Plane Analysis

For a system of linear differential equations $\underline{x}' = A\underline{x}$, the phase portrait is a representative set of its solutions, plotted as parametric curves (with t as the parameter) on the Cartesian plane tracing the path of each particular solution $(x, y) = (x_1(t), x_2(t))$ where $0 < t < \infty$. Thus, by evaluating $A\underline{x}$ at a large number of points and plotting the resulting vectors, one obtains a direction field of tangent vectors to solutions of the system of differential equations. This phase portrait is a graphical tool which assists us in visualizing how the solutions of a given system of differential equations would behave as time evolves. In this context, the Cartesian plane where the phase portrait resides is called the phase plane. The parametric curves traced by the solutions are sometimes also called their trajectories. A

qualitative understanding of the behavior of the solutions and local stability of the numerical solution near steady states can usually be gained from a direction field. More precise information can be discovered by including in the plot some solution curves or trajectories.

A phase portrait is able to assist us in establishing whether the trajectories of a solution will approach the equilibrium solution as t increases, where the equilibrium solution is obtained when $A\underline{x} = \underline{0}$. The behavior of these trajectories around equilibrium points provides further insight into the dynamics of the solution, particularly pertaining to varied parameter values.

4.2 Results

4.2.1 Compartmental Models for Pharmacokinetics

PK models deal with the mathematical description of the rates of the drug movement into, within and upon exiting the body. In this chapter we depict the whole system as two compartments; employing a two-compartment model is often more appropriate mathematically and physiologically when modeling the rate of a drug in the body. These models are used to predict the time course of drugs in the body and to allow maintenance of drug concentration in the therapeutic range by predicting drug levels in each compartment. In this work we will assume that the drug is uniformly distributed within each compartment. The compartments are also considered to be well-stirred and mixing of the drug is assumed to be rapid. Elimination is depicted as occurring in the central compartment, so the drug in the peripheral compartment must transfer back to the central compartment.

For the q-compartment, we have:

$$\frac{dc_i}{dt} = \sum_{j=0}^{q} (k_{ji}c_j - k_{ij}c_i), \tag{4.1}$$

where $c_i(t)$ is the concentration of the drug in compartment i, $i = 1, 2, ..., q$ and the rate constant k_{ij} governs the rate of the drug movement from the ith compartment to the jth-compartment and vice versa.

The variables of importance in this problem structure are as follows:

- c : Concentration of drug in central compartment.
- p : Concentration of drug in peripheral compartment.
- k_{12}: Transfer rate of drug from central to peripheral compartment.
- k_{21}: Degradation rate of drug in peripheral compartment.
- k_{10}: Clearance rate of drug leaving the central compartment.

The data relating to the pharmacokinetic of sisomicin, a new single component aminoglycoside antibiotic, were obtained from Péchère et al. [2] to test the model in this study. The elimination profile of this antibiotic follows two-compartment model kinetics after I.V. administration. The I.V. bolus injection is structured as the initial condition which has the units of concentration as mg/mL. In turn, the I.V. bolus infusion is administered as a dose, D, with unit mg/min, as shown in Table 4.1. The equations considered below are focused on obtaining the concentration in each compartment such that $C_p = \frac{A_p}{V_p}$ where A_p is the amount of drug present in the p^{th} compartment, V_p is the volume of the drug in the p^{th} compartment, with C_p representing the compartments: c (central) and p (peripheral) [50]. As such, we consider the infusion I to be defined as $\frac{D}{V_p}$ with the unit $\frac{mg/min}{ml}$ [2].

TABLE 4.1: Values for sisomicin kinetic parameters derived from two-compartment open model analysis of serum data after intravenous (I.V.) administration. These values are visualized in Figure 4.1 and are obtained from the work by Péchère et al. [2].

Parameter	Unit	Value: Subject 1	Value: Subject 2	Value: Subject 3	Value: Subject 4
k_{10}	min^{-1}	0.00940	0.01110	0.01030	0.01520
k_{12}	min^{-1}	0.04050	0.02504	0.02750	0.04120
k_{21}	min^{-1}	0.02910	0.02230	0.02830	0.02410
D	mg/min	1.00000	1.00000	1.00000	1.00000

Suppose we consider a two-compartment I.V. infusion model. We employ $c(t)$ and $p(t)$ to represent the drug in the central and peripheral compartment, respectively, within the two-compartment model as depicted in Figure 4.1. The central compartment is identified with the blood while the peripheral compartment describes soft tissue. The absorption phase is omitted because the drug was administered with I.V. infusion at time zero. Then, Equation (4.1) reads:

$$\begin{cases} \frac{dc}{dt} &= k_{21}p - k_{12}c - k_{10}c + I(t), \\ \frac{dp}{dt} &= k_{12}c - k_{21}p. \end{cases} \tag{4.2}$$

We will provide both analytical and numerical solutions to this equation for the case: $I(t) = 0$ and $I(t) = I_0$.

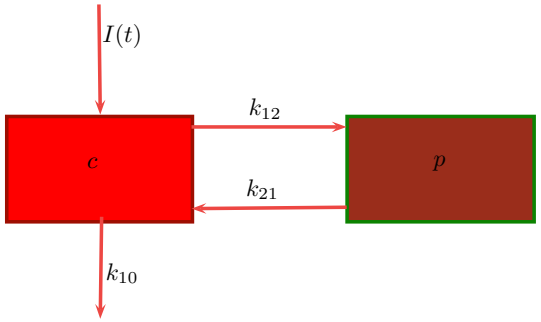

FIGURE 4.1: Two-compartment model with intravenous (I.V.) infusion introduced into the plasma compartment.

Case 1: $I(t) = 0$

If $I(t) = 0$ then (4.2) becomes a two-compartment I.V. bolus injection model, given as:

$$\begin{cases} \frac{dc}{dt} &= k_{21}p - k_{12}c - k_{10}c, \quad c(0) = 1, \\ \frac{dp}{dt} &= k_{12}c - k_{21}p \qquad\qquad p(0) = 0. \end{cases} \tag{4.3}$$

Case 2: $I(t) = I_0$

If $I(t) = I_0$ then (4.2) becomes a two-compartment I.V. infusion model, given as:

$$\begin{cases} \frac{dc}{dt} &= k_{21}p - k_{12}c - k_{10}c + I_0, \quad c(0) = 0, \\ \frac{dp}{dt} &= k_{12}c - k_{21}p \qquad\qquad\quad p(0) = 0. \end{cases} \tag{4.4}$$

The values considered are obtained from the work by Péchère et al. [2]. In this work sisomicin kinetic parameters were derived from a two-compartment open model analysis of serum data after I.V. administration. The values for Subjects 1–4 are employed for the dynamical systems analyses; for the numerical solutions obtained we considered the values of Subject 1. We have also considered different values of the dose; realistically these alternate values should correspond to different values of I_0, however the assumption is that the parameter values are within the correct range to provide us with at least a semblance of the correct dynamics.

4.2.2 Analytical Solution

4.2.2.1 Case 1

We obtain the analytical solution for the blood compartment $c(t)$ and tissue compartment $p(t)$ to Equation (4.3) via the Laplace transform $\mathcal{L}$. The Laplace transform is an integral transformation where the linear operator $\mathcal{L}\{f(t)\}$ transforms a function $f(t)$ with $t \in \mathcal{R}_{\geq 0}$ from the time domain to a function $f(s)$ with $s \in \mathcal{C}$ in an image domain [90, 91]. The main advantage of the Laplace transform is that differentiation and integration in the time domain corresponds to simple algebraic operations in the image domain. Transforming Equation (4.3) and writing Q_1, Q_2 for $\mathcal{L}\{c\}$ and $\mathcal{L}\{p\}$ respectively, we obtain:

$$\begin{cases} (s + k_{10} + k_{12})Q_1 - k_{21}Q_2 = 1 \\ -k_{12}Q_1 + (s + k_{21})Q_2 = 0, \end{cases} \tag{4.5}$$

upon substitution of the initial conditions and rearranging accordingly. These are simultaneous algebraic equations in Q_1 and Q_2; we can solve for these upon employing the method of elimination:

$$\begin{aligned} Q_2\left(-s^2 - sk_{21} - sk_{10} - k_{10}k_{21} - sk_{12} - k_{12}k_{21} + k_{12}k_{21}\right) &= -k_{12} \\ \left(s^2 + (k_{10} + k_{12} + k_{21})s + k_{10}k_{12}\right)Q_2 &= k_{12}, \end{aligned} \tag{4.6}$$

implies

$$Q_2 = \frac{k_{12}}{s^2 + (k_{10} + k_{12} + k_{21})s + k_{10}k_{12}} \tag{4.7}$$

providing,

$$Q_2 = \frac{k_{12}}{(s + \lambda_1)(s + \lambda_2)} \tag{4.8}$$

where,

$$\lambda_{1,2} = \frac{1}{2}\left(k_{10} + k_{12} + k_{21} \pm \sqrt{(k_{10} + k_{12} + k_{21})^2 - 4k_{10}k_{21}}\right) \tag{4.9}$$

such that,

$$\lambda_1 + \lambda_2 = k_{12} + k_{21} + k_{10}, \quad \lambda_1\lambda_2 = k_{21}k_{10}.$$

To obtain the solution for the peripheral compartment we take inverse Laplace transform of Equation (4.8) which gives:

$$\begin{aligned} \mathcal{L}^{-1}\{Q_2\} = p(t) &= \mathcal{L}^{-1}\left\{\tfrac{k_{12}}{(s+\lambda_1)(s+\lambda_2)}\right\} \\ &= k_{12}\mathcal{L}^{-1}\left\{\tfrac{A}{s+\lambda_1} + \tfrac{B}{(s+\lambda_2)}\right\}, \end{aligned} \tag{4.10}$$

where,

$$A = \frac{k_{12}}{\lambda_2 - \lambda_1}, \qquad B = \frac{-k_{12}}{\lambda_2 - \lambda_1},$$

such that,

$$p(t) = \frac{k_{12}}{\lambda_2 - \lambda_1} \left(\exp(-\lambda_1 t) - \exp(-\lambda_2 t)\right). \tag{4.11}$$

This then allows us to find $c(t)$ by eliminating Q_2 in Equation (4.5) or by substituting the solution for $p(t)$ in one of the equations given in (4.3). In this case, it will be simpler to substitute for $p(t)$ in the second equation of (4.3), giving,

$$\begin{aligned} k_{12}c = \frac{d}{dt}\left(\frac{k_{12}}{\lambda_2 - \lambda_1}\left(\exp(-\lambda_1 t) - \exp(-\lambda_2 t)\right)\right) + \\ k_{21}\left(\frac{k_{12}}{\lambda_2 - \lambda_1}\left(\exp(-\lambda_1 t) - \exp(-\lambda_2 t)\right)\right), \end{aligned} \tag{4.12}$$

from (4.12) we have

$$\begin{aligned} k_{12}c = \frac{k_{12}}{\lambda_2 - \lambda_1}\left(-\lambda_1 \exp(-\lambda_1 t) + \lambda_2 \exp(-\lambda_2 t)\right) + \\ \frac{k_{12}k_{21}}{\lambda_2 - \lambda_1}\left(\exp(-\lambda_1 t) - \exp(-\lambda_2 t)\right), \end{aligned} \tag{4.13}$$

such that,

$$c(t) = \frac{\lambda_1 - k_{21}}{\lambda_1 - \lambda_2}\exp(-\lambda_1 t) + \frac{k_{21} - \lambda_2}{\lambda_1 - \lambda_2}\exp(-\lambda_2 t).$$

The concentration in the central compartment is hence,

$$c(t) = E\exp(-\lambda_1 t) + (1 - E)\exp(-\lambda_2 t) \tag{4.14}$$

and the concentration of the drug in the peripheral compartment is:

$$p(t) = \frac{k_{12}}{\lambda_2 - \lambda_1}\left(\exp(-\lambda_1 t) - \exp(-\lambda_2 t)\right), \tag{4.15}$$

where $E = \frac{\lambda_1 - k_{21}}{\lambda_1 - \lambda_2}$.

4.2.2.2 Case 2

The general solution for (4.4) is of the form $q(t) = q_p + q_c$ where q_p is a particular solution and q_c is the complementary solution, i.e., the general solution of the homogeneous part of the Equation (4.4). To obtain a particular solution of Equation (4.4), we assume $c(t)$ and $p(t)$ to be constant, such that,

$$k_{21}p - k_{12}c - k_{10}c + I_0 = 0 \tag{4.16}$$

and,

$$k_{12}c - k_{21}p = 0. \tag{4.17}$$

Upon substituting (4.16) into (4.17) we obtain the particular solution of (4.4):

$$q_p = \begin{pmatrix} c(t) \\ p(t) \end{pmatrix} = \frac{I_0}{k_{10}} \begin{pmatrix} 1 \\ \frac{k_{12}}{k_{21}} \end{pmatrix}. \tag{4.18}$$

To find the complementary solution to Equation (4.4) at $I(t) = 0$) we consider,

$$\begin{pmatrix} c' \\ p' \end{pmatrix} = \begin{pmatrix} -k_{10} - k_{12} & k_{21} \\ k_{12} & -k_{21} \end{pmatrix} \begin{pmatrix} c \\ p \end{pmatrix} \tag{4.19}$$

providing the corresponding matrix,

$$A = \begin{pmatrix} -k_{10} - k_{12} & k_{21} \\ k_{12} & -k_{21} \end{pmatrix}. \tag{4.20}$$

We can find a fundamental set of solutions for the matrix by finding the eigenvalues and the corresponding eigenvectors. The matrix A has eigenvalues λ such that:

$$\lambda^2 + (k_{10} + k_{12} + k_{21})\lambda + k_{10}k_{21} = 0 \tag{4.21}$$

which, upon solution, provides the following eigenvalues:

$$\lambda_{1,2} = \frac{1}{2}\left(-k_{10} - k_{12} - k_{21} \pm \sqrt{(k_{10} + k_{12} + k_{21})^2 - 4k_{10}k_{21}}\right). \tag{4.22}$$

Suppose $\underline{v} = \begin{pmatrix} v_1 \\ v_2 \end{pmatrix}$ are the eigenvectors corresponding to the eigenvalues, then $(A - \lambda I)\underline{v} = 0$. Hence we have that,

$$\begin{pmatrix} -k_{10} - k_{12} - \lambda_{1,2} & k_{21} \\ k_{12} & -k_{21} - \lambda_{1,2} \end{pmatrix} \begin{pmatrix} v_1 \\ v_2 \end{pmatrix} = \begin{pmatrix} 0 \\ 0 \end{pmatrix}$$

or,

$$\begin{cases} (-k_{10} - k_{12} - \lambda_{1,2})v_1 + k_{21}v_2 = 0 \\ k_{12}v_1 + (-k_{21} - \lambda_{1,2})v_2 = 0. \end{cases} \tag{4.23}$$

From (4.23), we have that:

$$v_1 = \frac{k_{21} + \lambda_{1,2}}{k_{12}} v_2,$$

and,

$$v_2 = \frac{k_{10} + k_{12} + \lambda_{1,2}}{k_{21}} v_1.$$

Suppose $v_2 = 1$, then we have that,

$$v_1 = \frac{k_{21} + \lambda_{1,2}}{k_{12}},$$

and thus,

$$\underline{v} = \begin{pmatrix} v_1 \\ v_2 \end{pmatrix} = \begin{pmatrix} \frac{k_{21}+\lambda_{1,2}}{k_{12}} \\ 1 \end{pmatrix}.$$

Let $\tau_{1,2} = \frac{K_{21}+\lambda_{1,2}}{K_{12}}$, then we find the corresponding eigenvectors to the eigenvalues to be:

$$\underline{v} = \begin{pmatrix} v_1 \\ v_2 \end{pmatrix} = \begin{pmatrix} \tau_{1,2} \\ 1 \end{pmatrix}.$$

Substituting the value of $\lambda_{1,2}$ from (4.22), we have:

$$\tau_{1,2} = \frac{-k_{10} - k_{12} + k_{21} \pm \sqrt{(k_{10} + k_{12} + k_{21})^2 - 4k_{10}k_{21}}}{2k_{12}}.$$

We can now write our complementary solution as:

$$q_c(t) = A_1 e^{\lambda_1 t} \begin{pmatrix} \tau_1 \\ 1 \end{pmatrix} + A_2 e^{\lambda_2 t} \begin{pmatrix} \tau_2 \\ 1 \end{pmatrix}. \tag{4.24}$$

The general solution to (4.4) is then of the form $q(t) = q_p + q_c$, hence,

$$q(t) = \begin{pmatrix} c(t) \\ p(t) \end{pmatrix} = \frac{I_0}{k_{10}} \begin{pmatrix} 1 \\ \frac{k_{12}}{k_{21}} \end{pmatrix} + A_1 e^{\lambda_1 t} \begin{pmatrix} \tau_1 \\ 1 \end{pmatrix} + A_2 e^{\lambda_2 t} \begin{pmatrix} \tau_2 \\ 1 \end{pmatrix}, \tag{4.25}$$

giving,

$$c(t) = \frac{I_0}{k_{10}} + A_1\tau_1 e^{\lambda_1 t} + A_2\tau_2 e^{\lambda_2 t} \tag{4.26}$$

and,

$$p(t) = \frac{k_{12}I_0}{k_{10}k_{21}} + A_1 e^{\lambda_1 t} + A_2 e^{\lambda_2 t}. \tag{4.27}$$

Given the initial condition $\begin{pmatrix} c(0) \\ p(0) \end{pmatrix} = \begin{pmatrix} 0 \\ 0 \end{pmatrix}$, and employing Equations (4.26) and (4.27) we have:

$$\frac{I_0}{k_{10}} + A_1\tau_1 + A_2\tau_2 = 0, \tag{4.28}$$

$$\frac{k_{12}I_0}{k_{10}k_{21}} + A_1 + A_2 = 0. \tag{4.29}$$

With some algebraic manipulation we find the arbitrary constants:

$$A_1 = \frac{I_0}{k_{10}} \left(\frac{k_{12}\tau_2 - k_{21}}{k_{21}(\tau_1 - \tau_2)} \right) \tag{4.30}$$

and,

$$A_2 = \frac{I_0}{k_{10}} \left(\frac{k_{21} - k_{12}\tau_1}{k_{21}(\tau_1 - \tau_2)} \right). \tag{4.31}$$

Our final solution is then given as:

$$\begin{aligned} q(t) = \begin{pmatrix} c(t) \\ p(t) \end{pmatrix} = \frac{I_0}{k_{10}} \begin{pmatrix} 1 \\ \frac{k_{12}}{k_{21}} \end{pmatrix} + \frac{I_0}{k_{10}} \left(\frac{k_{12}\tau_2 - k_{21}}{k_{21}(\tau_1 - \tau_2)} \right) e^{\lambda_1 t} \begin{pmatrix} \tau_1 \\ 1 \end{pmatrix} \\ + \frac{I_0}{k_{10}} \left(\frac{k_{21} - k_{12}\tau_1}{k_{21}(\tau_1 - \tau_2)} \right) e^{\lambda_2 t} \begin{pmatrix} \tau_2 \\ 1 \end{pmatrix}. \end{aligned} \tag{4.32}$$

4.2.3 Remarks

As provided in Table 4.1 the parameter values for k_{10}, k_{12} and k_{21} were obtained from [2]. We also consider the case where $k_{12} = 0$ as a means of comparison; this case indicates that the transfer rate of the drug from the central to the peripheral compartment is zero.

Consider the dynamics presented in Figure 4.2 for the homogeneous case; we find that the transition from $k_{12} > 0$ to $k_{12} = 0$ does not change the nature of the equilibrium points. In both cases we find that $\lambda_1 < \lambda_2 < 0$, indicating that we have a node which is defined to be asymptotically stable. This has been checked for the range of parameter values given in Table 4.1, for Subjects 1–4. This indicates that when the transfer rate of the drug from the central to peripheral compartment is positive, or when there is no transfer, the system maintains the same dynamics.

Figure 4.3 shows that for the transition from $k_{12} > 0$ to $k_{12} = 0$, in the non-homogeneous case, our dynamics once again remain unchanged. We have a nodal sink—defined to be asymptotically stable—at a point where c and $p > 0$, such that the concentration in both compartments is positive. In the second instance

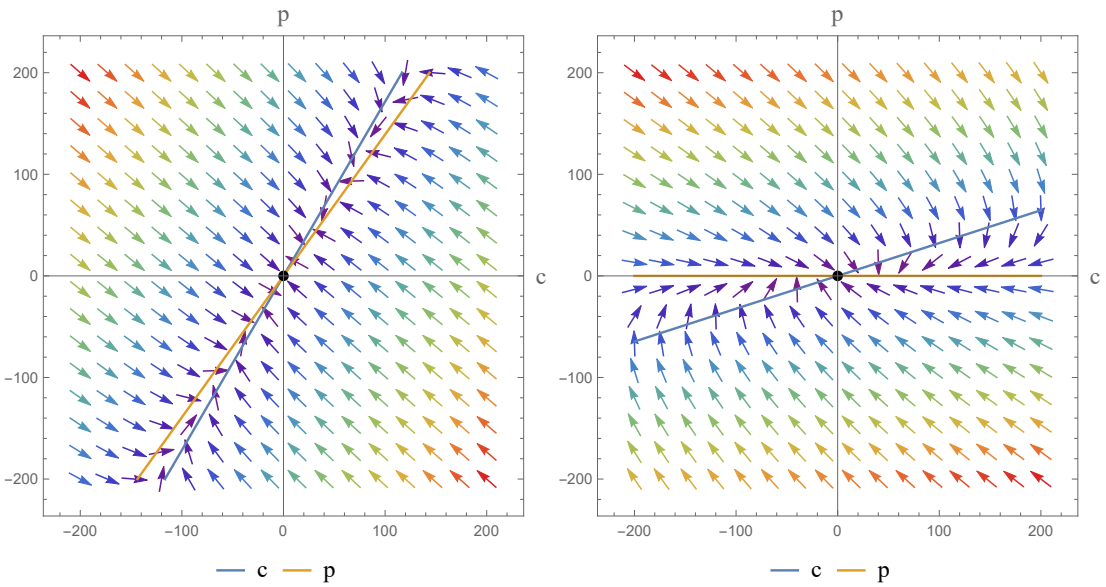

(a) $k_{10} = 0.0094$, $k_{12} = 0.0405$, $k_{21} = 0.0291$ (b) $k_{10} = 0.0094$, $k_{12} = 0.0$, $k_{21} = 0.0291$

FIGURE 4.2: Phase portrait representing $c(t)$ and $p(t)$. The arrows illustrates the trajectories of the system.

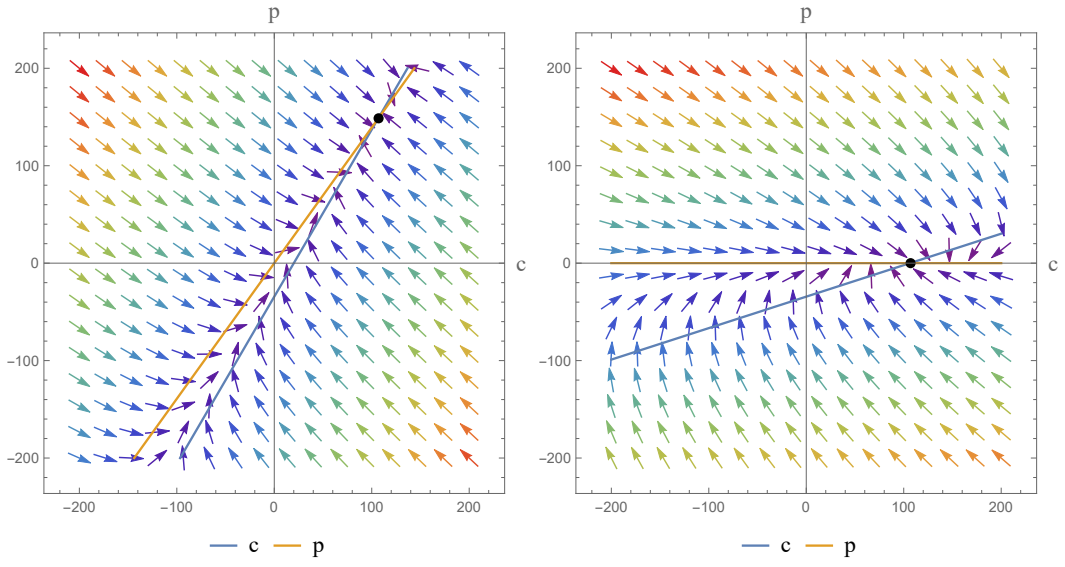

(a) $k_{10} = 0.0094$, $k_{12} = 0.0405$, $k_{21} = 0.0291$ and $I_0 = 1$. (b) $k_{10} = 0.0094$, $k_{12} = 0$, $k_{21} = 0.0291$ and $I_0 = 1$.

FIGURE 4.3: Phase portrait representing $c(t)$ and $p(t)$. The arrows illustrates the trajectories of the system.

($k_{12} = 0$) we obtain a point where $p = 0$, i.e., only the concentration in the central compartment is not zero. Thus, we further note that our results have shown that the case where $k_{10} > k_{12} = 0$ results in a lower steady-state drug concentration. We also note - as indicated in Figure 4.4 (a) - that the steady state concentration is directly proportional to the infusion rate I_0. Hence, a higher value of I_0 will result in a higher steady-state concentration. In Figure 4.4 (b) we note that a higher elimination rate (k_{10}) will result in a lower steady-state concentration.

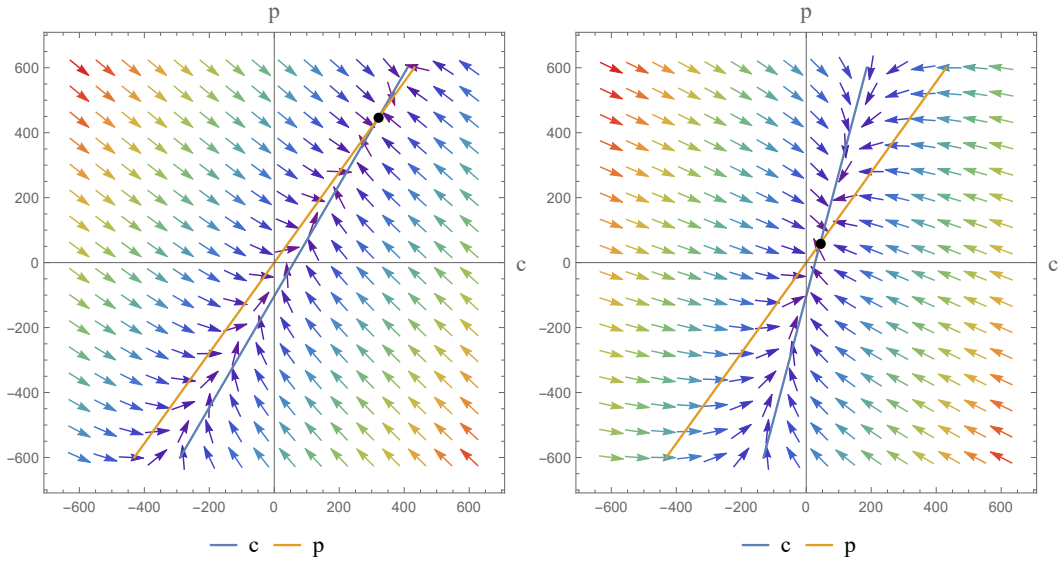

(a) $k_{10} = 0.0094$, $k_{12} = 0.0405$, $k_{21} = 0.0291$ and $I_0 = 3$.

(b) $k_{10} = 0.0694$, $k_{12} = 0.0405$, $k_{21} = 0.0291$ and $I_0 = 3$.

FIGURE 4.4: Phase portrait (**a**) shows the steady state concentration is directly proportional to the infusion rate (I_0). Thus, a higher I_0 will result in a higher steady-state concentration, and (**b**) shows a higher elimination rate (k_{10}) will result in a lower steady-state concentration.

In terms of an investigation of the impact of I_0 we note that the drug is given by I.V. infusion at a constant zero-order rate to allow accurate control of the drug concentration and to maintain the level of the drug in the body as constant. This allows us to predict the PK action. For physically meaningful results we can only consider constant values of the dose; at different constant values (I_0) we obtain a higher infusion rate which results in a higher steady state concentration. We find however, that an increase in I_0 does not have any effect on the dynamics of the system.

4.2.4 Nonstandard Finite Difference Scheme

4.2.4.1 Case 1

Before we discuss the implementation of the NSFD scheme we briefly review the SFD schemes of the system of equations given by (4.3) which are given as:

$$\frac{c_{n+1}-c_n}{h} = k_{21}p_n - k_{12}c_n - k_{10}c_n \tag{4.33}$$

$$\frac{p_{n+1}-p_n}{h} = k_{12}c_n - k_{21}p_n. \tag{4.34}$$

Via the SFD method the system may be written in explicit form as:

$$c_{n+1} = c_n + h(k_{21}p_n - k_{12}c_n - k_{10}c_n) \tag{4.35}$$

$$p_{n+1} = p_n + h(k_{12}c_n - k_{21}p_n). \tag{4.36}$$

We now turn to the focus of this section, which is the implementation of the concepts of the NSFD scheme to the linear PK model (4.3) under discussion [7]. Employing the NSFD method, Mickens [81] obtain NSFD scheme (4.37)-(4.38) which is the exact scheme of (4.3).

$$\frac{c_{n+1}-\varphi c_n}{\phi} = k_{21}p_n - k_{12}c_n - k_{10}c_n \tag{4.37}$$

$$\frac{p_{n+1}-\varphi p_n}{\phi} = k_{12}c_n - k_{21}p_n. \tag{4.38}$$

where,

$$\phi = \frac{e^{\lambda_1 h} - e^{\lambda_2 h}}{\lambda_1 - \lambda_2} \qquad \text{and} \qquad \varphi = \frac{\lambda_1 e^{\lambda_2 h} - \lambda_2 e^{\lambda_1 h}}{\lambda_1 - \lambda_2},$$

and λ_1 and λ_2 are given as per Equation (4.9).

4.2.5 Case 2:

As before, we present the SFD schemes of the system of equations given by (4.4) before discussing the relevant NSFD scheme. These are given as:

$$\frac{c_{n+1}-c_n}{h} = k_{21}p_n - k_{12}c_n - k_{10}c_n + I_0 \tag{4.39}$$

$$\frac{p_{n+1}-p_n}{h} = k_{12}c_n - k_{21}p_n. \tag{4.40}$$

This system may be written in explicit form as:

$$c_{n+1} = c_n + h(k_{21}p_n - k_{12}c_n - k_{10}c_n + I_0) \tag{4.41}$$

$$p_{n+1} = p_n + h(k_{12}c_n - k_{21}p_n). \tag{4.42}$$

We now turn to the NSFD implementation as a means of solution. In order to do so we start by considering the system of equations given by (4.4) which, under the requirement:

$$k_{10}k_{21} \neq 0, \tag{4.43}$$

gives the general solutions:

$$c(t) = \frac{1}{\lambda_1-\lambda_2}\left((k_{10}k_{21}-\lambda_2)c_0 + k_{21}p_0 + \frac{I_0(\lambda_2 - k_{10}k_{21} - k_{12})}{k_{10}}\right)e^{\lambda_1(t-t_0)} + \frac{1}{\lambda_1-\lambda_2}\left((\lambda_1-k_{10}k_{21})c_0 + k_{21}p_0 + \frac{I_0(k_{10}k_{21}-\lambda_2+k_{12})}{k_{10}}\right)e^{\lambda_2(t-t_0)} + \frac{I_0}{k_{10}}, \tag{4.44}$$

$$p(t) = \frac{\lambda_1+k_{10}+k_{12}}{k_{21}(\lambda_1-\lambda_2)}\left((k_{10}k_{21}-\lambda_2)c_0 + k_{21}p_0 + \frac{I_0(\lambda_2 - k_{10}k_{21} - k_{12})}{k_{10}}\right)e^{\lambda_1(t-t_0)} + \frac{\lambda_2+k_{10}+k_{12}}{k_{21}(\lambda_1-\lambda_2)}\left((\lambda_1-k_{10}k_{21})c_0 + k_{21}p_0 + \frac{I_0(k_{10}k_{21}-\lambda_2+k_{12})}{k_{10}}\right)e^{\lambda_2(t-t_0)} + \frac{k_{12}I_0}{k_{10}k_{21}}, \tag{4.45}$$

where λ_{12} is given in Equation (4.22).

The NSFD scheme of Equation (4.4) is obtained by making the following transformation in Equations (4.44) and (4.45):

$$\begin{cases} t_0 \to t_k = hk, \\ t \to t_{k+1} = h(k+1), \\ u_0 \to u_k, \\ u(t) \to u_{k+1}, \\ w_0 \to w_k, \\ w(t) \to w_{k+1}, \end{cases} \tag{4.46}$$

giving the following results:

$$c_{k+1} = \frac{1}{\lambda_1 - \lambda_2}\left((k_{10}k_{21} - \lambda_2)c_k + k_{21}p_k + \frac{I_0(\lambda_2 - k_{10}k_{21} - k_{12})}{k_{10}}\right) e^{\lambda_1 h} + \frac{1}{\lambda_1 - \lambda_2}\left((\lambda_1 - k_{10}k_{21})c_k + k_{21}p_k + \frac{I_0(k_{10}k_{21} - \lambda_2 + k_{12})}{k_{10}}\right) e^{\lambda_2 h} + \frac{I_0}{k_{10}}, \tag{4.47}$$

$$p_{k+1} = \frac{\lambda_1 + k_{10} + k_{12}}{k_{21}(\lambda_1 - \lambda_2)}\left((k_{10}k_{21} - \lambda_2)c_k + k_{21}p_k + \frac{I_0(\lambda_2 - k_{10}k_{21} - k_{12})}{k_{10}}\right) e^{\lambda_1 h} + \frac{\lambda_2 + k_{10} + k_{12}}{k_{21}(\lambda_1 - \lambda_2)}\left((\lambda_1 - k_{10}k_{21})c_k + k_{21}p_k + \frac{I_0(k_{10}k_{21} - \lambda_2 + k_{12})}{k_{10}}\right) e^{\lambda_2 h} + \frac{k_{12}I_0}{k_{10}k_{21}}. \tag{4.48}$$

When $I_0 = 0$, in equations (4.47) and (4.48) and with little manipulation as before, we obtained (4.37) and (4.38).

4.3 Discussion

In this study two-compartment models (the I.V. bolus injection and I.V. infusion models) are considered for simulations. The methods compared are the SFD

method, and the in-built function `ODE45` in MATLAB, with the focus of the study being the NSFD method. All the simulations were performed by using MATLAB. The absolute error is presented using the formula:

$$E_{\text{Absolute}} = |X_{\text{Analytical solution}} - X_{\text{Numerical solution}}|.$$

The first column, in each table presented, is the number of nodes chosen, the second column is the corresponding step size, the third column is the absolute error between the exact solution and the SFD scheme, the fourth column is the absolute error between the exact solution and `ODE45` in MATLAB, and the last column gives the absolute error between the exact solution and the NSFD scheme.

Once again, we remind the reader of the values provided in Table 4.1 for the parameters: k_{10}, k_{12} and k_{21} [2]. These were derived from a two-compartment open model analysis of serum of sisomicin after I.V. administration.

4.3.1 Case 1: Simulation Results

The results for this case clearly indicate the degree to which the NSFD method outperforms the SFD method, and in fact the in-built function as well - see Figure 4.5. For each step size employed the absolute error calculated is in fact zero, as per see Tables 4.2 and 4.3, given that the NSFD method produces "exact" solutions. More importantly, we see from Figures 4.6 and 4.7 that for large step sizes the NSFD method performs exceptionally well, matching the analytical solution for the entire time profile, while the SFD method is not able to do so.

The SFD method deviates from the exact solution the moment the solution changes gradient— see Figure 4.7. This is a known problem for methods of this nature; we find that as expected the NSFD method does not suffer from this weakness.

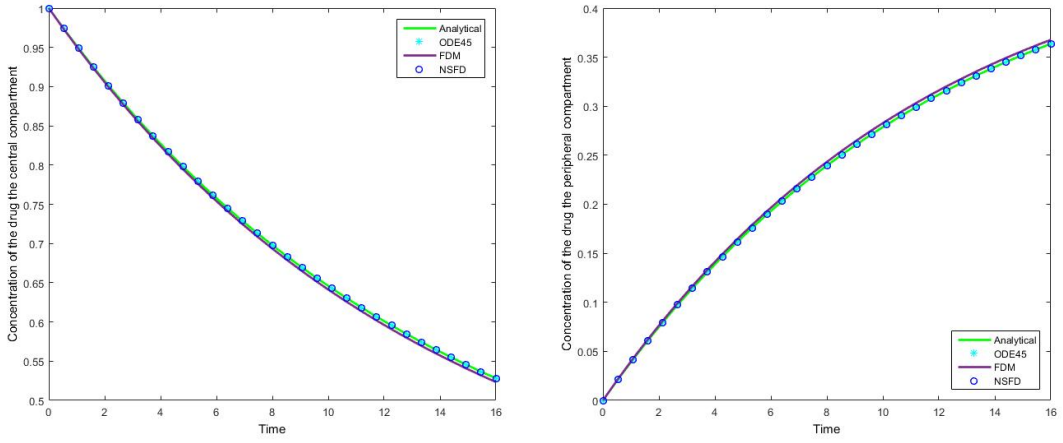

(**a**) (**b**)

FIGURE 4.5: The concentration of the drug for Case 1 where $h = 0.53333$ in the (**a**) central compartment, and (**b**) peripheral compartment.

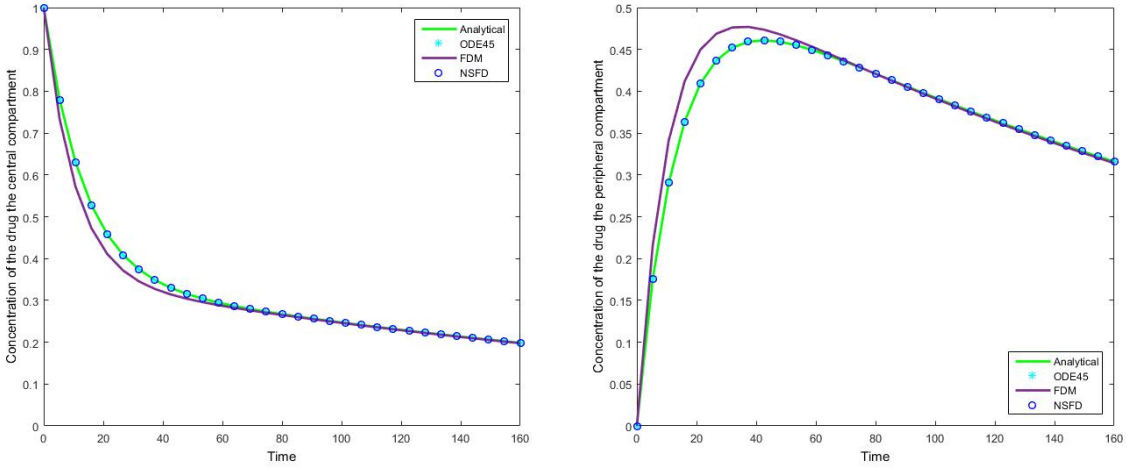

(**a**) (**b**)

FIGURE 4.6: The concentration of the drug for Case 1 where $h = 5.3333$ in the (**a**) central compartment, and (**b**) peripheral compartment for a large time interval.

4.3.2 Case 2: Simulation Results

Once more we find that for each step size employed the NSFD method outperforms those methods it is compared to - see Tables 4.4 and 4.5. In this case in particular, the structuring of the NSFD scheme is shown to be quite complex. The NSFD scheme in this case was obtained via an initial structuring of the exact solution of the problem and making the substitution provided in Equation (4.46). We

TABLE 4.2: The absolute error results for the system of equations given by (4.3) for $c(t)$ with parameter values $k_{10} = 0.0094$, $k_{12} = 0.0405$, and $k_{21} = 0.0291$.

Absolute Error for $c(t)$				
N	**h**	**Error in SFD**	**Error in ODE45**	**Error in NSFD**
2	10.00000	0.144913386	0.000000010	0.000000000
4	5.00000	0.053199386	0.000000010	0.000000000
8	2.50000	0.024396686	0.000000010	0.000000000
16	1.25000	0.011669111	0.000000022	0.000000000
32	0.62500	0.005719559	0.000000028	0.000000000
64	0.31250	0.002831162	0.000000028	0.000000000
128	0.15625	0.001408639	0.000000028	0.000000000
256	0.07812	0.000702591	0.000000028	0.000000000
512	0.03906	0.000350865	0.000000028	0.000000000
1024	0.01953	0.000175326	0.000000029	0.000000000

TABLE 4.3: The absolute error results for the system of equations given by (4.3) for p with parameter values $k_{10} = 0.0094$, $k_{12} = 0.0405$, and $k_{21} = 0.0291$.

Absolute Error for $p(t)$				
N	**h**	**Error in SFD**	**Error in ODE45**	**Error in NSFD**
2	10.00000	0.126270717	0.000000009	0.000000000
4	5.00000	0.046283217	0.000000009	0.000000000
8	2.50000	0.021180830	0.000000009	0.000000000
16	1.25000	0.010127446	0.000000019	0.000000000
32	0.62500	0.004961080	0.000000025	0.000000000
64	0.31250	0.002455508	0.000000025	0.000000000
128	0.15625	0.001221609	0.000000025	0.000000000
256	0.07812	0.000609284	0.000000025	0.000000000
512	0.03906	0.000304265	0.000000025	0.000000000
1024	0.01953	0.000152038	0.000000026	0.000000000

note from Figure 4.8 that the schemes reach the steady state as required. More importantly we observe the oscillations which occur for increasing step sizes h. It must be noted that these step sizes are realistic given that $t \in [0, 2000]$; as such in a range of $[0, 1]$ the value of $h = 10$ represents $\Delta t = 0.005$, whereas $h = 26.667$ is represented by $\Delta t = 0.013$. We can easily observe here the degree to which the NSFD method is able to outperform the other two numerical methods employed. The SFD scheme does not match the real dynamics of the system for higher step sizes; we observe oscillations of the SFD method for large h. As the step size increases there is complete blowup of the SFD scheme and the error in

`ODE45` increases.

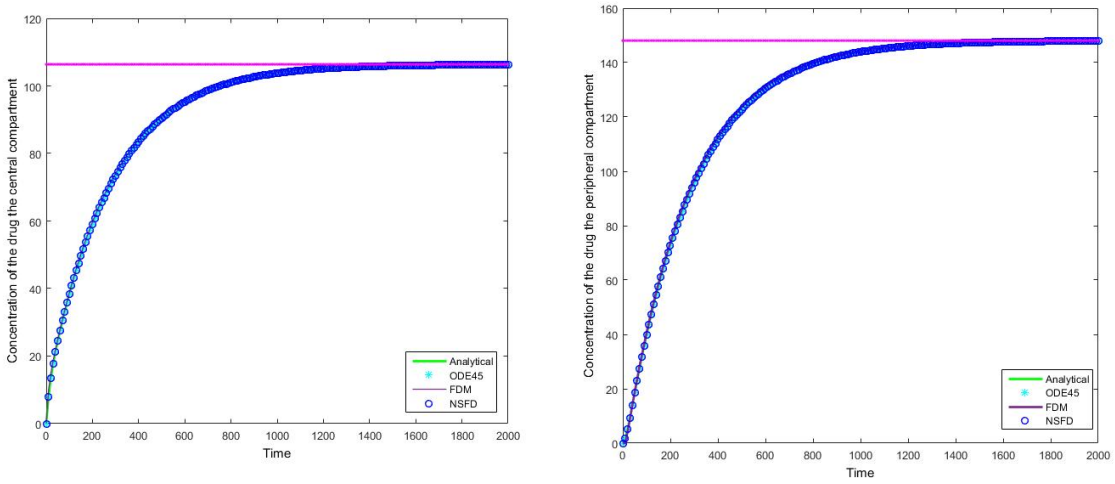

(**a**) (**b**)

FIGURE 4.7: The concentration of the drug for Case 2 where $h = 10$ in the (**a**) central compartment, and (**b**) peripheral compartment. At the steady state, the rate of drug infusion (I_0) is equal to the elimination rate (k_{10}).

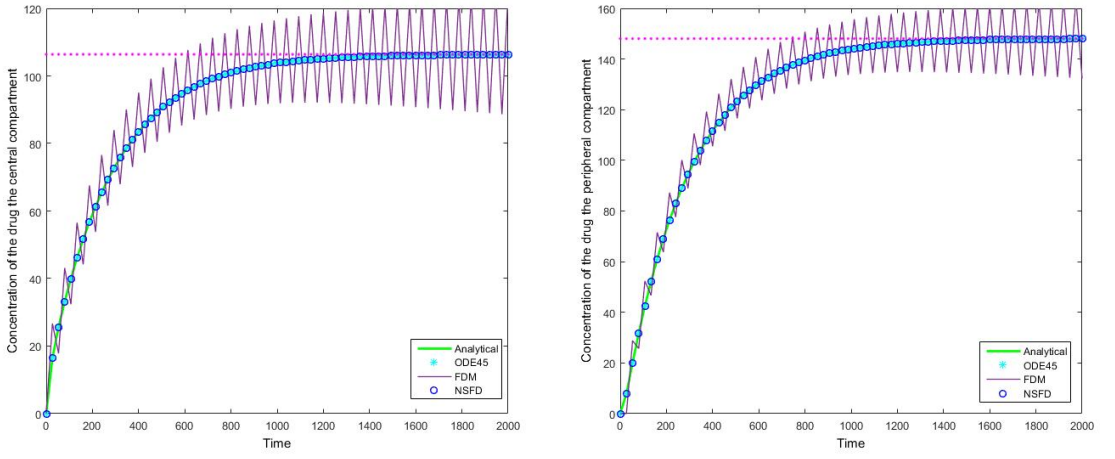

(**a**) (**b**)

FIGURE 4.8: The concentration of the drug for Case 2 where $h = 26.667$ in the (**a**) central compartment, and (**b**) peripheral compartment.

In terms of an investigation of the impact of I_0 we note that the drug is given by I.V. infusion at a constant zero-order rate to allow accurate control of the drug concentration and to maintain the level of the drug in the body as constant. This allows us predict PK action. For physically meaningful results we can only consider constant values of the dose; at different constant values (I_0) we obtain a higher infusion rate which results in a higher steady state concentration.

TABLE 4.4: The absolute error results for the system of equations given by (4.4) for $c(t)$ with parameter values $k_{10} = 0.0094$, $k_{12} = 0.0405$, $k_{21} = 0.0291$ and $I_0 = 1$.

Absolute Error for $c(t)$				
N	**h**	**Error in SFD**	**Error in ODE45**	**Error in NSFD**
2	10.00000	1.98326261	0.00000008	0.00000000
4	5.00000	0.73839463	0.00000010	0.00000000
8	2.50000	0.34211236	0.00000012	0.00000000
16	1.25000	0.16473051	0.00000018	0.00000000
32	0.62500	0.08083009	0.00000021	0.00000000
64	0.31250	0.04005593	0.00000019	0.00000000
128	0.15625	0.01993844	0.00000022	0.00000000
256	0.07812	0.00994725	0.00000023	0.00000000
512	0.03906	0.00496814	0.00000022	0.00000000
1024	0.01953	0.00248270	0.00000023	0.00000000

TABLE 4.5: The absolute error results for the system of equations given by (4.4) for $p(t)$ with parameter values $k_{10} = 0.0094$, $k_{12} = 0.0405$, $k_{21} = 0.0291$ and $I_0 = 1$.

Absolute Error for $p(t)$				
N	**h**	**Error in SFD**	**Error in ODE45**	**Error in NSFD**
2	10.00000	1.57898904	0.00000007	0.00000000
4	5.00000	0.56648904	0.00000009	0.00000000
8	2.50000	0.25172781	0.00000011	0.00000000
16	1.25000	0.12005326	0.00000016	0.00000000
32	0.62500	0.05860324	0.00000018	0.00000000
64	0.31250	0.02895478	0.00000017	0.00000000
128	0.15625	0.01439233	0.00000020	0.00000000
256	0.07812	0.00717515	0.00000021	0.00000000
512	0.03906	0.00358234	0.00000019	0.00000000
1024	0.01953	0.00178986	0.00000020	0.00000000

4.4 Conclusions

In this Chapter we structured and applied a NSFD numerical scheme to two systems of equations which are both PK models. The first model is an I.V. bolus injection two-compartment model while the second model is an I.V. infusion two-compartment model. The systems are homogeneous and non-homogeneous systems of differential equations, respectively. We present some absolute errors associated

with this method upon comparison to the relevant analytical solution, the SFD method and the in-built function `ODE45` in MATLAB. The NSFD results indicates superior performance over the SFD method and the in-built MATLAB function, confirming both its stability and robustness.

Chapter 5

Application of Nonstandard Finite Difference Method to 3-Compartment Pharmacokinetics Models

"The purpose of computation is insight, not numbers."

Richard Hamming

The work in this chapter appeared in:

Oluwaseun Francis Egbelowo. Nonstandard finite difference approach for solving 3-compartment pharmacokinetic models. Int J Numer Meth Biomed Engng. 2018;e3114. https://doi.org/10.1002/cnm.3114

5.1 Introduction

The development of analytical and sampling techniques for pharmacokinetic models has shown that some drugs follow a the three-compartment pharmacokinetic model.

Drug demonstrates the necessity of three-compartment model when either one or two compartment pharmacokinetic models are clearly insufficient to capture the complex nature of the pharmacokinetic' data exhibited by the drug. For example, if the drug concentrations after a single intravenous (I.V.) bolus dose on the semilog scale decline at three distinct rates, one or two compartmental pharmacokinetic models would not be enough to capture this phenomenon. Hence, the three-compartment pharmacokinetic models are mostly applicable to describe the progression of the drug administered. The three-compartment pharmacokinetic model comprises a central compartment and two peripheral compartments as shown in Figure 5.1. C_1 represents the central compartment, where elimination of the drug occurs. The other two are tissue compartment (C_2) and deep tissue compartment respectively [92]. An intravenously administered drug enters the central compartment and is redistributed to the other two compartments. The drug is eliminated from the central compartment by metabolism and excretion simultaneously. If the volume of the central compartment is known, then it is possible to calculate the drug concentration in the central compartment with simple mathematical models.

Obtaining an analytical solution for the three-compartment pharmacokinetic model requires the solution of a third-degree polynomial, whose roots are non-zero and difficult to solve [58, 93]. Due to the complex nature of the analytical solutions, many researchers have used numerical techniques to approximate the solution [53]. The easiest and the most used method to model the differential equations arising from three-compartment pharmacokinetic models is Euler's method [57]. The Euler's method numerical technique allows for the calculation of the approximate concentration of drug in each compartment at each update cycle [53, 57, 59]. This method has been used mostly for this type of problems. However, this method has a number of potential problems. Firstly, the modeling procedure is non-unique and the inappropriate modeling of the differential equations by the difference equations will lead to numerical instabilities [63]. Secondly, the positivity property of the exact solution is usually not transferred to the numerical solution. There are several

other numerical techniques that approximate the solution of the three-compartment pharmacokinetic models and are based on choosing small step-sizes [93] whereas this affects the speed of the simulation. Though, the method proposed by [53] is independent of step-size it does not solve for the concentrations in any compartment other than the central compartment and when it is necessary to target all the compartments rather than only the central compartment the technique suggested by [53] would not be able to capture this phenomenon. Since the drug concentration in each compartment is different because of differences in drug affinity to tissues, it is necessary to know the drug concentration in each compartment. The purpose of this Chapter is to give numerical solutions to three-compartment pharmacokinetic for two different inputs (I.V. bolus injection and I.V. bolus infusion) by determining the concentration of drug in each compartment. The nonstandard finite difference (NSFD) method, which was first suggested by Mickens [63] is used. Egbelowo [94] and Egbelowo et al. [87] applied NSFD methods to one and two compartment pharmacokinetic models respectively. In this chapter, we present the NSFD scheme for three compartment pharmacokinetic models, which gives the 'exact' numerical expressions of the drugs in each compartment when I.V bolus injection is considered. We also present a NSFD scheme that is dynamically consistency with contin uous differential equations when I.V bolus infusion model is considered.

TABLE 5.1: Pharmacokinetics of Remifentani parameters derived from three-compartment open model analysis after intravenous (I.V.) administration. These values are visualized in Figure 5.2 and are obtained from the work by Cascone et al. [3].

Description	**Parameter**	**Unit**	**Value**
Transfer rate of drug from central to tissue compartment	k_{12}	min^{-1}	0.3730
Degradation rate of drug in tissue compartment.	k_{21}	min^{-1}	0.1030
Transfer rate of drug from central to deep tissue compartment.	k_{13}	min^{-1}	0.0367
Degradation rate of drug in deep tissue compartment.	k_{31}	min^{-1}	0.0124
Clearance rate of drug leaving the central compartment.	k_{10}	min^{-1}	0.1720
Dose giving by I.V. bolus	D	$\mu g \cdot kg^{-1}$	5.0000

5.2 Mathematical Model

In the case where a drug is given by I.V. bolus injection the medications are released into the bloodstream. This system is often used when the rapid administration of a medication is needed as a result of the control it provides over dosage. To estimate the concentration of drugs at the different compartments, mathematical analysis is used to find optimal solutions to the concentration of the ingested drug. Three-compartment pharmacokinetic model with movement of the drugs from one compartment to another represented by inter-compartmental micro-rate constants k_{ij} is under consideration in this study. The inter-compartmental micro-rate constants k_{ij}, describe the exchange of drugs between the central and the peripheral compartments. The administration of the drug is considered in two cases: I.V. Bolus Injection and I.V. Bolus Infusion. Each compartment has at least two micro-rate constants, one for drug entry and one for drug exit. The micro-rate constants for the model under study are shown in Figure 5.1. We denote the concentration of drugs in the body in compartment i $(i = 1, 2, 3)$ at time by C_1, C_2, and C_3 as the concentrations of drug in the first, second, and third compartments, respectively. $k_{10}, k_{12}, k_{13}, k_{21}$, and k_{31} are the micro-rate constants defining the elimination and inter-compartmental transfer rates. It is assumed that the drug is injected into the plasma at a rate $I(t)$. Therefore, the mathematical model capturing the dynamics in Figure 5.1 is

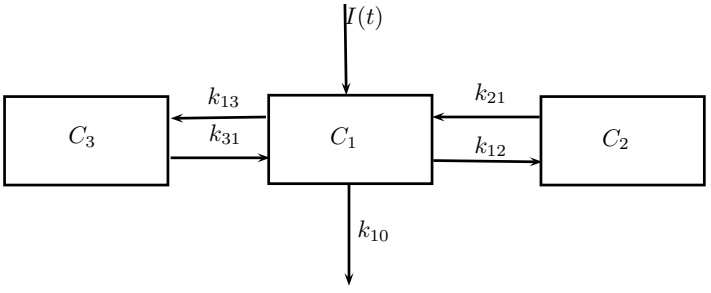

FIGURE 5.1: A three-compartment pharmacokinetic model which assumes that all drug elimination occurs via the central compartment.

$$\begin{cases} \frac{dC_1}{dt} = k_{21}C_2 + k_{31}C_3 - (k_{10} + k_{12} + k_{13})C_1 + I(t) \\ \frac{dC_2}{dt} = k_{12}C_1 - k_{21}C_2 \\ \frac{dC_3}{dt} = k_{13}C_1 - k_{31}C_3. \end{cases} \tag{5.1}$$

Equation (5.1) is a system of linear differential equations. We present the analytical and numerical solutions to this equation for $t > 0$ in the two cases: $I(t) = 0$; $C_1 = C_1(0) = D > 0$, $C_2(0) = 0$, $C_3(0) = 0$ and $I(t) = I_0$ a constant; $C_1(0) = 0$, $C_2(0) = 0$, $C_3(0) = 0$.

Case 1: $I(t) = 0$

In the case where $I(t) = 0$ in Figure 5.1, the drug is given as an I.V. bolus injection into compartment C_1 while exchanges take place with the two other compartments and the drug is excreted from compartment C_1. The I.V. bolus injection method allows the rapid drug administration and ensures that an entire dose enters the general circulation. This type of drug administration technique is given during an emergency to provide an immediate drug effect. The system of differential equations governing from this case are given as

$$\begin{cases} \frac{dC_1}{dt} = k_{21}C_2 - k_{12}C_1 + k_{31}C_3 - k_{13}C_1 - k_{10}C_1 & C_1(0) = D \\ \frac{dC_2}{dt} = k_{12}C_1 - k_{21}C_2 & C_2(0) = 0 \\ \frac{dC_3}{dt} = k_{13}C_1 - k_{31}C_3 & C_3(0) = 0. \end{cases} \tag{5.2}$$

Case 2: $I(t) = I_0$

When $I(t) = I_0$ in Figure 5.1, the drug is administered by I.V. bolus infusion. An I.V. bolus infusion is a controlled administration of medication into the bloodstream over time. In this case, the rate of change in each compartment is represented by a

series of differential equations given as

$$\begin{cases} \frac{dC_1}{dt} = k_{21}C_2 - k_{12}C_1 + k_{31}C_3 - k_{13}C_1 - k_{10}C_1 + I_0 & C_1(0) = 0 \\ \frac{dC_2}{dt} = k_{12}C_1 - k_{21}C_2 & C_2(0) = 0 \\ \frac{dC_3}{dt} = k_{13}C_1 - k_{31}C_3 & C_3(0) = 0. \end{cases} \tag{5.3}$$

We solved differential equations arising from case 1 and case 2 with nonstandard finite difference methods. We then compare the NSFD results with SFD.

5.3 Analytical Solution

In this section, we provide the analytical solutions for systems (5.2) (Case 1) and (5.3) (Case 2), respectively.

5.3.1 Case 1: Analtytical solution

From system (5.2), the denominator determinant B_1 is given by

$$B_1 = \begin{pmatrix} -k_{10} - k_{12} - k_{13} & k_{21} & k_{31} \\ k_{12} & -k_{21} & 0 \\ k_{13} & 0 & -k_{31} \end{pmatrix}. \tag{5.4}$$

We then find a fundamental set of solutions for the matrix B_1 by finding the eigenvalues and the corresponding eigenvectors of matrix B_1. The matrix B_1 has eigenvalues λ such that

$$\lambda^3 + i\lambda^2 + j\lambda + k = 0, \tag{5.5}$$

where

$$i = k_{10} + k_{12} + k_{13} + k_{21} + k_{31}, \tag{5.6}$$

$$j = k_{10}k_{21} + k_{13}k_{21} + k_{10}k_{31} + k_{12}k_{31} + k_{21}k_{31}, \tag{5.7}$$

$$k = k_{10}k_{21}k_{31}. \tag{5.8}$$

Letting $\lambda = x - \frac{i}{3}$ in Equation (5.5), it reduces to

$$x^3 + ax + b = 0, \tag{5.9}$$

where

$$a = \frac{1}{3}(3j - i^2), \qquad \text{and} \qquad b = \frac{1}{27}(2i^3 - 9ij + 27k). \tag{5.10}$$

For the solutions, let

$$\begin{cases} A = \sqrt[3]{-\frac{b}{2} + \sqrt{\frac{b^2}{4} + \frac{a^3}{27}}}, \\ B = -\sqrt[3]{+\frac{b}{2} + \sqrt{\frac{b^2}{4} + \frac{a^3}{27}}}. \end{cases} \tag{5.11}$$

Then the values of x will be given as,

$$\begin{cases} x_1 = A + B, \\ x_2 = -\frac{A+B}{2} + \frac{A-B}{2}\sqrt{-3}, \\ x_3 = -\frac{A+B}{2} - \frac{A-B}{2}\sqrt{-3}. \end{cases} \tag{5.12}$$

Therefore, the eigenvalues of (5.2) are given as

$$\begin{cases} \lambda_1 = A + B - \frac{i}{3}, \\ \lambda_2 = -\frac{A+B}{2} + \frac{A-B}{2}\sqrt{-3} - \frac{i}{3}, \\ \lambda_3 = -\frac{A+B}{2} - \frac{A-B}{2}\sqrt{-3} - \frac{i}{3}. \end{cases} \tag{5.13}$$

We solve system (5.2) using Laplace transforms, such that

$$\begin{cases} (s + k_{10} + k_{12} + k_{13})Q_1 - k_{21}Q_2 - k_{31}Q_3 = D \\ -k_{12}Q_1 + (s + k_{21})Q_2 = 0 \\ -k_{13}Q_1 + (s + k_{31})Q_3 = 0. \end{cases} \tag{5.14}$$

This equations can be written in matrix form as

$$\begin{pmatrix} s + k_{10} + k_{12} + k_{13} & -k_{21} & -k_{31} \\ -k_{12} & s + k_{21} & 0 \\ -k_{13} & 0 & s + k_{31} \end{pmatrix} \begin{pmatrix} Q_1 \\ Q_2 \\ Q_3 \end{pmatrix} = \begin{pmatrix} D \\ 0 \\ 0 \end{pmatrix}. \tag{5.15}$$

Let D_1 be the coefficient matrix of the system (5.15). The determinant of matrix D_1 is

$$D_1 = \begin{vmatrix} s + k_{10} + k_{12} + k_{13} & -k_{21} & -k_{31} \\ -k_{12} & s + k_{21} & 0 \\ -k_{13} & 0 & s + k_{31} \end{vmatrix}, \tag{5.16}$$

$$= s^3 + ps^2 + qs + r,$$

where

$$p = k_{10} + k_{12} + k_{13} + k_{21} + k_{31} \tag{5.17}$$

$$q = k_{10}k_{21} + k_{13}k_{21} + k_{10}k_{31} + k_{12}k_{31} + k_{21}k_{31} \tag{5.18}$$

$$r = k_{10}k_{21}k_{31}. \tag{5.19}$$

We then determine D_{Q_1}– the numerator determinant, D_{Q_2}– the numerator determinant and D_{Q_3}– the numerator determinant. Thus,

$$Q_1(s) = \frac{D_{Q_1}}{D_1}, \quad Q_2(s) = \frac{D_{Q_2}}{D_1} \quad \text{and} \quad Q_3(s) = \frac{D_{Q_3}}{D_1}. \tag{5.20}$$

For D_{Q_1}:

$$D_{Q_1} = \begin{vmatrix} D & -k_{21} & -k_{31} \\ 0 & s+k_{21} & 0 \\ 0 & 0 & s+k_{31} \end{vmatrix}, \tag{5.21}$$

$$= D\,(k_{21}+s)\,.\,(k_{31}+s)$$

Q_1 in Equation (5.14) is the Laplace transform of the drug concentration in compartment C_1 and is given by

$$Q_1(s) = \frac{D\,(k_{21}+s)\,(k_{31}+s)}{s^3+ps^2+qs+r}. \tag{5.22}$$

Taken the inverse Laplace of Equation (5.22) and considering λ_1, λ_2 and λ_3 in Equation (5.13) we have

$$\begin{aligned} \mathcal{L}^{-1}\{Q_1\} = C_1(t) =& D\left(\frac{(-k_{21}\lambda_1 - k_{31}\lambda_1 + \lambda_1^2 + k_{21}k_{31})\,e^{\lambda_1(-t)}}{(\lambda_1-\lambda_2)\,(\lambda_1-\lambda_3)}\right) \\ &+ D\left(\frac{(k_{21}\lambda_3 + k_{31}\lambda_3 - \lambda_3^2 - k_{21}k_{31})\,e^{\lambda_3(-t)}}{(\lambda_1-\lambda_3)\,(\lambda_3-\lambda_2)}\right) \\ &+ D\left(\frac{(k_{21}\lambda_2 + k_{31}\lambda_2 - \lambda_2^2 - k_{21}k_{31})\,e^{\lambda_2(-t)}}{(\lambda_1-\lambda_2)\,(\lambda_2-\lambda_3)}\right). \end{aligned} \tag{5.23}$$

For D_{Q_2}:

$$D_{Q_2} = \begin{vmatrix} s + k_{10} + k_{12} + k_{13} & D & -k_{31} \\ -k_{12} & 0 & 0 \\ -k_{13} & 0 & s + k_{31} \end{vmatrix}, \tag{5.24}$$

$$= Dk_{12}\left(k_{31} + s\right).$$

Q_2 in Equation (5.14) is the Laplace transform of the drug concentration in compartment C_2. We have that

$$Q_2(s) = \frac{Dk_{12}\left(k_{31} + s\right)}{s^3 + ps^2 + qs + r}. \tag{5.25}$$

Taking the inverse Laplace transform of $Q_2(s)$, we have

$$\begin{aligned} \mathcal{L}^{-1}\{Q_2\} = C_2(t) =& Dk_{12}\frac{\left(k_{31} - \lambda_1\right)e^{\lambda_1(-t)}}{\left(\lambda_1 - \lambda_2\right)\left(\lambda_1 - \lambda_3\right)} \\ &- Dk_{12}\frac{\left(k_{31} - \lambda_2\right)e^{\lambda_2(-t)}}{\left(\lambda_1 - \lambda_2\right)\left(\lambda_2 - \lambda_3\right)} \\ &- Dk_{12}\frac{\left(k_{31} - \lambda_3\right)e^{\lambda_3(-t)}}{\left(\lambda_1 - \lambda_3\right)\left(\lambda_3 - \lambda_2\right)}. \end{aligned} \tag{5.26}$$

Finally, for D_{Q_3}, we have $Q_3(s) = \frac{D_{Q_2}}{D_1}$:

$$D_{Q_3} = \begin{vmatrix} s + k_{10} + k_{12} + k_{13} & -k_{21} & D \\ -k_{12} & s + k_{21} & 0 \\ -k_{13} & 0 & 0 \end{vmatrix}, \tag{5.27}$$

$$= Dk_{13}\left(k_{21} + s\right).$$

Q_3 is the Laplace transform of the drug concentration in compartment C_3 and

$$Q_3(s) = \frac{Dk_{13}\,(k_{21}+s)}{s^3+ps^2+qs+r}. \tag{5.28}$$

Taking the inverse Laplace transform of $Q_3(s)$, we have

$$\begin{aligned}\mathcal{L}^{-1}\{Q_3\} = C_3(t) = Dk_{13}\frac{(k_{21}-\lambda_1)\,e^{\lambda_1(-t)}}{(\lambda_1-\lambda_2)\,(\lambda_1-\lambda_3)} - Dk_{13}\frac{(k_{21}-\lambda_2)\,e^{\lambda_2(-t)}}{(\lambda_1-\lambda_2)\,(\lambda_2-\lambda_3)} \\ - Dk_{13}\frac{(k_{21}-\lambda_3)\,e^{\lambda_3(-t)}}{(\lambda_1-\lambda_3)\,(\lambda_3-\lambda_2)}.\end{aligned} \tag{5.29}$$

So, our analytical solution to the three-compartment pharmacokinetic in (5.2) is given by (5.30) - (5.32) below.

$$\begin{aligned}C_1(t) =& D\left(\frac{(-k_{21}\lambda_1 - k_{31}\lambda_1 + \lambda_1^2 + k_{21}k_{31})\,e^{\lambda_1(-t)}}{(\lambda_1-\lambda_2)\,(\lambda_1-\lambda_3)}\right) \\ &+ D\left(\frac{(k_{21}\lambda_3 + k_{31}\lambda_3 - \lambda_3^2 - k_{21}k_{31})\,e^{\lambda_3(-t)}}{(\lambda_1-\lambda_3)\,(\lambda_3-\lambda_2)}\right) \\ &+ D\left(\frac{(k_{21}\lambda_2 + k_{31}\lambda_2 - \lambda_2^2 - k_{21}k_{31})\,e^{\lambda_2(-t)}}{(\lambda_1-\lambda_2)\,(\lambda_2-\lambda_3)}\right).\end{aligned} \tag{5.30}$$

$$\begin{aligned}C_2(t) = Dk_{12}\frac{(k_{31}-\lambda_1)\,e^{\lambda_1(-t)}}{(\lambda_1-\lambda_2)\,(\lambda_1-\lambda_3)} - Dk_{12}\frac{(k_{31}-\lambda_2)\,e^{\lambda_2(-t)}}{(\lambda_1-\lambda_2)\,(\lambda_2-\lambda_3)} \\ - Dk_{12}\frac{(k_{31}-\lambda_3)\,e^{\lambda_3(-t)}}{(\lambda_1-\lambda_3)\,(\lambda_3-\lambda_2)}.\end{aligned} \tag{5.31}$$

$$\begin{aligned}C_3(t) = Dk_{13}\frac{(k_{21}-\lambda_1)\,e^{\lambda_1(-t)}}{(\lambda_1-\lambda_2)\,(\lambda_1-\lambda_3)} - Dk_{13}\frac{(k_{21}-\lambda_2)\,e^{\lambda_2(-t)}}{(\lambda_1-\lambda_2)\,(\lambda_2-\lambda_3)} \\ - Dk_{13}\frac{(k_{21}-\lambda_3)\,e^{\lambda_3(-t)}}{(\lambda_1-\lambda_3)\,(\lambda_3-\lambda_2)}.\end{aligned} \tag{5.32}$$

5.3.2 Case 2: Analtytical Solution

The general solution for system (5.3) is of the form $C(t) = C_p + C_c$, where C_p is a particular solution and C_c is the complementary solution. Recall that the complementary solution is the the general solution of the homogeneous part of system (5.3). To obtain a particular solution for system (5.3), we assume $C_1(t)$,

$C_2(t)$ and $C_3(t)$ to be constant, such that

$$\begin{cases} k_{21}C_2 - k_{12}C_1 + k_{31}C_3 - k_{13}C_1 - k_{10}C_1 + I_0 = 0, \\ k_{12}C_1 - k_{21}C_2 = 0, \\ k_{13}C_1 - k_{31}C_3 = 0. \end{cases} \tag{5.33}$$

From system (5.33), we obtain the particular solution, C_p, of system (5.3) to be

$$C_p = \begin{pmatrix} C_1(t) \\ C_2(t) \\ C_3(t) \end{pmatrix} = \frac{I_0}{k_{10}} \begin{pmatrix} 1 \\ \frac{k_{12}}{k_{21}} \\ \frac{k_{13}}{k_{31}} \end{pmatrix}. \tag{5.34}$$

We find the complementary solution, C_c, for system (5.3) when $I_0 = 0$. Since we have already determined the eigenvalues $(\lambda_1, \lambda_2, \lambda_3)$, we proceed to find the corresponding eigenvector for each eigenvalue as follow;

$$\begin{pmatrix} -k_{10} - k_{12} - k_{13} - \lambda_{1,2,3} & k_{21} & k_{31} \\ k_{12} & k_{21} - \lambda_{1,2,3} & 0 \\ k_{13} & 0 & k_{31} - \lambda_{1,2,3} \end{pmatrix} \begin{pmatrix} V_1 \\ V_2 \\ V_3 \end{pmatrix} = \begin{pmatrix} 0 \\ 0 \\ 0 \end{pmatrix}. \tag{5.35}$$

From Equation (5.35), we have

$$\begin{cases} (-k_{10} - k_{12} - k_{13} - \lambda_{1,2,3})V_1 + k_{21}V_2 + k_{31}V_3 = 0, \\ k_{12}Q_1 + (-k_{21} - \lambda_{1,2,3})V_2 = 0, \\ k_{13}V_1 + (-k_{31} - \lambda_{1,2,3})V_3 = 0. \end{cases} \tag{5.36}$$

Solving system (5.36), we have that

$$\begin{pmatrix} V_1 \\ V_2 \\ V_3 \end{pmatrix} = \begin{pmatrix} 1 \\ \frac{k_{12}}{k_{21}+\lambda_{1,2,3}} \\ \frac{k_{13}}{k_{31}+\lambda_{1,2,3}} \end{pmatrix} = \begin{pmatrix} 1 \\ \beta_{1,2,3} \\ \gamma_{1,2,3} \end{pmatrix}, \tag{5.37}$$

β_i and γ_i written as

$$\begin{pmatrix} \beta_1 \\ \beta_2 \\ \beta_3 \end{pmatrix} = \begin{pmatrix} \frac{k_{12}}{k_{21}+\lambda_1} \\ \frac{k_{12}}{k_{21}+\lambda_2} \\ \frac{k_{12}}{k_{21}+\lambda_3} \end{pmatrix}, \begin{pmatrix} \gamma_1 \\ \gamma_2 \\ \gamma_3 \end{pmatrix} = \begin{pmatrix} \frac{k_{13}}{k_{31}+\lambda_1} \\ \frac{k_{13}}{k_{31}+\lambda_2} \\ \frac{k_{13}}{k_{31}+\lambda_3} \end{pmatrix}. \tag{5.38}$$

The general solution is of the form $C(t) = C_p + C_c$, hence

$$C(t) = \begin{pmatrix} C_1(t) \\ C_2(t) \\ C_3(t) \end{pmatrix} = \frac{I_0}{k_{10}} \begin{pmatrix} 1 \\ \frac{k_{12}}{k_{21}} \\ \frac{k_{13}}{k_{31}} \end{pmatrix} + A_1 e^{\lambda_1 t} \begin{pmatrix} 1 \\ \beta_1 \\ \gamma_1 \end{pmatrix} + A_2 e^{\lambda_2 t} \begin{pmatrix} 1 \\ \beta_2 \\ \gamma_2 \end{pmatrix} + A_3 e^{\lambda_3 t} \begin{pmatrix} 1 \\ \beta_3 \\ \gamma_3 \end{pmatrix}. \tag{5.39}$$

Given the initial condition $\begin{pmatrix} C_1(0) \\ C_2(0) \\ C_3(0) \end{pmatrix} = \begin{pmatrix} 0 \\ 0 \\ 0 \end{pmatrix}$, and using Equation (5.39), we have

$$\begin{cases} \frac{I_0}{k_{10}} + A_1 + A_2 + A_3 = 0 \\ \frac{k_{12}I_0}{k_{10}k_{21}} + A_1\beta_1 + A_2\beta_2 + A_3\beta_3 = 0 \\ \frac{k_{13}I_0}{k_{10}k_{31}} + A_1\gamma_1 + A_2\gamma_2 + A_3\gamma_3 = 0. \end{cases} \tag{5.40}$$

With some trivial algebraic manipulation we find the arbitrary constants A_1, A_2 and A_3

$$A_1 = \frac{I_0(a_1 + a_2)}{k_{10}k_{21}k_{31}d}, \tag{5.41}$$

$$A_2 = \frac{I_0\,(b_1 + b_2)}{k_{10}k_{21}k_{31}d}, \tag{5.42}$$

$$A_3 = -\frac{I_0\,(c_1 + c_2)}{k_{10}k_{21}k_{31}d}, \tag{5.43}$$

where

$$\begin{cases} a_1 = \gamma_2 k_{12}k_{31} - \gamma_3 k_{12}k_{31} - \beta_2 k_{13}k_{21} \\ a_2 = \beta_3 k_{13}k_{21} + \beta_2\gamma_3 k_{21}k_{31} - \beta_3\gamma_2 k_{21}k_{31} \\ b_1 = -\gamma_1 k_{12}k_{31} + \gamma_3 k_{12}k_{31} + \beta_1 k_{13}k_{21} \\ b_2 = -\beta_3 k_{13}k_{21} - \beta_1\gamma_3 k_{21}k_{31} + \beta_3\gamma_1 k_{21}k_{31} \\ c_1 = -\gamma_1 k_{12}k_{31} + \gamma_2 k_{12}k_{31} + \beta_1 k_{13}k_{21} \\ c_2 = -\beta_2 k_{13}k_{21} - \beta_1\gamma_2 k_{21}k_{31} + \beta_2\gamma_1 k_{21}k_{31} \\ d = \beta_2\gamma_1 - \beta_3\gamma_1 - \beta_1\gamma_2 + \beta_3\gamma_2 + \beta_1\gamma_3 - \beta_2\gamma_3. \end{cases} \tag{5.44}$$

final solution is

$$C(t) = \begin{pmatrix} C_1(t) \\ C_2(t) \\ C_3(t) \end{pmatrix} = \frac{I_0}{k_{10}} \begin{pmatrix} 1 \\ \frac{k_{12}}{k_{21}} \\ \frac{k_{13}}{k_{31}} \end{pmatrix} + A_1 e^{\lambda_1 t} \begin{pmatrix} 1 \\ \beta_1 \\ \gamma_1 \end{pmatrix} + A_2 e^{\lambda_2 t} \begin{pmatrix} 1 \\ \beta_2 \\ \gamma_2 \end{pmatrix} + A_3 e^{\lambda_3 t} \begin{pmatrix} 1 \\ \beta_3 \\ \gamma_3 \end{pmatrix}, \tag{5.45}$$

where A_1, A_2 and A_3 are given in (5.41), (5.42) and (5.43) respectively.

5.4 NSFD Scheme

This section provides NSFD schemes for systems (5.2) (case 1) and (5.3) (case 2), respectively.

5.4.1 Case 1: NSFD Scheme

System (5.2) can be written as

$$\begin{bmatrix} C_1 \\ C_2 \\ C_3 \end{bmatrix}' = \begin{bmatrix} -k_{10} - k_{12} - k_{13} & k_{21} & k_{31} \\ k_{12} & k_{21} & 0 \\ k_{13} & 0 & k_{31} \end{bmatrix} \begin{bmatrix} C_1 \\ C_2 \\ C_3 \end{bmatrix} \tag{5.46}$$

$$C' = A \quad C. \tag{5.47}$$

$C \in \mathbb{R}^3$ and A is a 3×3 matrix with constant coefficients of system (5.2). We denote the eigenvalues of A by α, β and γ.

Theorem 5.1 (Dang, 2017)**.** *Let A be any 3×3 matrix. Then, A is similar to the Jordan form matrices J of A depending on the set of its eigenvalues and the dimension of eigenspaces associated with the eigenvalues. Here, $\sigma(A)$ is the set of eigenvalues, $\chi_A(t)$ and $m_A(t)$ are characteristic and minimal polynomials of A, respectively.*

In our work, we only considered the case where matrix A has three distinct eigenvalues. The eigenvalues usually differ in size by about an order of magnitude. For Equation (5.47), the resulting Jordan system is

$$C' = JC, \tag{5.48}$$

where

$$J = \begin{pmatrix} \alpha & 0 & 0 \\ 0 & \beta & 0 \\ 0 & 0 & \gamma \end{pmatrix}. \tag{5.49}$$

The NSFD scheme for system (5.33) can be written as [95]

$$\frac{C_{k+1} - \psi C_k}{\phi} = A\left[\theta C_{k+1} + (1-\theta)C_k\right]. \tag{5.50}$$

Equation (5.50) can be transformed in terms of the Jordan matrix into

$$\frac{C_{k+1} - \psi C_k}{\phi} = J\left[\theta C_{k+1} + (1-\theta)C_k\right], \tag{5.51}$$

which is the NSFD scheme for Equation (5.48). ψ, ϕ and θ are obtained by solving Equations (5.48) and (5.51) with $\alpha, \beta, \gamma \neq 0$. This can be solved immediately since it decouples into three unrelated first-order equations. Equation (5.48) is written to the form

$$\begin{pmatrix} C_1 \\ C_2 \\ C_3 \end{pmatrix}' = \begin{pmatrix} \alpha & 0 & 0 \\ 0 & \beta & 0 \\ 0 & 0 & \gamma \end{pmatrix} \begin{pmatrix} C_1 \\ C_2 \\ C_3 \end{pmatrix}, \tag{5.52}$$

with initial conditions

$$\begin{pmatrix} C_1(t_0) \\ C_2(t_0) \\ C_3(t_0) \end{pmatrix} = \begin{pmatrix} C_1(0) \\ C_2(0) \\ C_3(0) \end{pmatrix}. \tag{5.53}$$

Making the following substitutions;

$$\begin{cases} t_0 \to t_k = hk, \\ t \to t_{k+1} = h(k+1), \\ C_0 \to C_k, \\ C(t) \to C_{k+1}, \end{cases} \tag{5.54}$$

we have exact scheme of Equation (5.52) to be

$$\begin{pmatrix} C_{1,k+1} \\ C_{2,k+1} \\ C_{3,k+1} \end{pmatrix} = \begin{pmatrix} C_{1,k}e^{\alpha h} \\ C_{2,k}e^{\beta h} \\ C_{3,k}e^{\gamma h} \end{pmatrix}. \tag{5.55}$$

Equation (5.51) can be written as

$$\begin{pmatrix} \frac{C_{1,k+1}-\psi C_{1,k}}{\phi} \\ \frac{C_{2,k+1}-\psi C_{2,k}}{\phi} \\ \frac{C_{3,k+1}-\psi C_{3,k}}{\phi} \end{pmatrix} = \begin{pmatrix} \alpha\left[\theta C_{1,k+1} + (1-\theta)C_{1,k}\right] \\ \beta\left[\theta C_{2,k+1} + (1-\theta)C_{2,k}\right] \\ \gamma\left[\theta C_{3,k+1} + (1-\theta)C_{3,k}\right] \end{pmatrix}. \tag{5.56}$$

Rearranging Equation (5.56), we have

$$\begin{pmatrix} C_{1,k+1} \\ C_{2,k+1} \\ C_{3,k+1} \end{pmatrix} = \begin{pmatrix} \frac{(\psi+\phi(1-\theta))C_{1,k}}{1-\phi\alpha\theta} \\ \frac{(\psi+\phi(1-\theta))C_{2,k}}{1-\phi\beta\theta} \\ \frac{(\psi+\phi(1-\theta))C_{3,k}}{1-\phi\gamma\theta} \end{pmatrix} \tag{5.57}$$

Equating Equations (5.55) and (5.57), we have

$$\begin{cases} e^{\alpha h} = \dfrac{\psi + \phi(1-\theta)}{1 - \phi\alpha\theta} \\ e^{\beta h} = \dfrac{\psi + \phi(1-\theta)}{1 - \phi\beta\theta} \\ e^{\gamma h} = \dfrac{\psi + \phi(1-\theta)}{1 - \phi\gamma\theta}. \end{cases} \tag{5.58}$$

Solving for ψ, ϕ and θ in system (5.58), we have

$$\begin{cases} \psi = \frac{\beta\gamma e^{h\alpha}\left(e^{h\beta}-e^{h\gamma}\right)+\alpha\left(\beta e^{h\gamma}\left(e^{h\alpha}-e^{h\beta}\right)-\gamma e^{h\beta}\left(e^{h\alpha}-e^{h\gamma}\right)\right)}{\beta\gamma\left(e^{h\beta}-e^{h\gamma}\right)+\alpha\left(\beta\left(e^{h\alpha}-e^{h\beta}\right)-\gamma\left(e^{h\alpha}-e^{h\gamma}\right)\right)} \\ \phi = \frac{\alpha\left(e^{h\alpha}-1\right)\left(e^{h\beta}-e^{h\gamma}\right)-\beta\left(e^{h\beta}-1\right)\left(e^{h\alpha}-e^{h\gamma}\right)+\gamma\left(e^{h\alpha}-e^{h\beta}\right)\left(e^{h\gamma}-1\right)}{\beta\gamma\left(e^{h\beta}-e^{h\gamma}\right)+\alpha\left(\beta\left(e^{h\alpha}-e^{h\beta}\right)-\gamma\left(e^{h\alpha}-e^{h\gamma}\right)\right)} \\ \theta = \frac{\alpha\left(e^{h\gamma}-e^{h\beta}\right)+\beta\left(e^{h\alpha}-e^{h\gamma}\right)-\gamma\left(e^{h\alpha}-e^{h\beta}\right)}{\alpha\left(e^{h\alpha}-1\right)\left(e^{h\beta}-e^{h\gamma}\right)-\beta\left(e^{h\beta}-1\right)\left(e^{h\alpha}-e^{h\gamma}\right)+\gamma\left(e^{h\alpha}-e^{h\beta}\right)\left(e^{h\gamma}-1\right)}. \end{cases} \tag{5.59}$$

Therefore, the 'exact' finite difference scheme is given by

$$\begin{cases} \frac{C_{1_{k+1}}-\psi C_{1_k}}{\phi} = (-k_{10}-k_{12}-k_{13})\left(\theta C_{1_{k+1}} + (1-\theta)C_{1_k}\right) + \\ k_{21}\left(\theta C_{2_{k+1}} + (1-\theta)C_{2_k}\right) + k_{31}\left(\theta C_{3_{k+1}} + (1-\theta)C_{3_k}\right) \\ \frac{C_{2_{k+1}}-\psi C_{2_k}}{\phi} = k_{12}\left(\theta C_{1_{k+1}} + (1-\theta)C_{1_k}\right) - \\ k_{21}\left(\theta C_{2_{k+1}} + (1-\theta)C_{2_k}\right) \\ \frac{C_{3_{k+1}}-\psi C_{3_k}}{\phi} = k_{13}\left(\theta C_{1_{k+1}} + (1-\theta)C_{1_k}\right) - \\ k_{31}\left(\theta C_{3_{k+1}} + (1-\theta)C_{3_k}\right), \end{cases} . \tag{5.60}$$

ϕ and ψ satisfy the necessary asymptotic properties equations (2.29) and (2.32) respectively and θ has asymptotic behaviour of the form

$$\theta(h) = \frac{1}{2} + \mathcal{O}(h). \tag{5.61}$$

Exact scheme (5.60) has exactly the same qualitative behaviour as the corresponding solution of the differential equation and it follows that the scheme will not have numerical instabilities for any step-size. Exact scheme (5.60) is compared with

SFD scheme:

$$\begin{cases} \frac{C_{1_{k+1}}-C_{1_k}}{h} = k_{21}C_{2_k} - k_{12}C_{1_k} + k_{31}C_{3_k} - k_{13}C_{1_k} - k_1C_{1_k} & C_1(0) = D \\ \frac{C_{2_{k+1}}-C_{2_k}}{h} = k_{12}C_{1_k} - k_{21}C_{2_k} & C_2(0) = 0 \\ \frac{C_{3_{k+1}}-C_{3_k}}{h} = k_{13}C_{1_k} - k_{31}C_{3_k} & C_3(0) = 0. \end{cases} \tag{5.62}$$

5.4.2 Case 2: NSFD Scheme

Our main aim in this section is to apply NSFD method to construct NSFD scheme for system (5.3). Models (5.3) represent the concentration of drug in the body in each compartment, it is necessary that the numerical schemes satisfy the Conservation Law [96]. Also, the NSFD schemes must preserve other properties of the continuous model for larger step sizes that some times the traditional schemes such as forward Euler, Runge–Kutta and others do not for extreme values in the parameters of the models [12]. We begin by adding system (5.3) and we obtained the conservation law [27, 96, 97]

$$\begin{aligned} -k_{10}(C_1 + C_2 + C_3) + I_0 \leq \frac{d}{dt}(C_1 + C_2 + C_3) \\ = -k_{10}P + I_0. \end{aligned} \tag{5.63}$$

When $P = C_1 + C_2 + C_3$, then

$$\frac{dP}{dt} \geq -k_{10}P + I_0, \tag{5.64}$$

we then get the conservation law giving by

$$\frac{dP}{dt} = -k_{10}P + I_0. \tag{5.65}$$

Equation (5.65) is the conservation law associated equation system (5.3). First it should be noted that Equation (5.65) is similar to the one compartment I.V

infusion model which the 'exact' finite difference as been determined to be

$$\frac{P_{k+1} - P_k}{\phi(h)} = I_0 - k_{10}P_k. \tag{5.66}$$

Equation (5.66) is the 'exact' finite difference scheme of (5.65). Where the denominator function $\phi(h)$ is

$$\phi(h) = \frac{1 - e^{-k_{10}h}}{k_{10}}. \tag{5.67}$$

ϕ is a denominator function which is a real-valued function and satisfies

$$\phi(h) = \phi + \mathcal{O}(h^2), \qquad \forall \quad h > 0. \tag{5.68}$$

It should be noted that system (5.3) has the mathematical structure required for positivity condition, i.e, for any non-negative initial condition, the iterations must remain non-negative [97]. Therefore, the negative part in the right-hand side of the differential model (5.3) is then dealt with by nonlocal approximation as shown in equation (5.73). Thus, $C_i (i = 1, 2, 3)$ from system (5.3) has the properties

$$\begin{cases} C_1 = C_{1,0} \geq 0, \\ C_2 = C_{2,0} \geq 0, \\ C_3 = C_{3,0} \geq 0, \end{cases} \tag{5.69}$$

equation (5.69) implies that

$$\begin{cases} C_1(t) \geq 0, \\ C_2(t) \geq 0, \\ C_3(t) \geq 0, \end{cases} \tag{5.70}$$

for $t > 0$. This called positivity condition. Consider the following discretization,

$$\begin{cases} t_0 \to t_k = hk, \\ t \to t_{k+1} = h(k+1), \\ C_1(t) \to C_{1,k}, \\ C_2(t) \to C_{2,k}, \\ C_3(t) \to C_{3,k}. \end{cases} \tag{5.71}$$

The positivity conditions, as stated in systems (5.69) and (5.70), translates to the discrete time situations as follows

$$\begin{cases} C_{1,k} \geq 0, \\ C_{2,k} \geq 0, \\ C_{3,k} \geq 0, \\ C_{1,k+1} \geq 0, \\ C_{2,k+1} \geq 0, \\ C_{3,k+1} \geq 0. \end{cases} \tag{5.72}$$

Using the notations above, we propose the following NSFD scheme to system (5.3) that follows the requirement of positivity. For example, because of positivity property, the $(-k_{10}C_1)$ term is discretized by the expression $(-k_{10}C_{1,k+1})$, $(-k_{21}C_1)$ as $(-k_{21}C_{2,k+1})$ and $(-k_{31}C_3)$ as $(-k_{31}C_{3,k+1})$.

$$\begin{cases} \frac{C_{1,k+1}-C_{1,k}}{\phi(h)} = k_{21}C_{2,k+1} + k_{31}C_{3,k+1} + I_0 - (k_{10}+k_{12}+k_{13})C_{1,k+1}, \\ \frac{C_{2,k+1}-C_{2,k}}{\phi(h)} = k_{12}C_{1,k+1} - k_{21}C_{2,k+1}, \\ \frac{C_{3,k+1}-C_{3,k}}{\phi(h)} = k_{13}C_{1,k+1} - k_{31}C_{3,k+1}, \end{cases} \tag{5.73}$$

where $\phi(h)$ is given in Equation (5.67). The same terms that occurs in each of the differential equations (5.3) are modeled discretely the same way in all equations (5.73) to preserved the conversation law. Therefore, the system of Equation (5.73) is the NSFD scheme for system (5.3) and it can be solved using the following concept

$$\begin{cases} (1+\phi k_{12}+\phi k_{13}+\phi k_{10})C_{1,k+1}-\phi k_{21}C_{2,k+1}-\phi k_{31}C_{3,k+1}=C_{1,k}+I_0, \\ -\phi k_{12}C_{1,k+1}+(1+\phi k_{21})C_{2,k+1}=C_{2,k}, \\ -\phi k_{13}C_{1,k+1}+(1+\phi k_{31})C_{3,k+1}=C_{3,k}. \end{cases} \tag{5.74}$$

The NSFD scheme (5.74) preserves conservation law while the exact scheme also preserve conservation law. Transforming system (5.74) into matrix form, we have a non-singular matrix

$$\begin{pmatrix} 1+\phi k_{12}+\phi k_{13}+\phi k_{10} & -\phi k_{21} & -\phi k_{31} \\ -\phi k_{12} & 1+\phi k_{21} & 0 \\ -\phi k_{13} & 0 & 1+\phi k_{31} \end{pmatrix} \begin{pmatrix} C_{1,k+1} \\ C_{2,k+1} \\ C_{3,k+1} \end{pmatrix} = \begin{pmatrix} C_{1,k}+\phi I_0 \\ C_{2,k} \\ C_{3,k} \end{pmatrix}. \tag{5.75}$$

Thus the concentration in each compartments is obtained by

$$\begin{pmatrix} C_{1,k+1} \\ C_{2,k+1} \\ C_{3,k+1} \end{pmatrix} = \begin{pmatrix} 1+\phi k_{12}+\phi k_{13}+\phi k_{10} & -\phi k_{21} & -\phi k_{31} \\ -\phi k_{12} & 1+\phi k_{21} & 0 \\ -\phi k_{13} & 0 & 1+\phi k_{31} \end{pmatrix}^{-1} \begin{pmatrix} C_{1,k}+\phi I_0 \\ C_{2,k} \\ C_{3,k} \end{pmatrix}. \tag{5.76}$$

For every positive initial value in Equation (5.76), C_1, C_2 and C_3 are positive since all parameters are positive constants. This is compare with SFD

$$\begin{cases} \frac{C_{1_{k+1}}-C_{1_k}}{h} = k_{21}C_{2_k} - k_{12}C_{1_k} + k_{31}C_{3_k} - k_{13}C_{1_k} - k_{10}C_{1_k} + I_0 \\ \frac{C_{2_{k+1}}-C_{2_k}}{h} = k_{12}C_{1_k} - k_{21}C_{2_k} \\ \frac{C_{3_{k+1}}-C_{3_k}}{h} = k_{13}C_{1_k} - k_{31}C_{3_k}. \end{cases} \tag{5.77}$$

5.5 Numerical Verifications and Comparison with other Schemes

All simulations were performed using MATLAB R2016b, and all model parameters used for simulation are provided in Table 5.1. We perform numerical simulations with different step sizes for the given parameter values in Table 5.1. The NSFD schemes are compare with SFD schemes and MATLAB ODE45. In the case of the three compartment model with I.V. bolus injection, the NSFD scheme produces

'exact' solution as these results are presented in Table 5.2- 5.4, Figures 5.2 and 5.3. In the case of the three compartment model with I.V. bolus infusion, the discretization using the SFD scheme produces a solution that does not converge to the steady state for a large step sizes as expect for this method. The NSFD scheme is consistent with the original system and is 'exact' for various step-sizes.

The results presented in the Table 5.2- 5.4 shows that the NSFD method is 'exact' for varies step sizes. Furthermore, The NSFD scheme are plotted for various step sizes in comparison with the SFD methods in Figures 3.17(a-c) and 3.13(a-c).

TABLE 5.2: The absolute error results for the system of equations given in Equation (5.2) for C_1 with parameter values in Table 5.1.

Maximum Error for C_1			
h	**Error in SFD**	**Error in ODE45**	**Error in NSFD**
1.00000	0.767610788	0.000000095	0.000000000
0.80000	0.547731359	0.000000159	0.000000000
0.60000	0.384525602	0.000000154	0.000000000
0.20000	0.112502579	0.000000021	0.000000000
0.02000	0.003338835	0.000000000	0.000000000

TABLE 5.3: The absolute error results for the system of equations given in Equation (5.2) for C_2 with parameter values in Table 5.1.

Maximum Error for C_2			
h	**Error in SFD**	**Error in ODE45**	**Error in NSFD**
1.00000	0.519334219	0.000000064	0.000000000
0.80000	0.369577553	0.000000108	0.000000000
0.60000	0.259767851	0.000000104	0.000000000
0.20000	0.075882694	0.000000014	0.000000000
0.02000	0.002259534	0.000000000	0.000000000

TABLE 5.4: The absolute error results for the system of equations given in Equation (5.2) for C_3 with parameter values in Table 5.1.

Maximum Error for C_3			
h	**Error in SFD**	**Error in ODE45**	**Error in NSFD**
1.00000	0.044438034	0.000000005	0.000000000
0.80000	0.031930115	0.000000009	0.000000000
0.60000	0.022346658	0.000000009	0.000000000
0.20000	0.0065701884	0.000000001	0.000000000
0.02000	0.000193153	0.000000000	0.000000000

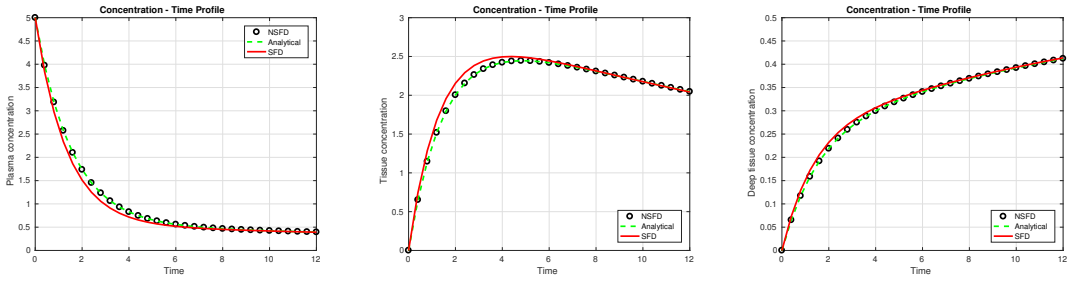

(a) C_1 (b) C_2 (c) C_3

FIGURE 5.2: *The NSFD scheme (5.60) plotted against the exact scheme (5.30) - (5.32) and SFD scheme (5.62) showing concentration of the drug in each compartment for a small time interval ($h = 0.4000$).*

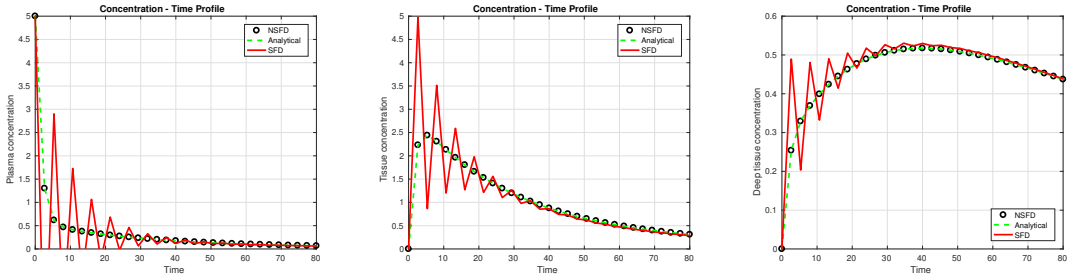

(a) C_1 (b) C_2 (c) C_3

FIGURE 5.3: *The NSFD scheme (5.60) plotted against the exact scheme (5.30) - (5.32) and SFD scheme (5.62) showing concentration of the drug in each compartment for a large time interval ($h = 2.6667$).*

The results for the three-compartment pharmacokinetic model with I.V. bolus infusion in Equation (5.3) are shown for different step sizes in Figures 5.4 and 5.5. Figure 5.4 shows results for a small step size ($h = 0.03$). All the methods are dynamically consistent with the physical observation of the system. However, when the step is considerable large ($h = 0.8299$) as shown in Figure 5.5, the SFD scheme

introduce extraneous solution (or spurious solution) while the NSFD replicate the dynamics of the system for any step size. Many simulations were carried out for various step sizes. In all cases, the NSFD results were consistent with all the step sizes and reflect the long-term behaviour of the continuous-time system accurately.

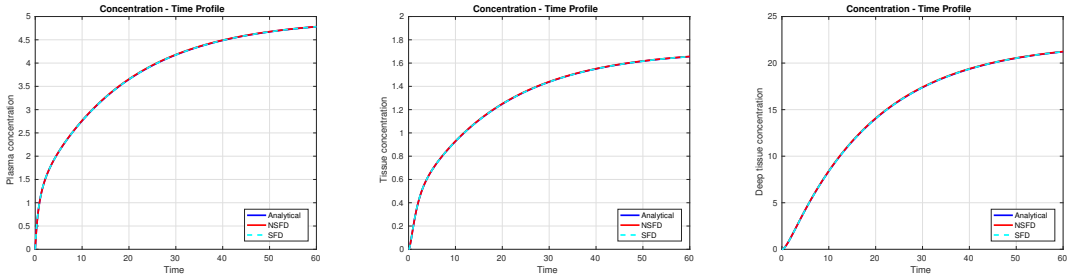

(a) C_1 (b) C_2 (c) C_3

FIGURE 5.4: *The NSFD scheme (5.73) plotted against the exact scheme (5.45) and SFD scheme (5.77) showing concentration of the drug in each compartment for a small time interval ($h = 0.03$). We observe for this step size, all the methods considered mimic the dynamic properties of the differential equation.*

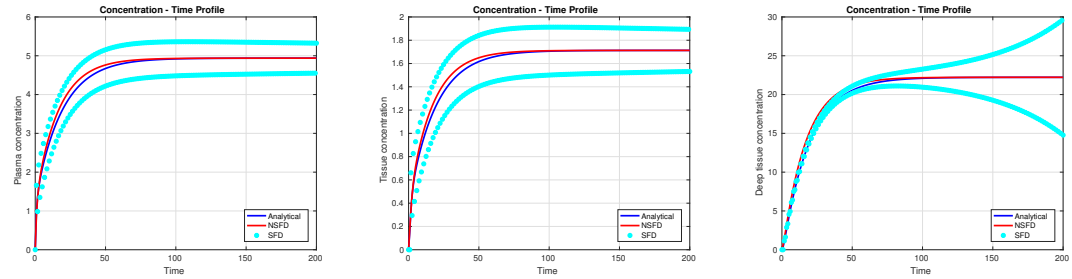

(a) C_1 (b) C_2 (c) C_3

FIGURE 5.5: *The NSFD scheme (5.73) plotted against the exact scheme (5.45) and SFD scheme (5.77) showing concentration of the drug in each compartment for a large time interval ($h = 0.8299$). We observe for this step size, the SFD method could not mimic the dynamic properties of the differential equation as it introduce spurious solution.*

The NSFD method results are very interesting and consistent with the physical interpretation of the systems under consideration. There is agreement between the NSFD results and the analytical results for different step sizes as shown in Figures 5.4 and 5.5. This further confirms the efficiency of the NSFD as a method of choice. We have seen from Figure 5.5 that when the step sizes in considerable large, the use of SFD method is not suitable as it introduced solutions that do not correspond exactly to solutions of the differential equations.

5.6 Conclusion

A NSFD method for the determination of the drug concentration in each of the three compartments at any time has been developed. Three-compartmental pharmacokinetic models are considered as the one depicted in Figure 5.1. The NSFD method is employed to find the time-course of drug concentrations in any given compartment of a three-compartment pharmacokinetic model. The first model is an I.V. bolus injection three-compartment model, while the second model is an I.V. infusion three-compartment model. For the first model, we present 'exact' finite difference scheme and the scheme produces exact results for various step-sizes. In the second model, we produce a scheme that is dynamically consistent with the original models. Several simulations were performed for different step sizes. The simulations shows that the SFD methods are consistent only for a very small step sizes. For comparatively large step sizes, it could not mimic the dynamic properties of the differential equation as it introduces spurious solution and numerical instabilities occur. The NSFD scheme is dynamically consistent with any step size and produces reliable numerical simulations that preserved the stability and positivity properties of the exact solution. NSFD are consistent with physical observations and our NSFD schemes allows large time steps. This saves the computational costs when integrating the system over a long time periods. The NSFD could be easily expanded to the PK models with more complex structure (e.g., having more than 3 compartments).

Chapter 6

Mathematical Analysis of Target-mediated Drug Disposition Models using Non-standard Finite Difference Methods

"In most sciences one generation tears down what another has built, and what one has established, another undoes. In mathematics alone each generation adds a new storey to the old structure."

Hermann Hankel

The work in this chapter has been submitted to Mathematical Biosciences.

6.1 Introduction

In the conventional pharamcokinetic-phamacodynamic system the amount of drug-target complex does not reflect in the pharmacokinetic characteristics of the drug. This implies that the plasma concentrations are modelled and then fixed as driving

functions in an appropriate pharmacodynamic model. In other words, it is assumed that the amount of the drug interacting with a pharmacological target is negligible and does not affect the pharmacokinetic profile [54]. Hence, studies of the rat tissues shed more light on this assumption. Levy [98] encountered high-affinity binding to pharmacokinetic target sites in his studies of the pharmacokinetic of warfarin in rats. Consequently, inferring from plasma concentration-time profiles that high-infinity binding to pharmacokinetic target sites is negligible is not appropriate; rather such an amount of drug-target complex does influence the pharmacokinetic characteristics of the drug.

Levy [98] used the term target mediated drug disposition (TMDD) to describe his observation that a drug is bound with high affinity and to a significant extent to its pharmacologic target sites such as receptors and enzymes. The first pharmacokinetic model exhibiting TMDD was formulated by Mager et al. [54]. Since then, several researchers have applied TMDD to various drugs ranging from small molecular weight compounds to relatively large proteins. Aston et al. [1] gives a compartmentalization representation of the physiological-based approach described by Levy [98] and they provide mathematical analysis with regard to the relationship between the target affinity of a monoclonal antibody (mAb) versus its in vivo potency. In this Chapter, we design NSFD scheme to gain insight into one and two-compartment TMDD models using the concept from Egbelowo [99]. We explore the dynamics of scheme design to preserve the quantitative properties of the original model. Also, global sensitivity analysis is carried out to determine the effect of each parameter on the model.

6.2 One-compartment TMDD Model

A bolus injection L_0 at the time zero of the ligand L (drug) is administered into the central compartment binds at a constant rate K_{on}, to the receptor R (or enzymatic sites) to form a ligand-receptor complex P. The ligand-receptor complex P may dissociate at the constant K_{off} and the unbound ligand will be directly eliminated

TABLE 6.1: Values and ranges for parameters for the one and two-compartment TMDD models, (6.1) and (6.17).

Parameter	Unit	Value	Source
$K_{e(L)}$	day^{-1}	0.0240	[1]
$K_{e(P)}$	day^{-1}	0.2010	[1]
K_{out}	day^{-1}	0.8230	[1]
K_{off}	day^{-1}	0.9000	[1]
K_{on}	$(nMday)^{-1}$	0.5920	[1]
K_{in}	$nMday^{-1}$	2.2122	[1]
K_{pt}	day^{-1}	0.0920	Assumed
K_{tp}	day^{-1}	0.0900	Assumed

at a constant rate $K_{e(L)}$. The elimination rate of the undissociated ligand-receptor complex is $K_{e(P)}$ while the receptor turnover and elimination are K_{in} and K_{out} respectively.

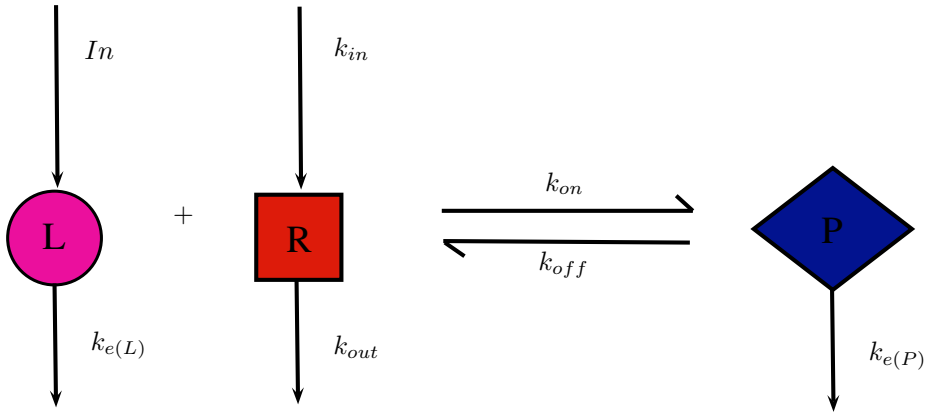

FIGURE 6.1: One-compartment TMDD reaction model [1].

The system described in Figure 6.1 can be defined by the following system of differential equations:

$$\begin{cases} \frac{dL}{dt} = -K_{e(L)}L - K_{on}LR + K_{off}P, \\ \frac{dR}{dt} = K_{in} - K_{out}R - K_{on}LR + K_{off}P, \\ \frac{dP}{dt} = K_{on}LR - K_{off}P - K_{e(P)}P. \end{cases} \tag{6.1}$$

Equation (6.1) is supplemented with the initial conditions by adding the bolus injection gives:

$$L(0) = L_0, \qquad R(0) = R_0 = \frac{K_{in}}{K_{out}}, \qquad P(0) = 0. \tag{6.2}$$

6.2.1 Mathematical Analysis of One-compartment TMDD Model

Positivity of Solutions

Theorem 6.1. *Let the initial data for the model (6.1) be $L(0)$, $R(0)$, $P(0) > 0$, then the solutions $L(t)$, $R(t)$, $P(t)$ of the model (6.1) are non-negative $\forall t \geq 0$.*

Proof. Suppose $L(t)$ non-positive, then there exists a first time, say $t^* > 0$, such that $L(t) > 0$ for $t \in [0, t^*)$ and $L(t^*) = 0$. By an inspection of equation $P(t)$ in (6.1), we have that

$$\frac{dP}{dt} \geq -(K_{off} + K_{e(P)})P, \quad \text{for} \quad t \in [0, t^*),$$

which gives

$$P(t) \geq KP(0)exp\left(-K_{off}t - K_{e(P)}t\right) \geq 0, \quad \text{for} \quad t \in [0, t^*).$$

Thus, it is clear from the first equation of model (6.1) that

$$\frac{dL}{dt} \geq -(K_{e(L)}L + K_{on}LR), \quad \text{for} \quad t \in [0, t^*)$$

with trivial algebraic manipulation and integration, we have that

$$\ln|L| \geq -\left(\int_0^t K_{on}Rdu + K_{e(L)}t + k\right),$$

therefore,

$$L(t) \geq KL(0)exp\left(-\int_0^t K_{on}Rdu - K_{e(L)}t\right) \geq 0, \quad \text{for} \quad t \in [0, t^*).$$

It follows that $L(t^*) > 0$, which contradicts $L(t^*) = 0$. Hence $L(t)$ is positive. It can be shown, using similar approach as that for $L(t)$, that $R(t) > 0$ and $P(t) > 0$. □

Steady state

We identify the biologically and non-biological relevant steady state of (6.1). We determine the stability of the biologically possible steady state. We identify the existence of two steady state analytically and confirm the existence of a single biologically relevant non-zero steady state. The first steady state of system is given by E_0:

$$L = 0, \quad R = \frac{k_{\text{in}}}{k_{\text{out}}}, \quad P = 0. \tag{6.3}$$

Notice that this equilibrium corresponds to the drug free equilibrium hypothetical situation in which there is no drug in the system. The second steady state is given by E_1:

$$L = \frac{-k_{\text{el}}k_{\text{ep}}k_{\text{out}} - k_{\text{el}}k_{\text{off}}k_{\text{out}} - k_{\text{ep}}k_{\text{in}}k_{\text{on}}}{k_{\text{el}}k_{\text{ep}}k_{\text{on}}}, \quad R = -\frac{k_{\text{el}}\left(k_{\text{ep}} + k_{\text{off}}\right)}{k_{\text{ep}}k_{\text{on}}}, \tag{6.4}$$
$$P = \frac{k_{\text{el}}k_{\text{ep}}k_{\text{out}} + k_{\text{el}}k_{\text{off}}k_{\text{out}} + k_{\text{ep}}k_{\text{in}}k_{\text{on}}}{k_{\text{ep}}^2k_{\text{on}}}.$$

Since all of the parameters are positive values, then E_1 is not biologically possible. Therefore, stability analysis of E_0 will only be carried out.

Theorem 6.2. *The steady state (6.3) of (6.1) is locally asymptotically stable.*

The Jacobian matrix J of system (6.1) is derived in other to determine the stability of the steady state. Evaluating the Jacobian matrix J of system (6.1) at the steady

state $E_0 = (0, \frac{k_{\text{in}}}{k_{\text{out}}}, 0)$, one obtain

$$J(E_0) = \begin{pmatrix} -k_{\text{el}} - \frac{k_{0\text{n}} k_{\text{in}}}{k_{\text{out}}} & 0 & k_{\text{off}} \\ -\frac{k_{0\text{n}} k_{\text{in}}}{k_{\text{out}}} & -k_{\text{out}} & k_{\text{off}} \\ \frac{k_{0\text{n}} k_{\text{in}}}{k_{\text{out}}} & 0 & -k_{\text{ep}} - k_{\text{off}} \end{pmatrix} \tag{6.5}$$

In this case, the eigenvalues are

$$\begin{cases} \lambda_1 = -k_{out} \\ \lambda_2 = \frac{-\sqrt{\left(k_{el}k_{out}+k_{ep}k_{out}+k_{in}k_{on}+k_{off}k_{out}\right)^2-4\left(k_{el}k_{ep}k_{out}^2+k_{el}k_{off}k_{out}^2+k_{ep}k_{in}k_{on}k_{out}\right)}-k_{el}k_{out}-k_{ep}k_{out}-k_{in}k_{on}-k_{off}k_{out}}{2k_{out}} \\ \lambda_3 = \frac{\sqrt{\left(k_{el}k_{out}+k_{ep}k_{out}+k_{in}k_{on}+k_{off}k_{out}\right)^2-4\left(k_{el}k_{ep}k_{out}^2+k_{el}k_{off}k_{out}^2+k_{ep}k_{in}k_{on}k_{out}\right)}-k_{el}k_{out}-k_{ep}k_{out}-k_{in}k_{on}-k_{off}k_{out}}{2k_{out}} \end{cases} \tag{6.6}$$

Since all of the parameter values are positive, we notice that the eigenvalues of the Jacobian matrix evaluated at the steady state E_0 are all real and negative indicative of a steady state that is locally asymptotically stable.

6.2.2 Construction and Analysis of the NSFD

We design NSFD scheme for the system (6.1) which has the similar quantitative properties as the continuous-time model (6.1). The NSFD scheme is constructed by replacing the classical denominator h in the derivatives of model (6.1) with a function $\phi(h) = h + \mathcal{O}(h^2)$. For example, the conventional denominator h of the derivative for L(t) in model (6.1):

$$\frac{dL}{dt} \to \frac{L_{k+1} - L_k}{h} + \mathcal{O}(h) \quad \text{as} \quad h \to 0, \tag{6.7}$$

is replaced by

$$\frac{dL}{dt} \to \frac{L_{n+1} - L_n}{\phi(h)} + \mathcal{O}(\phi(h)) \quad \text{as} \quad h \to 0, \tag{6.8}$$

where $\phi(h)$ is a nonnegative function given by

$$\phi(h) = h + \mathcal{O}(h^2). \tag{6.9}$$

Since a conservation law does not exists, the denominator function for each equation in (6.1) will be different. Using the above notations and terminology, we propose the following explicit NSFD scheme

$$\begin{cases} \frac{L_{n+1}-L_n}{\phi_1(h)} = -K_{e(L)}L_n - K_{on}L_{n+1}R_n + K_{off}P_n, \\ \frac{R_{n+1}-R_n}{\phi_2(h)} = K_{in} - K_{out}R_n - K_{on}L_{n+1}R_n + K_{off}P_n, \\ \frac{P_{n+1}-P_n}{\phi_3(h)} = K_{on}L_{n+1}R_n - K_{off}P_n - K_{e(P)}P_n. \end{cases} \tag{6.10}$$

Whereas, a possible explicit-implicit scheme of the model is given as

$$\begin{cases} \frac{L_{n+1}-L_n}{\phi_4(h)} = -K_{e(L)}L_{n+1} - K_{on}L_{n+1}R_n + K_{off}P_n, \\ \frac{R_{n+1}-R_n}{\phi_5(h)} = K_{in} - K_{out}R_{n+1} - K_{on}L_{n+1}R_n + K_{off}P_n, \\ \frac{P_{n+1}-P_n}{\phi_6(h)} = K_{on}L_{n+1}R_n - K_{off}P_{n+1} - K_{e(P)}P_{n+1}, \end{cases} \tag{6.11}$$

with initial data approximated as

$$L_n = L_n(t_n) \geq 0, \quad R_n = R_n(t_n) \geq 0 \quad P_n = P_n(t_n) = 0. \tag{6.12}$$

The two NSFD schemes above are two of the many possible NSFD schemes for equation (6.1). The non-linear terms in model (6.1) are approximated in a non-local way to arrive at the explicit and explicit-implicit schemes (6.10) and (6.11) respectively. These leads to different denominator function for the schemes (6.10) and (6.11). The denominator function depend on the scheme. In this study, the denominator functions for explicit scheme (6.10) are considered to be

$$\begin{cases} \phi_1(h, K_{e(L)}) = \dfrac{1 - e^{-hK_{e(L)}}}{K_{e(L)}}, \quad \phi_2(h, K_{out}) = \dfrac{1 - e^{-hK_{out}}}{K_{out}}, \\ \phi_3(h, K_{off}, K_{e(P)}) = \dfrac{1 - e^{-h(K_{off}+K_{e(P)})}}{K_{off} + K_{e(P)}}. \end{cases} \tag{6.13}$$

while the denominator functions for the explicit-implicit (6.11) are considered to be

$$\begin{cases} \phi_4(h, K_{e(L)}) = \dfrac{e^{hK_{e(L)}} - 1}{K_{e(L)}}, \quad \phi_5(h, K_{out}) = \dfrac{e^{hK_{out}} - 1}{K_{out}}, \\ \phi_6(h, K_{off}, K_{e(P)}) = \dfrac{e^{h(K_{off}+K_{e(P)})} - 1}{K_{off} + K_{e(P)}}. \end{cases} \tag{6.14}$$

Simplifying (6.10) we have that

$$\begin{cases} L_{n+1} = \frac{L_n(1+\phi_1 K_{e(L)})+\phi_1 K_{off} P_n}{1+\phi_1 K_{on} R_n}, \\ R_{n+1} = R_n + \phi_2 K_{in} - \phi_2 K_{out} R_n - \phi_2 K_{on} L_{n+1} R_n + \phi_2 K_{off} P_n, \\ P_{n+1} = P_n + \phi_3 K_{on} L_{n+1} R_n - \phi_3 K_{off} P_n - \phi_3 K_{e(P)} P_n. \end{cases} \tag{6.15}$$

Similarly, (6.11) is simplified to be

$$\begin{cases} L_{n+1} = \frac{L_n+\phi_4 K_{off} P_n}{1+\phi_4 K_{e(L)}+\phi_4 K_{on} R_n}, \\ R_{n+1} = \frac{R_n+\phi_5 K_{in}-\phi_5 K_{on} L_{n+1} R_n+\phi_5 K_{off} P_n}{1+\phi_5 K_{out}}, \\ P_{n+1} = \frac{P_n+\phi_6 K_{on} L_{n+1} R_n}{1+\phi_6 K_{off}+\phi_6 K_{e(P)}}. \end{cases} \tag{6.16}$$

Numerical experiment were performed using the parameter values in Table 6.1. The result presented in [1] is replicate with scheme (6.16) as shown in Figures 6.2 and 6.3.

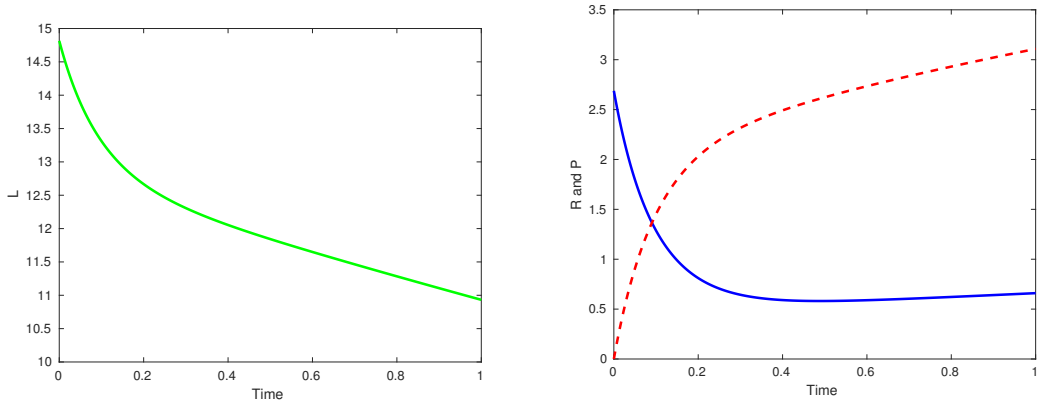

(a) (b)

FIGURE 6.2: The NSFD scheme (6.11) showing the concentration-time profile for $0 \leq t \leq 1$ of (a) the free ligand L, and (b) the free receptor R (blue) and the ligand-receptor complex P (red).

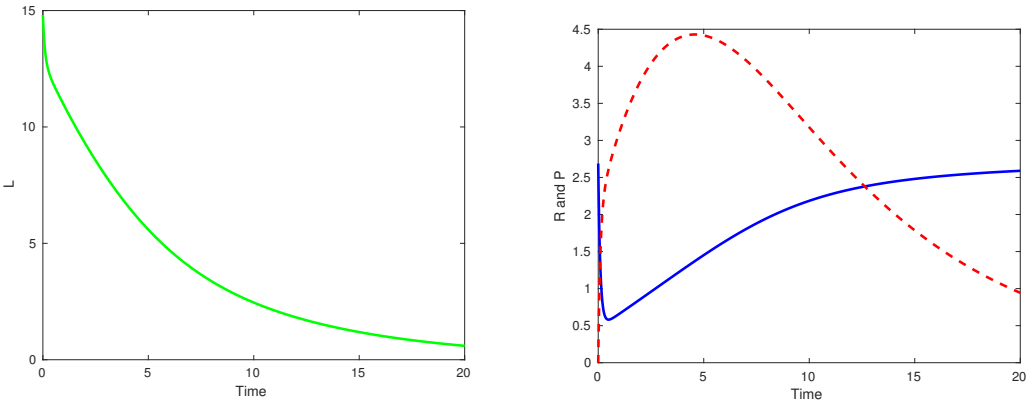

(a) (b)

FIGURE 6.3: The NSFD scheme (6.11) showing the concentration-time profile for $0 \leq t \leq 20$ of (a) the free ligand L, and (b) the free receptor R (blue) and the ligand-receptor complex P (red).

6.3 Two-compartment TMDD Model

The mathematical model of two compartment TMDD was adopted from literature [54, 100]. The model composed of four compartments: The ligand, tissue, receptor and ligand-receptor compartments. A bolus infusion L_0 at the time zero of the ligand L (drug) is administered into the central compartment. K_{on} is the binding rate of the ligand L to the receptor R (or enzymatic sites) to form a ligand-receptor complex P. The unbound drug can be directly eliminated at constant rate, K_{el} or subjected to non-specific tissue transfer between the central compartment, L and tissue M compartment at constants order rate, K_{pt} and K_{tp}. Unlike one-compartment TMDD model, the two compartment TMDD model assume that only unbound drug can move into the peripheral compartment while other ligands remain in the central compartment [54]. L , R and P are the concentrations of the unbound drug, the receptor and ligand-receptor complex in the central compartment respectively. The ligand-receptor complex P may dissociate at the constant rate K_{off} and $K_{e(L)}$ is the linear elimination rate. The elimination rate of the undissociated ligand-receptor complex is $K_{e(p)}$ while the receptor production and elimination rate constants are K_{in} and K_{out} respectively. The system described

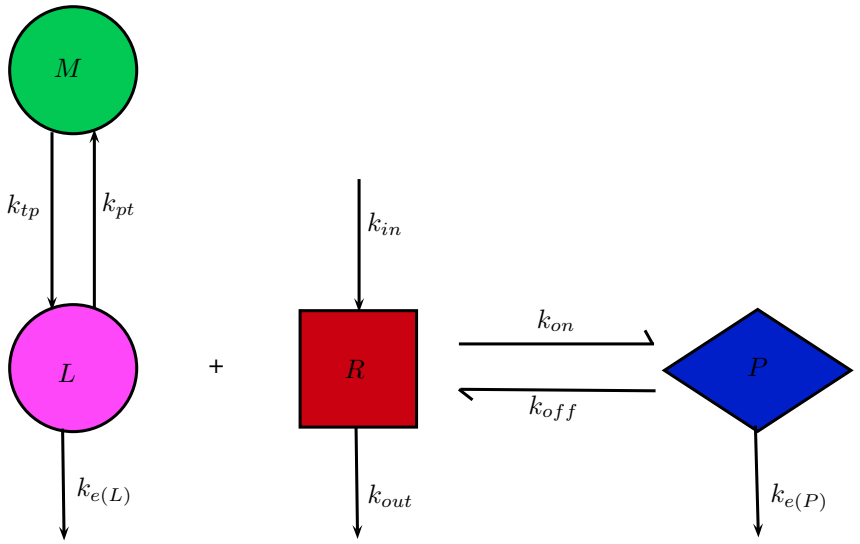

FIGURE 6.4: Two-compartment TMDD reaction model.

in Figure 6.4 can be defined by the following system of differential equations:

$$\begin{cases} \frac{dL}{dt} = -K_{e(L)}L - K_{on}LR + K_{off}P - K_{pt}L + K_{tp}M, \\ \frac{dM}{dt} = K_{pt}L - K_{tp}M, \\ \frac{dR}{dt} = K_{in} - K_{out}R - K_{on}LR + K_{off}P, \\ \frac{dP}{dt} = K_{on}LR - K_{off}P - K_{e(P)}P. \end{cases} \tag{6.17}$$

with initial conditions

$$L(0) = L_0, \qquad M(0) = 0, \qquad R(0) = R_0 = \frac{K_{in}}{K_{out}}, \qquad P(0) = 0. \tag{6.18}$$

6.3.1 Mathematical Analysis of Two-compartment TMDD Model

Steady state

We identify the existence of two steady states and confirm the presence of a single biologically relevant non-zero steady state. The first steady state of system (6.17)

is given by E_0:

$$\hat{L} = 0, \quad \hat{M} = 0, \quad \hat{R} = \frac{k_{\text{in}}}{k_{\text{out}}}, \quad \hat{P} = 0. \tag{6.19}$$

In a similar fashion with one compartment TMDD model, the steady state (6.19) corresponds to the drug free equilibrium hypothetical situation in which there is no drug in the system while steady state E_1 given by

$$\begin{cases} \hat{L} = \frac{-k_{\text{el}}k_{\text{ep}}k_{\text{out}} - k_{\text{el}}k_{\text{off}}k_{\text{out}} - k_{\text{ep}}k_{\text{in}}k_{\text{on}}}{k_{\text{el}}k_{\text{ep}}k_{\text{on}}}, \quad \hat{M} = -\frac{k_{\text{pt}}(k_{\text{el}}k_{\text{ep}}k_{\text{out}} + k_{\text{el}}k_{\text{off}}k_{\text{out}} + k_{\text{ep}}k_{\text{in}}k_{\text{on}})}{k_{\text{el}}k_{\text{ep}}k_{\text{on}}k_{\text{tp}}}, \\ \hat{R} = -\frac{k_{\text{el}}(k_{\text{ep}} + k_{\text{off}})}{k_{\text{ep}}k_{\text{on}}}, \quad \hat{P} = \frac{k_{\text{el}}k_{\text{ep}}k_{\text{out}} + k_{\text{el}}k_{\text{off}}k_{\text{out}} + k_{\text{ep}}k_{\text{in}}k_{\text{on}}}{k_{\text{ep}}^2 k_{\text{on}}}. \end{cases} \tag{6.20}$$

is not biological possible. Evaluating the Jacobian matrix at the steady state $E_0 = (0, 0, \frac{k_{\text{in}}}{k_{\text{out}}}, 0)$ we get the matrix

$$J(E_0) = \begin{pmatrix} -k_{el} - k_{pt} - \frac{k_{on}k_{in}}{k_{out}} & k_{tp} & 0 & k_{\text{off}} \\ k_{pt} & -k_{tp} & 0 & 0 \\ -\frac{k_{on}k_{in}}{k_{out}} & 0 & -k_{out} & k_{off} \\ \frac{k_{on}k_{in}}{k_{out}} & 0 & 0 & -k_{\text{ep}} - k_{\text{off}} \end{pmatrix}. \tag{6.21}$$

Using the parameter values in Table 6.1, the eigenvalues of the Jacobian matrix in (6.21) are $\lambda_1 = -2.98244$, $\lambda_2 = -0.823$, $\lambda_3 = -0.593762$ and $\lambda_4 = -0.0800727$. These eigenvalues are all real and negative indicative that steady state E_0 is asymptotically stable.

6.3.2 Construction and Analysis of the NSFD

NSFD scheme for the system (6.17) which has the similar quantitative properties as the continuous-time model (6.17) is constructed. Using notations and terminology

introduced in (6.7) - (6.9), the following NSFD scheme is proposed

$$\begin{cases} \dfrac{L_{n+1}-L_n}{\phi_7(h)} = -K_{e(L)}L_{n+1} - K_{on}L_{n+1}R_n + K_{off}P_n - K_{pt}L_{n+1} + K_{tp}M_k, \\ \dfrac{M_{n+1}-M_n}{\phi_8(h)} = K_{pt}L_n - K_{tp}M_{k+1}, \\ \dfrac{R_{n+1}-R_n}{\phi_9(h)} = K_{in} - K_{out}R_{n+1} - K_{on}L_{n+1}R_n + K_{off}P_n, \\ \dfrac{P_{n+1}-P_n}{\phi_{10}(h)} = K_{on}L_{n+1}R_n - K_{off}P_{n+1} - K_{e(P)}P_{n+1}. \end{cases} \tag{6.22}$$

This can be rearranged to

$$\begin{cases} L_{n+1} = \dfrac{L_n + \phi_7 K_{off}P_n + \phi_7 K_{tp}M_n}{1 + \phi_7 K_{e(L)} + \phi_7 K_{on}R_n + \phi_7 K_{pt}}, \\ M_{n+1} = \dfrac{M_n + \phi_8 K_{pt}L_n}{1 + \phi_8 K_{tp}}, \\ R_{n+1} = \dfrac{R_n + \phi_9 K_{in} - \phi_9 K_{on}L_{n+1}R_n + \phi_9 K_{off}P_n}{1 + \phi_9 K_{out}}, \\ P_{n+1} = \dfrac{P_n + \phi_{10} K_{on}L_{n+1}R_n}{1 + \phi_{10}K_{off} + \phi_{10}K_{e(P)}}. \end{cases} \tag{6.23}$$

The denominator functions for the NSFD scheme (6.22) are considered to be

$$\begin{cases} \phi_7(h, K_{e(L)}, K_{pt}) = \dfrac{e^{h(K_{e(L)}+K_{pt})} - 1}{K_{e(L)} + K_{pt}}, \quad \phi_8(h, K_{tp}) = \dfrac{e^{hK_{tp}} - 1}{K_{tp}}, \\ \phi_9(h, K_{out}) = \dfrac{e^{hK_{out}} - 1}{K_{out}}, \qquad \phi_{10}(h, K_{off}, K_{e(P)}) = \dfrac{e^{h(K_{off}+K_{e(P)})} - 1}{K_{off} + K_{e(P)}}. \end{cases} \tag{6.24}$$

6.3.2.1 Analysis of the NSFD

The steady state of the NSFD scheme (6.22) was investigated. The idea was to determine if the discrete scheme has introduce extraneous (spurious) solution or not. We begin by finding the steady state $(\hat{L}^0, \hat{M}^0, \hat{R}^0, \hat{P}^0)$ of (6.22). This can be

found by solving

$$\begin{cases} F_L^0(\hat{L}^0, \hat{M}^0, \hat{R}^0, \hat{P}^0) = \hat{L}^0, \\ F_M^0(\hat{L}^0, \hat{M}^0, \hat{R}^0, \hat{P}^0) = \hat{M}^0, \\ F_R^0(\hat{L}^0, \hat{M}^0, \hat{R}^0, \hat{P}^0) = \hat{R}^0, \\ F_P^0(\hat{L}^0, \hat{M}^0, \hat{R}^0, \hat{P}^0) = \hat{P}^0. \end{cases} \tag{6.25}$$

F_L^0, F_M^0, F_R^0 and F_P^0 are the right sides of (6.23), i.e.

$$\begin{cases} F_L^0(\hat{L}^0, \hat{M}^0, \hat{R}^0, \hat{P}^0) = \frac{\hat{L}^0+\phi_7 K_{off}\hat{P}^0+\phi_7 K_{tp}\hat{M}^0}{1+\phi_7 K_{e(L)}+\phi_7 K_{on}\hat{R}^0+\phi_7 K_{pt}}, \\ F_M^0(\hat{L}^0, \hat{M}^0, \hat{R}^0, \hat{P}^0) = \frac{\hat{M}^0+\phi_8 K_{pt}\hat{L}^0}{1+\phi_8 K_{tp}}, \\ F_R^0(\hat{L}^0, \hat{M}^0, \hat{R}^0, \hat{P}^0) = \frac{\hat{R}^0+\phi_9 K_{in}-\phi_9 K_{on}\hat{L}^0\hat{R}^0+\phi_9 K_{off}\hat{P}^0}{1+\phi_9 K_{out}}, \\ F_P^0(\hat{L}^0, \hat{M}^0, \hat{R}^0, \hat{P}^0) = \frac{\hat{P}^0+\phi_{10} K_{on}\hat{L}^0\hat{R}^0}{1+\phi_{10} K_{off}+\phi_{10} K_{e(P)}}. \end{cases} \tag{6.26}$$

The stability of a steady state for a discrete dynamical model is important in understanding how that particular mathematical model behaves. The discrete dynamical model given by (6.25) is solved to obtain $\hat{E}_0$:

$$\hat{L} = 0, \quad \hat{M} = 0, \quad \hat{R} = \frac{k_{\text{in}}}{k_{\text{out}}}, \quad \hat{P} = 0. \tag{6.27}$$

and $\hat{E}_1$:

$$\begin{cases} \hat{L} = \frac{-k_{\text{el}}k_{\text{ep}}k_{\text{out}}-k_{\text{el}}k_{\text{off}}k_{\text{out}}-k_{\text{ep}}k_{\text{in}}k_{\text{on}}}{k_{\text{el}}k_{\text{ep}}k_{\text{on}}}, & \hat{M} = -\frac{k_{\text{pt}}(k_{\text{el}}k_{\text{ep}}k_{\text{out}}+k_{\text{el}}k_{\text{off}}k_{\text{out}}+k_{\text{ep}}k_{\text{in}}k_{\text{on}})}{k_{\text{el}}k_{\text{ep}}k_{\text{on}}k_{\text{tp}}}, \\ \hat{R} = -\frac{k_{\text{el}}(k_{\text{ep}}+k_{\text{off}})}{k_{\text{ep}}k_{\text{on}}}, & \hat{P} = \frac{k_{\text{el}}k_{\text{ep}}k_{\text{out}}+k_{\text{el}}k_{\text{off}}k_{\text{out}}+k_{\text{ep}}k_{\text{in}}k_{\text{on}}}{k_{\text{ep}}^2 k_{\text{on}}}. \end{cases} \tag{6.28}$$

It is clear that (6.17) has exactly the same properties as the solutions obtained for (6.23):

- Equation (6.23) has two fixed points located at $\hat{E}_0$ and $\hat{E}_1$.
- Fixed points $\hat{E}_0$ is biologically possible while $\hat{E}_1$ is biologically impossible.

From the above fact, it is has been shown that (6.17) and (6.23) have the same steady states. Numerical experiment were performed using the parameter values

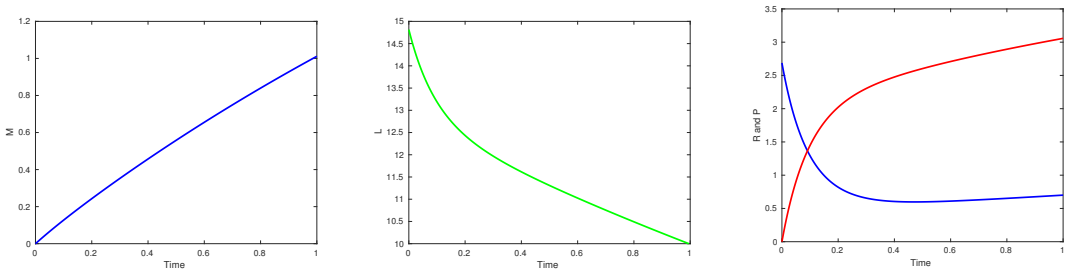

(a) (b) (c)

FIGURE 6.5: The NSFD scheme (6.23) showing the concentration-time profile for $0 \leq t \leq 1$ of (a) tissue M, (b) the free ligand L, and (c) the free receptor R (blue) and the ligand-receptor complex P (red).

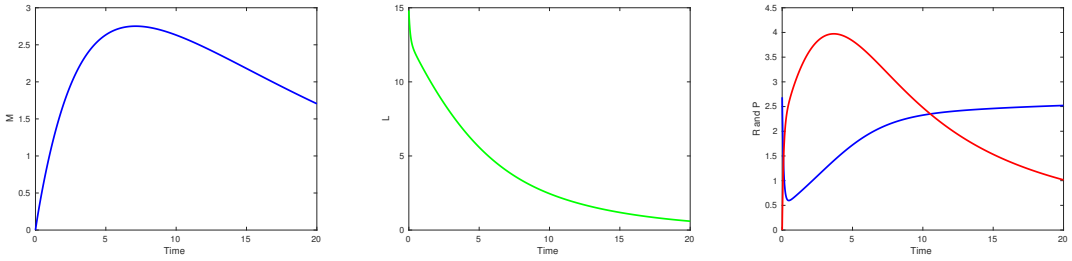

(a) (b) (c)

FIGURE 6.6: The NSFD scheme (6.23) showing the concentration-time profile for $0 \leq t \leq 20$ of (a) tissue M, (b) the free ligand L, and (c) the free receptor R (blue) and the ligand-receptor complex P (red).

in Table 6.1. The NSFD result presented in equation (6.23) as shown in Figures 6.5 and 6.6 which are the expected behaviour of the model.

6.4 Global Sensitivity Analysis

6.4.1 Background

Global sensitivity analysis (GSA) studies how uncertainty in the output of a model can be apportioned to different source of uncertainty in the model input [101, 102].

The advantage of GSA is that it simultaneously varies parameter over the entire parameters space rather than at a point in that space (local sensitivity analysis). GSA is conducted using a group of techniques that are applied to a model to gain more confidence and insight about the behaviour of the model and also to investigate the robustness of the model. This is done in order to determine the most contributing parameter values or non-influential parameter. Several types of global sensitivity analysis have been suggested by a handful authors. Among all, the sensitivity indices, based on decomposition of variance developed by Sobol [103] is the most powerful and as such it will be employed in our analysis. For a general form of Sobol's sensitivity indices, let consider model input vector denoted by

$$X = (X_1, X_2, X_2, \cdots, X_k) \in \mathcal{R}, \tag{6.29}$$

and output $Y \in \mathcal{R}$. Then we have model of the form

$$Y = F(X). \tag{6.30}$$

According to the result by [103], the variance of the output can be decomposed as sum of variances in an increasing order i.e

$$Var(Y) = \sum_{i=1}^{k} V_i + \sum_{i<j}^{k} V_{ij} + \cdots + V_{i,j\ldots k} \tag{6.31}$$

where

$$V_i = Var\left(\mathbb{E}(Y|X_i)\right). \tag{6.32}$$

V_i is called first order variances. V_{ij} is the second order variances and its presented as

$$V_{ij} = Var\left(\mathbb{E}(Y|X_i, X_j)\right). \tag{6.33}$$

Therefore, the Sobol sensitivity indices are obtained as follows

$$S_i = \frac{V_i}{Var(Y)} = \frac{Var\left(\mathbb{E}(Y|X_i)\right)}{Var(Y)}, \tag{6.34}$$

S_i is the first order index for input, X_i which measure the proportion of variance which is due to main effect of input on output. Similarly,

$$S_{ij} = \frac{V_{ij}}{Var(Y)} = \frac{Var\left(\mathbb{E}(Y|X_i, X_j)\right)}{Var(Y)}, \tag{6.35}$$

S_{ij} is the second order index for X_i and X_j. It measures the proportion of total variance which is explained by the interaction between X_i and X_j. The number of indices grows. For k parameters, there are $2^k - 1$ indices. The total variance index was introduced by [104] in order determine the total variance which is due to the main effect of input and its interaction with every other inputs. This total sensitivity indices is presented mathematically as

$$S_{Ti} = \frac{V_i + \sum_j V_{ij} + \sum_{jk} V_{ijk} + \cdots}{Var(Y)} = \frac{\mathbb{E}\left(Var\left(Y|X_{-i}\right)\right)}{Var(Y)} = 1 - \frac{Var\left(\mathbb{E}\left(Y|X_{-i}\right)\right)}{Var(Y)} \tag{6.36}$$

where $X_{-i} = (X_1, X_2, \cdots, X_{i-1}, X_{i+1}, \cdots X_k)$. In practice, only the first order indices and the total indices are computed in other to get information on the model sensitivities.

6.4.2 Result

The GSA explained above was applied to one and two-compartment TMDD models to gain insight into the global sensitivity of the model parameters. The sensitivity estimates offered by Jansen [105, 106] was used for simulation by running 10,000 iterations. The first order effect and total order effect for the one-compartment TMDD model parameters are presented in Table 6.2.

For the one-compartment TMDD model, it was found that $K_{e(P)}$ is the most sensitive parameter, followed by $K_{e(L)}$, K_{off}, K_{out}, K_{in} and K_{on} as shown in Figure 6.7. Reducing $K_{e(P)}$ would have a significant effect on the concentration of the drug regardless of other parameter values. For the two-compartment TMDD model, similar behaviour was found as for the one-compartment TMDD model as it presented in Figure 6.8. In each of the model considered, we observed that total

TABLE 6.2: First order indices and the total indices for one-compartment TMDD model.

Global Sensitivity Analysis		
Parameters	**First order indices**	**Total indices**
$K_{e(L)}$	0.0345	0.0620
K_{on}	0.0002	0.0077
$K_{e(P)}$	0.8553	0.962
K_{out}	0.0071	0.0494
K_{off}	0.0070	0.0154
K_{in}	0.0051	0.0535

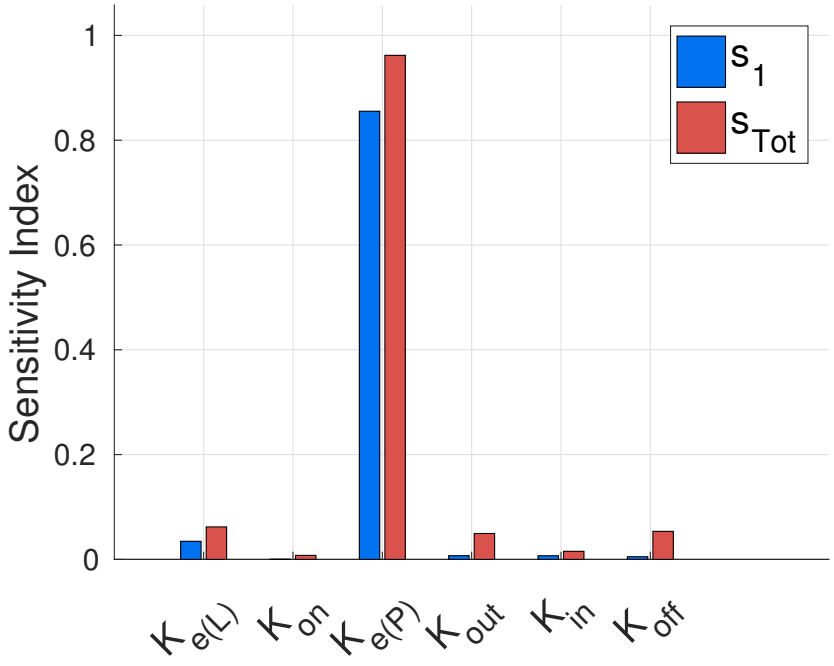

FIGURE 6.7: First order effects $S_1(blue)$ and total effects S_{Tot} (red) of the six parameters using Sobol's method of Sensitivity Analysis for one-compartment TMDD model.

effect and first order effect have similar behaviour, which indicate no significant second order interaction between the parameters.

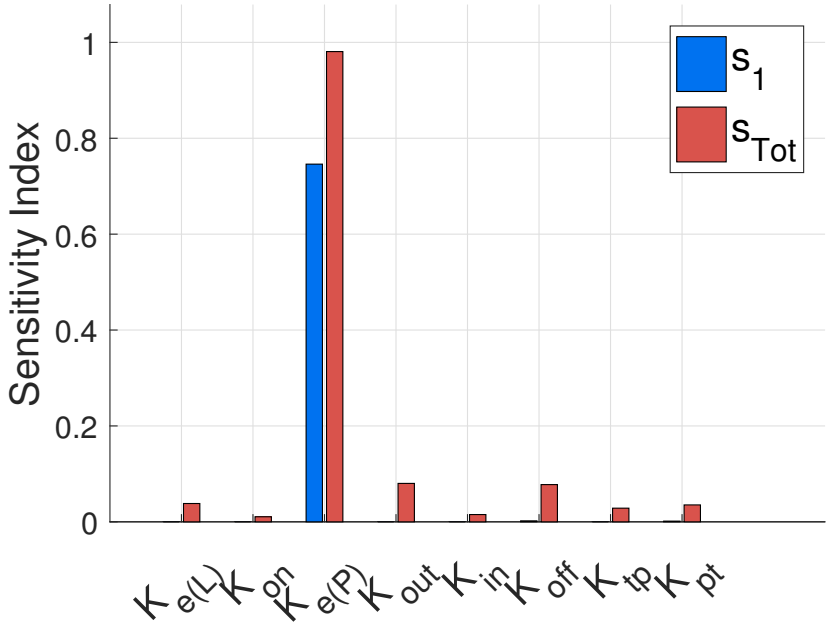

FIGURE 6.8: First order effects $S_1(blue)$ and total effects S_{Tot} (red) of thesix parameters using Sobol's method of Sensitivity Analysis for two-compartment TMDD model.

6.5 Concluding Remarks

NSFD schemes were constructed for one and two-compartment TMDD models and their qualitative behaviour was studied. The NSFD schemes developed were found to have the same quantitative properties as the continuous-time models. We prove the existence of positive solutions for the models. The GSA was carried out to ascertain the most contributing parameters. From the results obtained in Figures 6.7 and 6.8 we found that the model result will be highly influenced by any change in $K_{e(P)}$.

Chapter 7

Conclusion

"All scientific work is incomplete – whether it be observational or experimental."

Hill, Austin Bradford (1965)

Due to its simplicity, the compartment pharmacokinetic model often serves as a "first model" that requires further refinement in order to describe the physiological and drug distribution processes in the body accurately. While this may be the case, non-compartment models have gained popularity in the literature due to their ability to easily relate experimental data to mathematical models via parameter fitting. Foste [107] points out that upon comparing non-compartment with compartment models, it is not a question of declaring one method better than the other. It is a question of (1) what information is desired from the data; and (2) what is the most appropriate method to obtain this information. Known limitations of non-compartment models include the fact that they do not allow for meta-analysis and the deeper insight that the physiological-based PK models allow for [108]. Another important limitation of non-compartment PK analysis is that it lacks the ability to predict PK profiles when there are alterations in a dosing regimen, which compartment PK methods are capable of [109]. Furthermore, compartmental approaches allow for some level of "physiological" interpretation of what the body does to the drug (i.e., consistency with physiologically reasonable pathways of drug

elimination can be maintained). Shargel et al. [49] note that, in comparison to non-compartment models, compartment models are particularly useful when little information is known about the tissues of the compartment(s). In this study non-compartment models are not of interest, not due to their limitations but because non-compartment analysis is based on algebraic equations, whereas compartment models are based on linear or nonlinear differential equations. This thesis instead investigates the use of a method (Nonstandard finite difference method) which is designed for the effective solution of differential equations, and as such turn our attention away from non-compartment models.

7.1 Nonstandard Finite Difference Method

The flexibility afforded by the NSFD scheme, in terms of its construction, means that the scheme secures consistency with the continuous pharmacokinetic models arising from compartmental or physiological models with respect to the different dynamical characteristics of the systems [11]. As a consequence, we were able to investigate the dynamics of the models and the impact of the parameter value choices employed. Also, we were able to study the dynamics of the models and ensure the method under consideration do not introduce extraneous (or spurious) solutions.

This thesis, provided numerical solution to compartmental pharmacokinetic models and target mediated drug disposition. These models are one, two and three-compartment pharmacokinetic models. All models were solved using NSFD method. The results presented in this thesis are helpful in understanding the long time behaviour of the drug in the body. Some of the main findings in this thesis are:

7.1.1 One-compartment Pharmacokinetic Models

In Chapter 3, we introduced and substantiated the use of NSFD schemes capable of solving one-compartment pharmacokinetic models. These models are comprised

of linear and nonlinear ordinary differential equations. 'Exact' finite difference schemes were provided for the linear models while the NSFD rules based on Mickens' [29] idea of transferring nonlinear models into discrete schemes was applied to the nonlinear models. The method was compared with established methods to verify the efficiency and the accuracy of the method. The one-compartment pharmacokinetic models were considered for different routes of administration: I.V. bolus injection, I.V. bolus infusion and extravascular administration. With the results obtained in Chapter 3, we have provided an alternative solution to the problem of no solution often encountered in the literature when the absorption and elimination rate constants are equal [110].

7.1.2 Two-compartmnet Pharmacokinetic Models

The NSFD method of solution to the study of a drug that follows first order two-compartment pharmacokinetic was presented in Chapter 4. NSFD schemes were structured for the relevant system of equations which models this pharmacokinetic process. The results obtained were compared to standard methods. The scheme is dynamically consistent and reliable in replicating complex dynamic properties of the relevant continuous models for varying step sizes. This study provides assistance in understanding the long-term behavior of the drug in the system, and validation of the efficiency of the nonstandard finite difference scheme as the method of choice.

7.1.3 Three-compartment Pharmacokinetic Models

The complex nature of the analytical solutions to three-compartment pharmacokinetic model lead to the discrete approximation of the continuous differential equation been mostly used [53]. NSFD schemes for solving three compartment pharmacokinetic models were derived. For the case when the system is homogeneous (models arising from I.V. bolus injection mode of administration), 'exact'

finite difference scheme was obtained for any step-size while in the case of non-homogeneous (models arising from I.V. bolus infusion route of administration), positivity-preserving scheme that has the same qualitative behaviour as the analytical solution for all step-sizes was constructed [96]. It was shown computationally that the NSFD scheme for three compartment pharmacokinetic model with I.V. bolus mode of administration is exact while three-compartment pharmacokinetic model with I.V. infusion is dynamically consistent with the continuous model for all step-sizes. The problem encountered by [53] of not being able to determine concentration of drug in each compartment except at the central compartment as been resolved in Chapter 5.

7.1.4 Target-mediated Drug Disposition Models

Chapter 6 was mainly devoted to the application of NSFD method to the study of one and two-compartment TMDD models and characterization of the model parameters by conducting GSA. From the qualitative analysis of the models we found that the models exhibit two steady states for any positive parameters values. One of the steady state is biologically possible while the other is not biological possible since all the model parameters are positive values. The same phenomena was experienced when analysis of the NSFD schemes was carried out. This indicates that the new schemes preserves the qualitative properties of solutions. With the use of GSA we are able to determine the most contributing parameter in the models.

7.2 Final note

The goal of pharmacokinetic is to obtain the desired drug concentration in the body by optimizing the dosage regimen and dosage form. Hence, with an understanding of pharmacokinetic models, health-care providers can increase effectiveness (or increase patient compliance with a therapeutic regimen) and decrease drug toxicity. These goals can only be achieved when the solutions to pharmacokinetic models are

fully understood. The need for improvement relates to an interest in considering more complex models (for instance non-linear or multi-compartmental models) in which simplifying assumptions need not be made.

In order to do so one would require an effective, robust and stable numerical method the dynamics of which can be investigated since the scheme maintains the appropriate qualitative behavior. This numerical technique allows calculation of the concentration of drug in each compartment at each update cycle with improved accuracy and reduced computational costs when compared with standard numerical techniques. In this thesis, we have succeeded in developing nonstandard schemes for various pharmacokinetic models. These schemes preserve the significant properties of their continuous analogues and consequently give reliable numerical results. It was found that the NSFD schemes were stable for large step sizes and display qualitatively accurate results, allowing one to assess and predict the long time behaviour of the drug in the system. Given that the NSFD method produces "exact" numerical schemes when the model is linear, we may conclude that they are well-suited for the solution of pharmacokinetic models.

Bibliography

[1] P. J. Aston, G. Derks, A. Raji, B. M. Agoram, and P. H. van der Graaf. Mathematical analysis of the pharmacokinetic-pharmacodynamic (pkpd) behaviour of monoclonal antibodies: Predicting in vivo potency. *Theoretical Biology*, 281:133–121, 2011.

[2] J.-C. Péchère, M.-M. Péchère, and R. Dugal. Clinical pharmacokinetics of sisomicin: Two-compartment model analysis of serum data after i.v. and i.m. administration. *Eur. J. Clin. Pharmacol.*, 10:251–256, 1976.

[3] S. Cascone, G. Lamberti, G. Titomanlio, and O. Piazza. Pharmacokinetics of remifentanil: a three-compartmental modeling approach. *Translational Medicine @ UniSa*, 7(4):18–22, 2013.

[4] R. E. Mickens. Exact solutions to a finite-difference model of a nonlinear reaction-advection equation: Implications for numerical analysis. *Numerical Methods for Partial Differential Equations*, 5(1):313–325, 1989.

[5] B. F. Woods. Numerical instabilities in finite-difference models of ordinary differential equations. *Master Thesis, Atlanta University, Atlanta, USA*, 1989.

[6] R.E. Mickens. Application of nonstandard finite difference schemes, 1st ed. *World Scientific: Singapore*, 2000.

[7] R.E. Mickens. Nonstandard finite difference schemes for differential equations. *J. Differ. Equ. Appl.*, 8:823–847, 2002.

[8] R.E. Mickens. A nonstandard finite difference scheme for the diffusionless burgers equation with logistic reaction. *Math. Comput. Simul.*, 62:117–124, 2003.

[9] R.E. Mickens. Dynamic consistency: A fundamental principle for constructing nonstandard finite difference schemes for differential equations. *J. Differ. Equ. Appl.*, 11:645–653, 2005.

[10] R.E. Mickens. A numerical integration technique for conservative oscillators combining nonstandard finite-difference methods with a hamilton's principle. *J. Sound Vib.*, 285:477–482, 2005.

[11] C. Liao and X. Ding. Nonstandard finite difference variational integrators for nonlinear schrödinger equation with variable coefficients. *Adv. Differ. Equ.*, 2013:1–22, 2013.

[12] A.J. Arenas, G. González-Parra, and B.M. Chen-Charpentier. A nonstandard numerical scheme of predictor- corrector type for epidemic models. *Comput. Math. Appl.*, 59:3740–3749, 2010.

[13] G. González-Parra, A.J. Arenas, and B.M. Chen-Charpentier. Combination of nonstandard schemes and richardson's extrapolation to improve the numerical solution of population models. *Math. Comput. Model.*, 52:1030–1036, 2010.

[14] P.M. Jordan. A nonstandard finite difference scheme for nonlinear heat transfer in a thin finite rod. *J. Differ. Equ. Appl.*, 9:1015–1021, 2003.

[15] A. Malek. Applications of nonstandard finite difference methods to nonlinear heat transfer problems. *In Heat Transfer—Mathematical Modelling, Numerical Methods and Information Technology, InTech: Rijeka, Croatia, 2011; doi:10.5772/14439.*

[16] R. E. Mickens and A. Smith. Finite-difference models of ordinary differential equations: Influence of denominator functions. *Journal of Franklin Institute*, 327(1):143–149, 1990.

[17] R. E. Mickens and I. Ramadhani. Finite-difference schemes having the correct linear stability properties for all finite step-sizes iii. *Computers Math. Applic.*, 27(4):77–84, 1994.

[18] R. E. Mickens. Novel explicit finite-difference schemes for time-dependent schrodinger equations. *Computer Physics Communications*, 63:203–208, 1991.

[19] R. E. Mickens. Best finite-difference scheme for the fisher equation. *Numerical Method for partial Differential Equations*, 10(5):581–585, 1994.

[20] R. Anguelov and J.M.-S. Lubuma. Contributions to the mathematics of the nonstandard finite difference method and applications. *Numer Methods Partial Differential Eq.*, 71:518–543, 2001.

[21] J. M.-S. Lubuma and K. C. Patidar. Advances in the application of nonstandard finite difference schemes. *World Scientific Publishing Co., Singapore, Chapter 12*, pages 513–560, 2005.

[22] J. B. Cole. High-accuracy realization of the yee algorithm using non-standard finite differences. *IEEE Transactions on Microwave Theory and Techniques*, 45(6):991–996, 1997.

[23] E. Momoniat. A modified equation approach to selecting a nonstandard finite difference scheme applied to the regularized long wave equation. *Hindawi Publishing Corporation Abstract and Applied Analysis*, 2014, 2014.

[24] B. M. Chen and F. Solis. Dicretizations of nonlinear differential equations using explicit finite order method. *Journal of Computational and Applied Mathematics*, 90(2):171–183, 1998.

[25] R. E. Mickens. Dicretizations of nonlinear differential equations using explicit finite order method. *Computational and Applied Mathematics*, 110(1):181–185, 1999.

[26] A. S. de Markus and R. E. Mickens. Suppression of numerically induced chaos with nonstandard finite difference schemes. *Computational and Applied Mathematics*, 106(2):317–324, 1999.

[27] R. Anguelov, Y. Dumont, J.M.-S. Lubuma, and M. Shillor. Dynamically consistent nonstandard finite difference schemes for epidemiological models. *J Comput Appl Math*, 255:161–182, 2014.

[28] J. C. Kamgang and G. Sallet. Computation of threshold conditions for epidemiological models and global stability of the disease equilibrium (dfe). *Mathematical Biosciences*, 213:1–12, 2008.

[29] R.E. Mickens. Nonstandard finite difference models of differential equations. *World Scientific: Singapore*, 1994.

[30] R. Anguelov, Y. Dumont, and J.M.-S. Lubuma. On nonstandard finite difference schemes in biosciences. *AIP Conference Proceedings*, 1487(1): 212–223, 2012.

[31] S. Elsheikh, R. Ouifki, and K. C. Patidar. A non-standard finite difference method to solve a model of hiv-malaria co-infection. *Difference Equations and Applications*, 20(3):354–378, 2014.

[32] D. Ding, Q. Ma, and X. Ding. A non-standard finite difference scheme for an epidemic model with vaccination. *Difference Equations and Applications*, 19(2):179–190, 2013.

[33] H. A. Obaid, R. Ouifki, and K. C. Patidar. An unconditionally stable nonstandard finite difference method applied to mathematical model of hiv infection. *Int. J. Appl. Math. Comput. Sci.*, 23(2):357–372, 2013.

[34] J. M.-S. Lubuma and Y. A. Terefe. A non-standard volterra difference equation for the sis epidemiological model. *RACSAM*, 109:597–602, 2015.

[35] R. Anguelov, Y. Dumont, .M.-S. Lubuma, and M. Shillor. Dynamical consistent non-standard finite difference schemes for the mseir epidemiological model. *AIP Proceedings 1168*, 1213(1), 2009.

[36] R. Anguelov, Y. Dumont, J.M.-S. Lubuma, and M. Shillor. Comparison of some standard and nonstandard numerical methods for the mseir epidemiological model. *AIP Proceedings 1168*, 1209, 2009. URL doi:10.1063/1.3241285.

[37] M. Chapwanya, J. M.-S. Lubuma, and R. E. Mickens. From enzyme kinetics to epidemiological models with michaelis–menten contact rate: Design of nonstandard finite difference schemes. *Comput Math Appl.*, 64(1):201–213, 2012.

[38] S.M. Garba, A.B. Gumel, and J.M.-S. Lubuma. Dynamically-consistent non-standard finite difference method for an epidemic model. *Mathematical and Computer Modelling*, 53(1):131–150, 2011.

[39] J.M.-S. Lubuma, E. W. Mureithi, and Y. A. Terefe. Nonstandard discretizations of the sis epidemiological model with and without diffusion. *Department of Mathematics and Applied Mathematics, University of Pretoria*, (1), January 2014.

[40] K. C. Patidar. On the use of nonstandard finite difference methods†. *Difference Equations and Applications*, 11(8):735–758, 2005.

[41] K. C. Patidar. Nonstandard finite difference methods: recent trends and further developments. *Difference Equations and Applications*, 22(6):817–849, 2016.

[42] A. Buchanan. Physiologic effects of the inhalation of ether. *Lond. Med. Gaz.*, 39:715–717, 1847.

[43] L. Michealis and M.L. Menten. Die kinetik der invertinwirking. *Biochem. Z.*, 49:333–369, 1913.

[44] E. Widmark and J. Tandberg. Uber die bedingungen f'tir die akkumulation indifferenter narkoliken theoretische bereckerunger. *Biochem. Z.*, 147:358–369, 1924.

[45] T. Teorell. Kinetics of distribution of substances administered to the body. i. the extravascular modes of administration. *Arch. Int. Pharmacodyn. Ther.*, 57:205–225, 1937.

[46] N.H.G. Holford and L.B. Sheiner. Kinetics of pharmacologic response. *Pharmacol. Ther.*, 16:143–166, 1982.

[47] S.-M. Huang, D.R. Abernethy, Y. Wang, P. Zhao, and I. Zineh. The utility of modelling and simulation in drug development and regulatory review. *J. Pharm. Sci.*, 102:2912–2923, 2013.

[48] P. L. Bonate. Pharmacokinetic-pharmacodynamic modelling and simulation. *Springer: New York, NY, USA*, page 2, 2011.

[49] L. Shargel, A. Yu, and S. Wu-Pong. Introduction to biopharmaceutics and pharmacokinetics. *Applied Biopharmaceutics & Pharmacokinetics, 6th ed., McGraw-Hill: New York, NY, USA, Chapter 1*, pages 1–17, 2012.

[50] L. Shargel, A. Yu, and S. Wu-Pong. Multicompartment models: Intravenous bolus administration. *Applied Biopharmaceutics & Pharmacokinetics, 6th ed., McGraw-Hill: New York, NY, USA, Chapter 4*, pages 58–79, 2012.

[51] L. Shargel, A. Yu, and S. Wu-Pong. Physiologic pharmacokinetic models, mean residence time, and statistical moment theory. *Applied Biopharmaceutics & Pharmacokinetics, 6th ed., McGraw-Hill: New York, NY, USA, Chapter 22*, pages 658–690, 2012.

[52] M. Beňová, D. Gombárska, and B. Dobrcký. Using euler's and taylor's expansion method for solution of non-linear differential equation system in pharmacokinetics. *Electr. Rev.*, 89:259–261, 2013.

[53] J. M. Bailey and S. L. Shafer. A simple analytical solution to the three-compartment pharmacokinetic model suitable for computer-controlled. *IEEE transaction on biomedical engineering*, 38(6):522–525, 1991.

[54] D. E. Mager and W. J. Jusko. General pharmacokinetic model for drugs exhibiting target-mediated drug disposition. *Pharmacokinetics and Pharmacodynamics*, 28(6):248–252, 2001.

[55] L. Shargel, S. Wu-Pong, and A. B. C. Yu. Applied biopharmaceutics & pharmacokinetics, 5th edition, chapter 9. *McGraw-Hill*, 64.

[56] M. Benova and B. Dobrucky D. Gombarska. Using euler's and taylor's expansion method for solution of non-linear differential equation system in pharmacokinetics. *University of Zilina*, 2013.

[57] S. L. Shafer, L. C. Siegel, J. E. Cooke, and J. C. Scott. Testing computer-controlled infusion pumps by simulation. *Anesthesiology*, 68:261–266, 1988.

[58] R. N. Upton. Calculating the hybrid (macro) rate constants of a three-compartment mamillary pharmacokinetic model from known micro-rate constants. *JPTME*, 49:65–68, 2004.

[59] D. B. Raemer, A. Buschman, J. R. Varvel, B. K. Philip, M. D. Johnson, D. A. Stein, and S. L. Shafer. The prospective use of population pharmacokinetics in a computer-driven infusion system for alfentanil. *Anesthesiology*, 73:66–72, 1990.

[60] Runge-kutta methods. *Accessed on 15 September 2017*, . URL http://web.mit.edu/10.001/Web/Course_Notes/Differential_Equations_Notes/node5.html.

[61] R. Anguelov and Jean M.-S. Lubuma. Nonstandard finite difference method by nonlocal approximation. *Math Comput Simul.*, 61(1):465–475, 2003.

[62] K.F. Gurski. A simple construction of nonstandard finite-difference schemes for small nonlinear systems applied to sir models. *Computers and Mathematics with Applications*, 66(1):2165–2177, 2013.

[63] R.E. Mickens. Lie methods in mathematical modelling: Difference equation models of differential equation. *Math. Comput. Model.*, 11:528–530, 1988.

[64] What is the difference between consistency, stability and convergence for the numerical treatment of any pde. available online. *Accessed on 9 September 2017*, . URL https://www.researchgate.net/post/What_is_the_difference_between_consistency_stability_and_convergence_for_the_numerical_treatment_of_any_PDE.

[65] J. C. Butcher. The numerical analysis of ordinary differential equations. *John Wiley & Sons, Chapter 1*, pages 16–46, 1989.

[66] Numerical instability. available online. *Accessed on 9 September 2017*, . URL https://www.revolvy.com/topic/Numerical%20instability&item_type=topic.

[67] R. Anguelov, Y. Dumont, J.M.-S. Lubuma, and M. Shillor. Topological dynamic consistency of non-standard finite difference schemes for dynamical systems. *Journal of Difference Equations and Applications*, 17:1769–1791, (2011.

[68] R.E. Mickens. Nonstandard finite difference schemes for differential equations. *J. Differ. Equations Appl.*, 8(9):823–847, 2002.

[69] K. R. Sharma. On single compartment pharmacokinetic model systems that obey michaelis-menten kinetics and systems that obey krebs cycle kinetics. *JEAS*, 1(1):43–50, 2011.

[70] F. R. Villatoro. Exact finite-difference methods based on nonlinear means. *J. Differ. Equations Appl.*, 14(7):681–691, 2008.

[71] R. E. Mickens, K. Oyedeji, and S. Rucker. Exact finite difference scheme for second-order, linear odes having constant coefficients. *J. Sound Vib.*, 287(1): 1052–1056, 2005.

[72] L. W. Roeger. Exact finite-difference schemes for two-dimensional linear systems with constant coefficients. *J. Comput. Appl. Math.*, 219(1):102–109, 2008.

[73] E. A. Ibijola and A. A. Obayomi. Derivation of new non-standard finite difference schemes for non-autonomous ordinary differential equation. *AJSIR*, 2012.

[74] P. M. Manning and G. F. Margrave. Introduction to non-standard finite-difference modelling. *CREWES Research Report 18*, 219(1):102–109, 2006.

[75] R. E. Mickens. Application of nonstandard finite difference schemes. *1st edn. World Scientific,Singapore*, pages 995–1006, 2000.

[76] R. E. Mickens. A nonstandard finite difference scheme for the diffusionless burgers equation with logistic reaction. *Math. Comput. Simul.*, 62(1):117–124, 2003.

[77] R. E. Mickens. Dynamic consistency: a fundamental principle for constructing nonstandard finite difference schemes for differential equations. *J. Differ. Equ. Appl.*, 11(7):645–653, 2005.

[78] R. E. Mickens. A numerical integration technique for conservative oscillators combining nonstandard finite-difference methods with a hamilton's principle. *J. Sound Vib.*, 285(1):477–482, 2005.

[79] J. Sunday. On exact finite-difference scheme for numerical solution of initial value problems in ordinary differential equations. *PJST*, 11(2):260–267, 2010.

[80] J.J. Gander and R. Meyer-Spasche. An introduction to numerical integrators preserving physical properties, in applications of nonstandard finite difference schemes., in r.e. mickens ed. *World Scientific*, 1(1):181–246, 2000.

[81] R.E. Mickens. Nonstandard finite difference models of differential equations. *World Scientific, Singapore*, 1994.

[82] R.E. Mickens. Difference equation models of differential equations. *Math. Comput. Modelling*, 11(1):528–530, 1988.

[83] T. Sanyi and X. Yanni. One-compartment model with michaelis-menten elimination kinetics and therapeutic window: an analytical approach. *J Pharmacokinet Pharmacodyn*, 34(1):807–827, 2007.

[84] R. E. Mickens. An exact discretization of michaelis–menten type population equations. *J Biol Dyn.*, 5(5):391–397, 2011.

[85] M. Chapwanya, J. M.-S. Lubuma, and R. E. Mickens. Nonstandard finite difference schemes for michaelis-menten type reaction-diffusion equations. 2012.

[86] R.E. Mickens. Numerical integration of population models satisfying conservation laws: Nsfd methods. *J. Biol. Dyn.*, 1(4):427–436, 2007.

[87] O. Egbelowo, C. Harley, and B. Jacobs. Nonstandard finite difference method applied to a linear pharmacokinetics model. *Bioengineering*, 4(2):40, 2017.

[88] E. M. P. Widmark. Die theoretischen grundlagen und die praktische verwendbzrkeit der gerichtlichmedizinischen alkoholbestimmung. *Berlin*, 1932.

[89] Introduction to non-standard finite-difference modelling. available online. *Accessed on 1 January 2016.* URL https://www.crewes.org/ForOurSponsors/ResearchReports/2006/2006-46.pdf.

[90] G. Koch. Modeling of pharmacokinetics and pharmacodynamics with application to cancer and arthritis. *Ph.D. Thesis, University of Konstanz, Konstanz, Germany*, 2012.

[91] D.V. Widder. The laplace transform. *Princeton University Press: Princeton, NJ, USA*, 1966.

[92] S. Kreuer, A. Hauschild, T. Fink, J. I. Baumbach, S. Maddula, and T. Volk. Two different approaches for pharmacokinetic modeling of exhaled drug concentrations. *Sci. Rep.*, 4:5423, 2014.

[93] Y. Plusquelle. Analytical study of three-compartment pharmacokinetic models: concentration, area under curves, mean residence time. *J. Biomed. Eng*, 11:345–351, 1989.

[94] O. Egbelowo. Nonlinear elimination of drugs in one-compartment pharmacokinetic models: Nonstandard finite difference approach for various routes of administration. *Math. Comput. Appl.*, 23:27, 2018.

[95] D. Q. A and H. M. Tuan. Exact finite difference schemes for three-dimensional linear systems with constant coefficients. *Vietnam J. Math,DOI 10.1007/s10013-017-0249-8.*

[96] R.E. Mickens. Numerical integration of population models satisfying conservation laws: Nsfd method. *J. Biol. Dyn*, 1:427–436, 2007.

[97] R. E. Mickens. A note on a non-standard finite difference scheme for the reluga x–y–z model. *J. Differ. Equations Appl.*, 16(12):1501–1504, 2010.

[98] G. Levy. General pharmacologic target-mediated drug disposition. *Clinical Pharmacol. Ther.*, 56:248–252, 1994.

[99] O. Egbelowo. Nonstandard finite difference approach for solving 3-compartment pharmacokinetic models. *Int J Numer Meth Biomed Engng.*, e3114, 2018. URL https://doi.org/10.1002/cnm.3114.

[100] P. Dua, E. Hawkins, and PH van der Graaf. A tutorial on target-mediated drug disposition (tmdd) models. *CPT Pharmacometrics Syst. Pharmacol*, 4: 324–337, 2015.

[101] A. Saltelli, P. Annoni, I. Azzini, F. Campolongo, M. Ratto, and S. Tarantola. Variance based sensitivity analysis of model output. design and estimator for the total sensitivity index. *Computer Physics Communications*, 181:259–270, 2010.

[102] B. Iooss and P. Lemaître. A review on global sensitivity analysis methods. c. meloni and g. dellino. uncertainty management in simulation-optimization of complex systems: Algorithms and applications. *Springer*, pages 1–24, 2015.

[103] I. M. Sobol. Sensitivity estimates for nonlinear mathematical models. *Mathematical Modelling and Computational Experiment*, 4(1):407–414, 1993.

[104] T. Homma and A. Saitelli. Importance measures in global sensitivity analysis of nonlinear models. *Reliability Engineering and System Safety*, 52:1–17, 1996.

[105] M. J. W. Jansen. Analysis of variance designs for model output. *Computer Physics Communication*, 117:35–43, 1999.

[106] M. J. W. Jansen, W. A. H. Rossing, and R. A. Daamen. Monte carlo estimation of uncertainty contributions from several independent multivariate sources, in: J. gasmanand and g. van straten (eds.), predictability and nonlinear modelling in natural sciences and economics. *Kluwer Academic Publishers, Dordrecht*, pages 334–343, 1994.

[107] D.M. Foster. Noncompartmental versus compartmental approaches to pharmacokinetic analysis. *In Principles of Clinical Pharmacology,2nd ed., Atkinson, A.J., Abernethy, D.R., Daniels, C.E., Dedrick, R.L., Markey, S.P., Eds.; Academic Press: New York, NY, USA*, pages 89–105, 2014.

[108] Z. Wang, S. Kim, S.K. Quinney, J. Zhou, and L. Li. Non-compartment model to compartment model pharmacokinetics transformation meta-analysis–a multivariate nonlinear mixed model. *BMC Syst. Biol.*, 4:S8, 2010.

[109] G.R. Jang, R.Z. Harris, and D.T. Lau. Pharmacokinetics and its role in small molecule drug discovery research. *Med. Res. Rev.*, 21:382–396, 2001.

[110] H. P. Wijnand. Pharmacokinetic model equations for the one- and two-compartment models with first-order processes in which the absorption and exponential elimination or distribution rate constants are equal. *Pharmacokinetics and Biopharmaceutics*, 16(1), 1988.